High-temperature superconductors: growth of single crystals

L. N. Dem'yanets

A. V. Shubnikov Institute of Crystallography, Academy of Sciences of the USSR, Moscow
(Submitted 7 June 1990; resubmitted 6 September 1990)
Usp. Fiz. Nauk **161**, 71–142 (January 1991)

The crystal structure of twenty structurally different types of high-temperature oxide superconductors is discussed. This is followed by a detailed review of the phase relationships and the growth of single crystals belonging to the following systems: La–Sr–Cu–O, Ba–Y–Cu–O, Bi–Sr–Ca–Cu–O, Nd–Ce–Cu–O, Tl–Ba–Ca–Cu–O, Ba–K–Bi–O, and Ba–Rb–Bi–O.

1. INTRODUCTION

The discovery in 1986, of the high-temperature superconductivity in the class of lanthanum–alkaline-earth cuprates[1] has stimulated a mighty flood of papers reporting the search for, synthesis, and determination of physical properties of an enormous number of different oxide compounds, mainly those based on copper cuprates.

The first result of this search was the discovery of $YBa_2Cu_3O_{7-x}$ superconductors.[2] At the time of writing of this review the transition to the superconducting state at temperatures above 30 K has been detected in over 20 structural types of layer cuprates listed in Table I; the compositions of the majority of these compounds, based on single-crystal data, are given in Refs. 1–42. Table I includes oxide semiconductors with $T_c \gtrsim 10$ K. The great majority are various cuprates and only three complex oxides do not contain copper. The first two of these among the oxide compounds in Table I have relatively low values of T_c and belong to an earlier "quiet" period of investigation of high-temperature superconductors: one is an *Li* spinel and the other is barium bismuthate plumbate with $T_c \gtrsim 10$ K. The complex cuprates which follow these three materials in Table I have been the object of intensive studies in the last three years.

The reports of Michel *et al.*[20] and of Akimitsu *et al.*[21] of the superconductivity in the Bi–Sr–Cu–O system with T_c from 7 to 22 K have triggered extensive investigations of superconducting materials that do not contain rare earths. A major increase in T_c to 120 K has been achieved by increasing the complexity of the composition (addition of calcium) to the Bi–Sr–Ca–Cu–O system.[22]

The next increase in the temperature of the superconducting transition has been achieved for Tl alkaline-earth cuprates[29,34–37] also free of rare earths. Three phases have initially been identified for this family of compounds and then become superconducting at 85, 95–108, and 114–125 K. At present eleven Tl compounds with different types of structure are known. Among the compounds listed in Table I certain structural types appear repeatedly only for Tl and Bi compounds with doubled Tl(Bi) layers and they are known as the 2201, 2212, 2223, and 2234 phases (these phases are identified by asterisks in Table I). The other compounds have each an individual structure type different in respect of the sequence, type of packing, number of layers per unit cell, and chemical composition of the layers (consisting of M, MO, MO_2, O_2, etc.). It should be pointed out that the chemical composition of the compounds listed in Table I becomes much more complex by introduction of various isomorphous impurities (almost all the chemical elements of the periodic systems have by now been tried as such impurities). If an isomorphous substitution of this type does not alter the type of structure, then a material of this type is not listed in Table I. The only exceptions to this rule are isostructural compounds in which one of the chemical elements of the host crystal is replaced completely (isostructural Tl and Bi compounds are listed separately).

The development of the chemistry of high-temperature superconductors and the search for new compounds have followed the path of increasing complication of the chemical composition and assembly of compounds whose structure combines fragments of the already known superconducting cuprates. Typical examples are $(Y_{1-x}Ca_x)Sr_2(Cu_{3-y}Pb_y)O_{7-\delta}$ (Ref. 42), $Tl_2Ba_2(Ln_{1-y}Ce_y)_2Cu_2O_{10}$ (Ref. 37), and (Tl, Pb) $M_2M'_2Cu_2O_9$ ($M = Sr_{1-x}La_x$, $M' = Ln_{1-y}Ce_y$, Ln = Nd, Gd, Y).[32] The first compound belongs, in spite of its complex chemical composition, to the 123 ($YBa_2Cu_3O_{7-\delta}$) structure type, the second includes in its structure fragments of the 2212 Tl phase and of $(Nd, Ce, Sr)_2CuO_4$, whereas the third contains fragments of the 1212 Tl phase and of $(Nd, Ce, Sr)_2CuO_4$. These phases are listed in Table I as individual structure types.

In the investigation of each of the systems in Table I the main tasks during the initial stages have been identification of the individual phases in a multiphase polycrystalline material and identification of those phases which are responsible for the superconductivity. The problem of growth of single crystals has increased in importance in subsequent stages of research. Bulk single crystals are essential for the understanding and development of various aspects of the study of the superconductivity. The most important of these aspects are: a) determination of the anisotropy of the properties such as the electrical conductivity, critical current, critical magnetic fields, etc.; b) comparison of the main characteristics of single-crystal and polycrystalline materials in order to identify the nature of the superconductivity and the role of defects, grain boundaries, twin boundaries, etc.; c) acquisition of reliable data on the crystal chemistry of superconducting materials with the aim of identifying the optimal paths in the search for new better superconductors.

The review given below provides an analysis of the methods and conditions of growth of single crystals of high-temperature superconductors.

The review covers the work carried out from the time of

 0038-5670/91/010036-38$01.00

TABLE I. Oxide semiconductors with $T_c \gtrsim 10$ K.

System	Compound	T_c, K	Ref.
Li—Ti—O	$Li_{1+x}Ti_{2+x}O_4$ ($0,35 \leqslant x \leqslant 0,2$)	13,7	[3]
Ba—Pb—Bi—O	$BaPb_{1-x}Bi_xO_3$ ($x \sim 0,25$)	13,4	[4—6]
Ba—K—Bi—O	$Ba_{1-x}K_xBiO_3$ ($x \sim 0,40$)	30	[7, 8]
La—Cu—O	$La_2CuO_{4+\delta}$ ($\delta \leqslant 0,08$)	15	[10]
La—Sr—Cu—O	$La_{2-x}Sr_xCuO_4$ ($0 \leqslant x \leqslant 0,15$)	36	[1, 11]
Nd—Ce—(Sr)—Cu—O	$Nd_{2-x}Ce_xCuO_4$ ($x \sim 0,15$)	24	[12]
(Nd = Pr, Sm)	$Nd_{2-x-y}Sr_xCe_yCuO_4$ ($x=0,41$, $y=0,27$)	28	[13—15]
Y—Ba—Cu—O	$YBa_2Cu_3O_{7-\delta}$ (123)	92	[2, 9, 16]
(Y = Ln)	$YBa_2Cu_{3,5}O_{7,5}$ (247)	40	[17]
	$YBa_2Cu_4O_8$ (248)	82	[18]
	1) $Bi_2(Sr_{1-x}Ca_x)_{1+n}Cu_nO_y$:		[5, 6, 19—28]
Bi—Sr—Ca—Cu—O	$Bi_2Sr_2CuO_6$ (2201) ($n=1$)	10 (20)	[20, 21]
	$Bi_2Sr_2CaCu_2O_8$ (2212, 4334) ($n=2$)	80—85	[22, 23]
	$Bi_2Sr_2Ca_2Cu_3O_{10}$ (2223) ($n=3$)	120	[24—26]
	$Bi_2Sr_2Ca_3Cu_4O_{12}$ (2234) ($n=4$)	<120	[27]
	2) $TlBa_2Ca_{n-1}Cu_nO_y$:		[29, 30]
Tl—Ba—Ca—Cu—O	$TlBa_2CuO_5$ (1201) ($n=1$)	10	
	$TlBa_2CaCu_2O_7$ (1212) ($n=2$)	78—80	
	$TlBa_2Ca_2Cu_3O_9$ (1223) ($n=3$)	110—120	
	$TlBa_2Ca_3Cu_4O_{11}$ (1234) ($n=4$)	120	
	$TlBa_2Ca_4Cu_5O_{13}$ (1245) ($n=5$)	106—118	
	$(Tl, Pb)Ba_2CaCu_6O_{15}$ (1256) ($n=6$)	70	[31]
Tl—Pb—Sr—La—Ln—Ce—Cu—O (Ln = Nd, Gd, Y)	$(Tl, Pb)(Sr, La)_2(Ln, Ce)_2Cu_2O_9$ (1222)	17	[32]
	3) $Tl_2Ba_2Ca_{n-1}Cu_nO_y$:		[29, 33—36]
Tl—Ba—Ca—Cu—O	$Tl_2Ba_2CuO_{4+\delta}$ (2201) * ($n=1$)	80	
	$Tl_2Ba_2CaCu_2O_8$ (2212) * ($n=2$)	108	
	$Tl_2Ba_2Ca_2Cu_3O_{10}$ (2223) * ($n=3$)	116—120	
	$Tl_2Ba_2Ca_3Cu_4O_{12}$ (2234) * ($n=4$)	102	
Bi—Sr—Ln—Cu—O	$Bi_2Sr_2(Ln, Ce)_2Cu_2O_{10}$ (2222)	23—30	[37]
(Ln = Sm, Eu, Gd)	$Bi_2(Sr, Ce)_2(Gd, Ce)_2Cu_2O_{10}$		[38]
Tl—Ba—Ln—Cu—O (Ln = Sm, Eu, Gd)	$Tl_2Ba_2(Ln_{1-x}Ce_x)_2Cu_2O_{10+\delta}$ (2222)		[37]
Pb—Y—Sr—Cu—O	$Pb_2Sr_2(Y, Ca)Cu_3O_{8+\delta}$	70	[39]
	$(Pb, Bi)_2(La, Sr)_2Cu_2O_6$	32	[40]
Ln′—Ln″—Ba—Cu—O (Ln′ = Nd, Sm, Eu Ln″ = Ce)	$(Ln_{1-x}Ce_x)_2(Ba_{1-y}Ln_y)_2Cu_3O_{10}$ ($\times 3 = Eu_6Ba_4Ce_2Cu_9O_x$)	25—43	[41]
Ln—Sr—Ca—Cu—Pb—O	$(Y_{1-x}Ca_x)Sr_2(Cu_{3-y}Pb_y)O_{7-\delta}$ (123) ($0,25 \leqslant x \leqslant 0,35$, $y=0,65$)	17	[42]

discovery of the high-temperature superconductivity (end of 1986) to the first half of 1990.

The work on the growth of single crystals peaked in the period from 1988 to the beginning of 1989; this was a time when the main chemical compositions of the high-temperature superconductors and their structures became known, and ways of preparing single crystals were determined. The next period saw a considerable fall in the number of original papers on the growth of single crystals. The search for various ways of preparing single crystals of high-temperature superconductors was followed by attempts to gain a deeper understanding of the growth mechanisms and to find ways of improving the quality of crystals by modernization of the existing methods.

This review of the methods and results of research and growth of single crystals begins with a brief description of the main types of structure of high-temperature superconductors, since the characteristic features of their structure (layer configuration, similarity of different types of structure, ease of twinning, presence of modulated structures, etc.) determine the difficulties encountered in the preparation of single crystals.

2. STRUCTURE OF HIGH-TEMPERATURE SUPERCONDUCTORS WITH $T_c > 10$ K

The structures of high-temperature superconductors studied intensively in recent years have proved to be derivatives of the well-known structural types of the ABO_3 perovskite or the K_2NiF_4 layer perovskite. The present review gives only a general description of the main principles of the way these compounds are built without an analysis of the structural details, such as distortions of the component polyhedra, occupancy of various positions, types of twinning, etc. A description of the main structural types will be given in the course of subsequent description necessary for a clearer understanding of the published material on the growth of single crystals of those high-temperature superconductors which are considered below. For each structure we shall identify the initial matrix, the sequence of the layers,

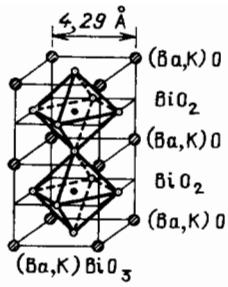

FIG. 1. Structure of $Ba_{1-x}K_xBiO_3$.

the principle of formation of a unit cell, and the type of the copper–oxygen polyhedra (in the case of cuprates).

$Ba_{1-x}K_xBiO_3$

In this case the initial matrix is monoclinic $BaBiO_3$, which is a semiconductor. Potassium replaces Ba isomorphously (Fig. 1) and solid solutions with compositions in the range $0.04 < x < 0.25$ are characterized by orthorhombic symmetry, whereas superconductivity is exhibited by solid solutions with $0.25 \leqslant x \leqslant 0.40$ and cubic symmetry.[8,7]

$BaPb_{1-x}Bi_xO_3$

The initial matrix is the same and replacement of Bi with Pb produces $BaPb_{1-x}Bi_xO_3$ solid solutions. The superconductor $BaPb_{1-x}Bi_xO_3$ was discovered in 1975 (Ref. 4). The superconducting properties are exhibited by solid solutions in a fairly narrow range of values of x: $0.05 \leqslant x \leqslant 0.25$; the maximum T_c corresponds to $x \sim 0.25$. The conductivity of the $x \sim 0.35$ material is metallic and the terminal member of the series $BaBiO_3$ is a semiconductor. The same type of structure is exhibited by the Sb-substituted variety, but in this case T_c is much lower: 3.5 K. Superconductivity is exhibited by the compounds with $x < 0.35$; the unit cell is tetragonal with $a = 6.028$ Å and $c = 8.511$ Å (Ref. 43). The symmetry of the polycrystalline materials with compositions $0.35 \leqslant x \leqslant 0.40$ is cubic with $a = 4.254$ Å ($x = 0.40$).

$La_{2-x}SrCuO_{4-\delta}$

The initial matrix is orthorhombic La_2CuO_4 which at temperatures above ~530 °C becomes tetragonal. The transition to the tetragonal phase is initiated also by partial La–Sr substitution ($La_{2-x}Sr_xCuO_4$, $x \leqslant 0.1$).[44,45] The tetragonal phase with $x \lesssim 0.25$ is a high-temperature superconductor and T_c is maximal (36 K) for $x = 0.16$. The temperature of the superconducting transition depends strongly on the strontium content and to a lesser extent on the oxygen stoichiometry. The compounds with these compositions belong to the structural type of the K_2NiF_4 layer perovskite and the structure is based on $[CuO_6]$ octahedra linked by shared vertices, whereas the orthorhombic distortion is due to rotation of these octahedra. The La and Cu atoms form metal–oxygen layers perpendicular to the c axis and alternating in the sequence ...LaO–CuO_2–LaO–LaO–CuO_2–...; each Cu atom is surrounded by six oxygen atoms (Fig. 2).

The $La_2CuO_{4+\delta}$ phase can also be a high-temperature superconductor if additional O atoms are introduced. The high-temperature superconducting phase $La_2CuO_{4+\delta}$ has the orthorhombic symmetry with the space group *Fmmm* (Refs. 10 and 46) in the range $0 \leqslant \delta \leqslant 0.08$ or *Cmca* (Ref. 47) for $\delta = 0.032$, in contrast to the orthorhombic semiconductor La_2CuO_4 with the space group *Bmab* (Ref. 10).

$Nd_{2-x}Ce_xCuO_4$

In the cuprate just discussed one of the elements of the host matrix is replaced with an element of lower valence (La^{3+}–Sr^{2+}, p-type conduction), whereas in the Nd system superconductivity appears for two substitution variants: by an element with a higher typical valence (Nd^{3+}–Ce^{4+}, n-type conduction) or with Ce^{4+} and Sr^{2+}, simultaneously. Transformation of the initial Nd_2CuO_4 matrix[13] is demonstrated in Fig. 2. A special feature of the original Nd_2CuO_4 structure is the presence of CuO_2 layers consisting of $[CuO_4]$ squares between which there are packets of Nd–O_2–Nd layers. The coordination number of copper in Nd_2CuO_4 is 4. In the Nd(Ce, Sr)-substituted cuprate the coordination number of Cu is 5. Three-layer Nd–O_2–Nd packets are located between the CuO_2 layers joined by the bases of the $[CuO_5]$ pyramids. The geometric dimensions of the cells are similar.[15]

$YBa_2Cu_3O_{7-\delta}$ (123 phase)

Separation of the positions occupied by the Ba and Y atoms in the perovskite sublattice triples the unit cell of $YBa_2Cu_3O_x$ along the c axis (Fig. 3). Depending on the oxygen content x and on temperature, we can have two polymorphic modifications of the 123 phase: tetragonal in the range $x \lesssim 6.5$ and orthorhombic for $6.5 \lesssim x \lesssim 7$. The ortho-

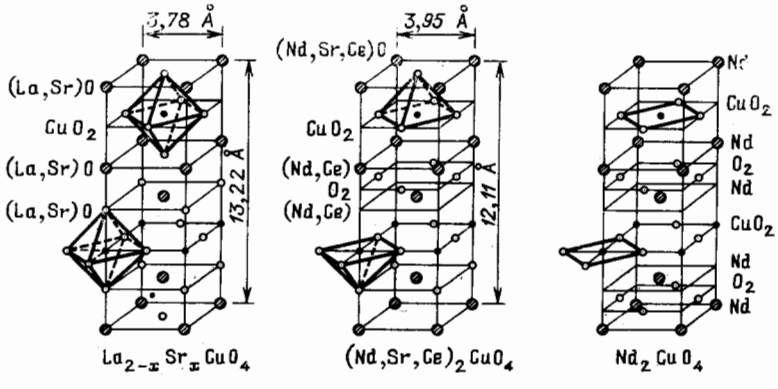

FIG. 2. Structure types of $La_{2-x}Sr_xCuO_4$, $(Nd, Sr, Ce)_2CuO_4$, and Nd_2CuO_4 based on the data reported in Refs. 1, 11, and 15.

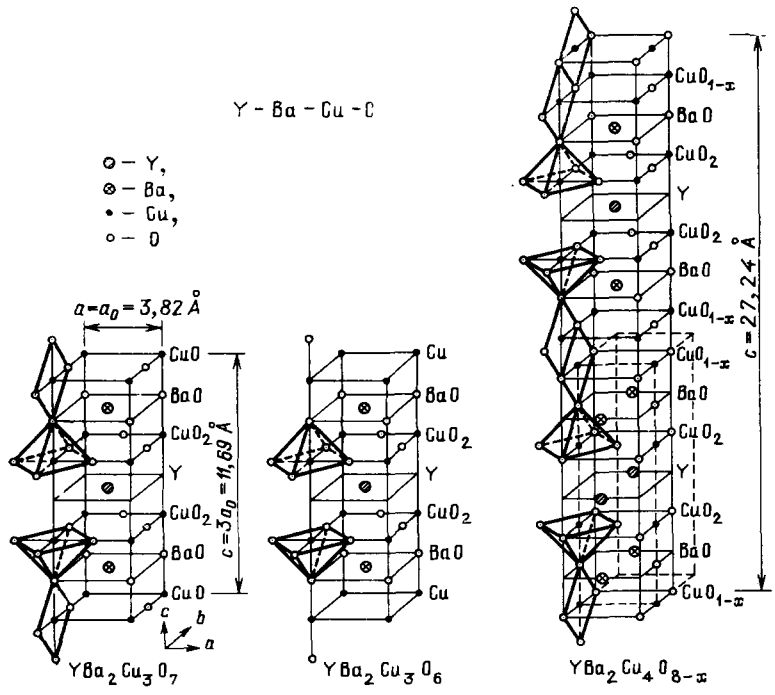

FIG. 3. Structure types of Y–Ba cuprates.[16-18]

rhombic ($Pmmm$) phase is a high-temperature superconductor and a reduction in the number of the oxygen atoms reduces the degree of the orthorhombic distortion, so that the structure becomes tetragonal ($P4/mmm$) at $x \sim 6.5$. The oxygen-deficient tetragonal phase is a semiconductor. The structural phase transition is of the order–disorder type. Heating above 540 °C at a pressure up to 1 atm initiates the loss of oxygen so that at 900–950 °C the oxygen content is $x = 6$. The higher is the external pressure of O_2, the higher is the temperature of the transition from the orthorhombic to the tetragonal phase.[48] According to Ref. 49, a reversible phase transition takes place at 575 °C. By analogy with the L–Sr cuprate, the structural phase transition in the Y–Ba cuprate occurs when the number of carriers changes: the value of x in $La_{2-x}Sr_xCuO_4$ increases on transition from the orthorhombic to the tetragonal symmetry, whereas δ decreases on transition of $YBa_2Cu_3O_{7-\delta}$ from the tetragonal to the orthorhombic phase. The coordination number of copper is 5, representing a pyramid with its base facing a Y layer.

The general formula is $YBa_2Cu_3O_{7-\delta}$, where $0 \leqslant \delta \leqslant 1$, and the compounds in question form a homologous series whose terms differ in respect of the oxygen content in the Cu–O chains along the b axis (Fig. 3).[50] For all the variations of the oxygen content the Cu(2) atom always has the coordination number 5 (pyramid), whereas the coordination number of Cu(1) is $4d$ or 2 (square or dumbbell). The CuO_2 layers alternate with the layers of Y.

The compound $YBa_2Cu_3O_{7-\delta}$ is the base of the phases differing in respect of the number of additional Cu layers.[17,18] In the 124 phase the additional CuO_2 layer is formed by a shift of the 123-type subcell by 1/2 along the b axis (Fig. 3) and the unit cell of the 124 phase has the parameter $c = 27.24$ Å.

The 12(3, 5) or the 247 compound has a unit cell consisting of four blocks of the 123 type alternating along the b axis in the following sequence: 123 block → shift by 1/2 along the b axis → translation along c → shift by 1/2 along $-b$.

Bi and Tl high-temperature superconductors

Historically the first discovered were the Bi superconductors and this was followed by the discovery of the Tl materials, giving rise to two homologous branches with single and paired TlO layers and with gradually increasing numbers of the Cu–O layers.

The layer structures containing Bi and Tl can be described by the general formula $(A^{III}O)_xA^{II}_2Ca_{n-1}Cu_nO_{2n+2}$, where A^{III} = Tl, Bi, Bi + Pb, Bi + Tl, Tl + Pb; A^{II} = Ba, Sr. These tetragonal compounds exhibit, as already mentioned, two homologous series with $x = 1$ or 2 for Tl and with $x = 2$ for Bi (Ref. 51). The structural types for the $x = 1$ series formed by transformation of the initial $TlBa_2CuO_5$ matrix are shown in Fig. 4. The structures consist of perovskite-like blocks containing one, two, or three CuO_2 layers separated by one or two TlO layers. The Cu coordination polyhedron in the terminal member of the $TlBa_2CuO_5$ series is the octahedron, whereas introduction of additional Cu–O layers (Fig. 4) produces a packet of two CuO_2 layers joined by the bases of $[CuO_5]$ pyramids separated by a layer of Ca atoms (1212 structure). A further increase in the number of CuO_2 layers (and also of Ca layers) results in a structure where the additional layers with the Ca–CuO_2–Ca-... sequence are located between the same CuO_2 layers joined by the bases of the $[CuO_5]$ pyramids. The unit cell "spreads apart," while the parameter a (3.85 Å) remains the same and the parameter c gradually increases: $c = 6.3 + 3.2$ Å, which is true of the structures with a single Bi (or Tl) layer.[51]

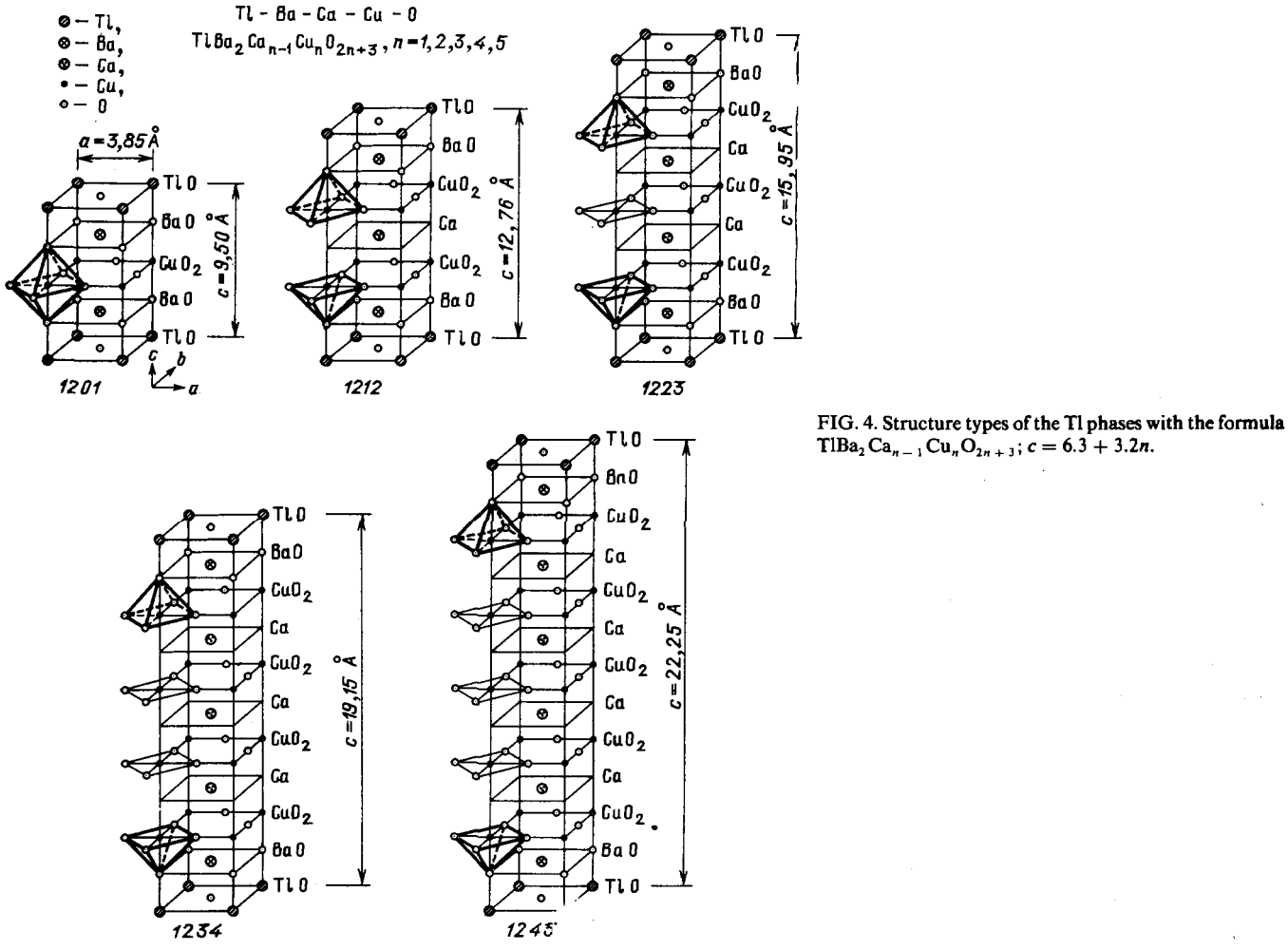

FIG. 4. Structure types of the Tl phases with the formula $TlBa_2Ca_{n-1}Cu_nO_{2n+3}$; $c = 6.3 + 3.2n$.

Attempts to modify further the structures based on Tl cuprates with single layers have led to the discovery of a new Tl 1222 family (Table I), where the repeated block consists of consecutive TlO–MO–CuO_2–M′–O_2–M′–CuO_2–MO–TlO layers, where $M = Sr_{1-x}La_x$ and $M' = La_{1-y}Ce_y \times (Ln = Nd, Gd, Y)$. The tetragonal cell parameters of such phases are $a = 3.846$ Å, $c = 29.436$ Å [composition $Tl(Sr_{0.6}La_{0.4})_2(Gd_{0.85}Ce_{0.15})_2Cu_2O_z$] or $a = 3.848$ Å, $c = 29.413$ Å [composition $(Tl_{0.5}Pb_{0.5})(Sr_{0.8}La_{0.2}) \times (Gd_{0.85}Ce_{0.15})Cu_2O_z$].[32] In the structure of these phases we can readily identify blocks typical of the Tl phases of the Tl-1212 type and of Ce- or Sr-substituted neodymium cuprate (M′–O_2–M′ networks).

The compounds with doubled Tl layers and the formula $Tl_2Ba_2Ca_{n-1}Cu_nO_{2n+4}$ also form a homologous series in which each consecutive term can be obtained formally by the addition of $CaCuO_3$ (layer of CuO_2 and layer of Ca) and the number of layers deduced using electron microscopy can reach six (Refs. 29 and 52–54). Phases with a similar structure form also in the Bi–Sr–Ca–Cu–O system.

In the simplest structure of doubled Bi (or Tl) layers (2201 structure) the Cu–O layers consist of distorted [CuO_6] octahedra, exactly as in $La_{2-x}Sr_xCuO_4$. An increase in the number of Cu–O layers in a cell is accompanied by an increase in the number of Ca layers which act as spacers adjoining the CuO_2 layers formed by the bases of the CuO_5 pyramids (2212 structure), by analogy with the compound $YBa_2Cu_3O_{7-\delta}$ (Fig. 5).

The compound 2223 retains two such pyramidal layers, but between them there is an additional layer joined by the planar CuO_4 squares (copper with the coordination number 4), separated from the pyramidal layers of the CuO_2 composition by the Ca layers. A further increase in the number of the Cu–O layers should result in a compound with the composition characterized by 2234 ratio of the main elements. Such a compound has not yet been prepared in the form of single crystals, but we may assume that its structure is similar to that of 2223, except that the central CuO_2 layer is replaced by two such layers separated by planes containing Ca atoms and O vacancies,[56] and the unit cell parameters are $a = 3.853$ and $c = 41.98$ Å (Ref. 57).

In this family of compounds the unit cells are constructed as a result of displacement of a repeated set of planar networks by $\frac{1}{2}(a + b)$ and increasing the number of the Cu–O layers, which increases the parameter c: from 24.65 Å (Bi–2201) to 30.69 Å (Bi–2212), and 36.8 Å (Bi-2223) in the case of the Bi phases;[19] from 29.25 Å (Tl-2212) to 36.26 Å (Tl-2223), and 41.98 Å (Tl-2234) in the case of Tl phases.[57]

The similarity of the structural modifications of the single-layer (Tl) and double-layer (Bi, Tl) cuprates accounts for the ease of mutual intergrowth and for the high sensitiv-

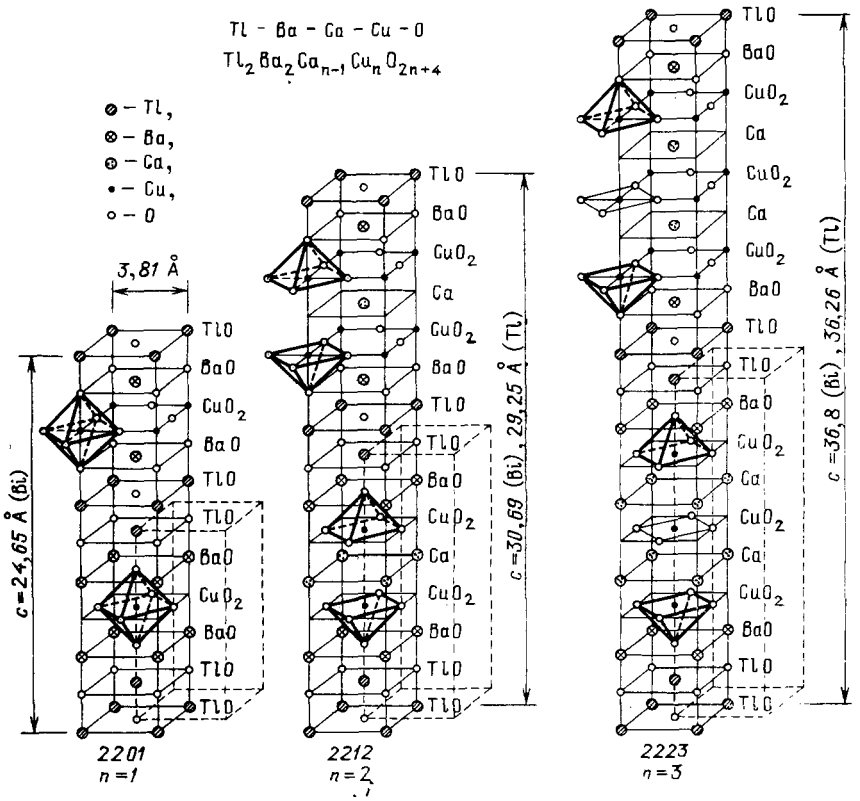

FIG. 5. Structures of Tl(Bi) phases with the formula $Tl_2Ba_2Ca_{n-1}Cu_nO_{2n+4}$; $c = 16.4 + 6.4n$ (based on the data from Refs. 19, 55, and 56).

ity to the conditions during synthesis or subsequent treatment resulting in a disturbance of the packing sequence of the individual fragments of the structure. The problem is further complicated by the existence of modulated structures of these compounds.

There is a general tendency for T_c to increase with the number of Cu–O layers, at least up to $n = 4$ in the case of the structures with one Tl layer, followed by a fall of T_c for $n = 5$.

$Pb_2Sr_2ACu_3O_{8+\delta}$

This new family of the layer cuprates with a high T_c and with the general formula $Pb_2Sr_2ACu_3kO_{8+\delta}$ was described in Ref. 39. According to Ref. 58, the anion A can be Y, Ln + Sr, or Ln + Ca/Sr.

The perovskite-like cell has the dimensions $a = b = 2a_0$ and $c = 4a_0$, where a_0 is the unit cell parameter of perovskite.[40] The parameters of the c-centered cell with the orthorhombic distortion[58] are as follows: $a = 5.40$ Å, $b = 5.43$ Å, $c = 15.74$ Å.

The structure of these compounds differs from the structures of the Y–Ba–Cu–O, Bi–Sr–Ca–Cu–O, and Tl–Ba–Ca–Cu–O systems considered above in respect of the composition of the layers separating the CuO_2–Y–CuO_2 packets. These layers represent alternate metal-oxide layers and a layer of Cu atoms in the following sequence: ...–SrO–PbO–Cu–PbO–SrO–... . The Pb atoms are distributed in coordination polyhedra in the form of pyramids (Fig. 6a).[58,59]

$(Ln_{1-x}Ce_x)_2(Ba_{1-y}Ln_y)_2Cu_3O_{10-\delta}$

This new family of superconducting cuprates was discovered in 1989 (Ref. 41). The structure retains the characteristics of the known types: the layer configuration is retained, the parameter is $a \sim 3.8$ Å, and the copper atoms have teristics of the known types: the layer configuration is retained, the parameter is $a \sim 3.8$ Å, and the copper atoms have the coordination numbers 6 (octahedra) and 5 (pyramids). The Cu–O layers are interleaved with the BaO layers, while the central layer of such a CuO_2–BaO–CuO_2–BaO–CuO_2 packet exhibits a random occupancy of the positions by the oxygen atoms. The large rare-earth cations form a fragment already encountered in Nd_2CuO_4 and $Nd_{2-x}Ce_xCuO_4$: there are two layers of rare-earth atoms separated by a layer of oxygen atoms. The unit cell contains two such blocks [CuO_2–BaO–CuO_{2-x}–BaO–CuO_2]–[(Ln, Ce)–O_2–(Ln, Ce)] as shown in Fig. 6b; the second block was linked to the first by the $\frac{1}{2}(a + b)$ translation.

An analysis of the composition and structure of the compounds with the superconducting transition temperature $T_c \gtrsim 30$ reveals the following series of features exhibited by all the known phases.

1. Practically all the superconducting materials with $T_c \gtrsim 30$ K are nonstoichiometric phases, which are frequently metastable under normal conditions. These phases are characterized by a nonstoichiometry in respect of the cations (substition of a rare-earth element Ln with an alkaline earth and the Ln^{3+}–Ln^{4+} replacement) as well as by the oxygen nonstoichiometry. The random disordering of the original matrices and the change in the carrier density usually result from introduction of isomorphous impurities during growth and these impurities have a typical valence state different from the host ions (heterovalent isomorphism of the La–Sr, Ba–K, Nd–Ce, Nd–Sr, etc. type) or such disordering is due to introduction of an excess number of the O atoms by special treatments after growth.

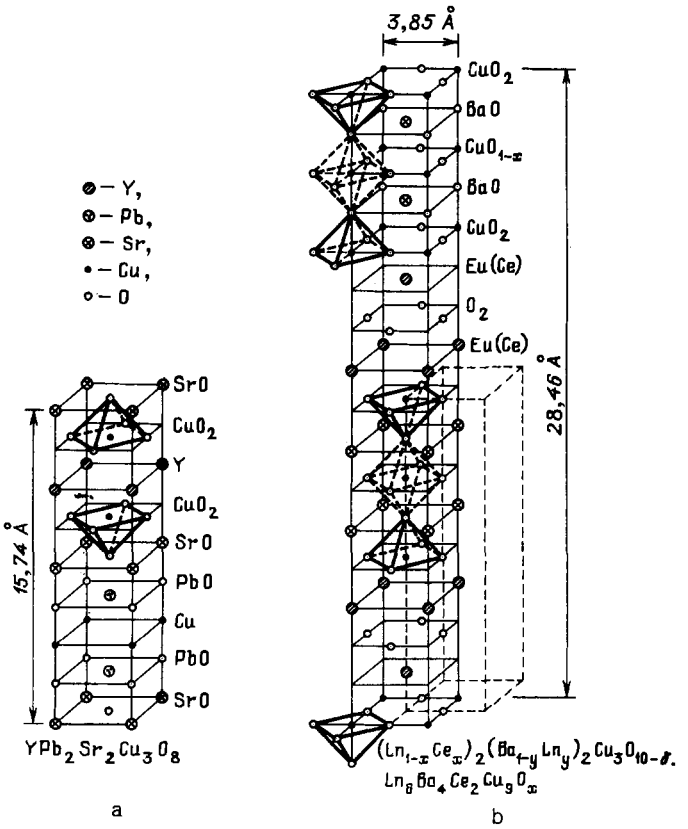

FIG. 6. Structures of: a) $YPb_2Sr_2Cu_3O_8$ (Ref. 58); b) $Yb_6Ba_4Ce_2Cu_9O_x$ (Ref. 41).

2. All the compounds have layer perovskite-like structures with different numbers and different sequences of metal–oxygen layers. The structures permit isomorphous substitutions within fairly wide limits without a change in the structure type. Modification due to changes in the structure type occurs as a result of addition of new layers of the M, MO, CuO_2, CuO_{1-x}, or O_2 type, where M represents an element with one or more (two, three, four) charges. The crystallographic parameter c of such structures can reach ~ 50 Å.

3. All the compounds with $T_c \gtrsim 30$ K belong to the cuprate class, i.e., the main element has the mixed valence 1–3, has in crystals the local environment consisting of two, four, five, or six oxygen atoms, and is a typical metal. The complex superconducting cuprates with $T_c = 10$ K known up to June 1990 can be described by 21 structure types of perovskite-like compounds.

4. All the high-temperature superconducting compounds contain an element capable of forming perovskite compounds (Ca, Sr, Ba, K), i.e., able to form O_2^{2-} pairs.

3. GROWTH OF HIGH-TEMPERATURE SUPERCONDUCTING SINGLE CRYSTALS

The search for possible ways of growing single crystals began practically immediately after the discovery of the high-temperature superconductivity by Bednorz and Müller.[1] The following methods have been used to obtain bulk single crystals of high-temperature superconductors:

solid-phase synthesis,
crystallization from stoichiometric and nonstoichiometric melts,
partial melting of nonstoichiometric compositions,
Bridgman method,
zone melting,
pedestal method,
Czochralski method,
crystallization from a molten solution (melting of stoichiometric and nonstoichiometric charges in the presence of a mineralizer,
partial recrystallization of glass,
hydrothermal synthesis.

The first attempts to prepare single crystals were made by *solid-phase synthesis* involving growth of individual grains of a ceramic under certain thermal conditions characterized by considerable duration of the process; the stoichiometric composition has been usually the starting point, the temperatures have been close to the melting point, and this has been followed by prolonged annealing.

The advantage of this method is its simplicity, the absence of a crucible (partial dissolution of the crucible results in deterioration of the quality of the grown crystals), lack of any stringent requirements in respect of temperature or duration of the process, and fairly low temperatures (lying below the melting point or the temperature of decomposition).

The shortcomings of the method are the inability to control the process, the low growth rates because of the slow diffusion in the solid phase, the long duration of the process, the small dimensions (usually up to 500 μm) of the resultant crystals, and the difficulties encountered in separating these crystals (without damage) from the surrounding aggregate.

There are two ways of using the method of solid-phase synthesis in growing single crystals. The first is the direct

synthesis by heating a mechanical mixture of oxides or of salts which readily dissociate during heating and contain the necessary components. The second way involves annealing of quenched melts (both stoichiometric and nonstoichiometric in relation to the required phase) at certain temperatures and in various atmospheres.

In the second case the size of the resultant crystals is slightly greater than that obtained in the first case. Solid-phase synthesis can be applied to any of the investigated oxide superconductors; it was used for the first time to prepare Y–Ba and La–Sr cuprates and the details of this process will be considered later in a discussion of the crystallization of different types of high-temperature superconductors.

This group of methods for the preparation of single crystals includes *partial recrystallization of glass* formed as a result of fast quenching, for example, in the Bi–Ca system.[60]

Since melting of the majority of high-temperature superconducting compounds is accompanied by decomposition, the method of crystallization from stoichiometric melts is unacceptable for this class of materials (at least under normal pressures).

For example, the preparation of cuprates of the 123 type from the melt is prevented by peritectic decomposition into Y_2BaCuO_5 and a copper-rich but yttrium-depleted liquid phase. Crystallization from almost-stoichiometric melts can be used in the case of the Bi system because of the high stability of the melts and because of the polytypism of the resultant cuprates. It is usual to employ the growth of melts by slow cooling of certain compositions which in practically all cases produces crystals with other than the initial compositions.[34] Direct melting (*pedestal method and laser heating*) has been used to prepare fiber crystals of the Bi system[28] but this method has failed to give positive results in the case of the La–Sr and Y–Ba cuprates because of their strong dissociation before melting and the loss of CuO, although single crystals of these compounds have indeed been obtained by this method.[28,61,62]

The characteristic features of the chemical composition and structure of the cuprate superconducting materials are such that for the majority of them it is *a priori* clear that the main growth method is *the crystallization from nonstoichiometric melts*, which is a variant of the crystallization from a molten solution when the melt does not contain any additional elements that are not components of the required compound. This method has been used in the preparation of both La–Sr, Y–Ba, as well as Bi and Tl cuprates. The method has been used most extensively in the growth of 123 single crystals.

The growth occurs during slow (usually multistage) reduction in the melt temperature or under isothermal conditions or in the presence of a vertical (or a horizontal) temperature gradient in the furnace. The imagination of the experimentalists has created a great variety of modifications of this method (seeding from above, introduction of "foreign" seeds, pulling of a crystal, growth in specially created cavities in a thin layer of the melt, etc.; horizontal or vertical movement of the heater or crucible; different types of heaters, and so on). Examples of ways of growing single crystals of high-temperature superconducting materials by this method will be given later.

One of the variants of the method of crystallization from nonstoichiometric melts is known as *the partial melting*, in which crystals are grown in quasiclosed cavities formed as a result of evolution of gases (O_2) due to dissociation of CuO or because of forced introduction of gas into a ceramic.[62,63]

The many variants of *directional crystallization* are used widely in the preparation of high-temperature superconducting materials (they include the method of zone melting or zone recrystallization, with horizontal or vertical variants, crystallization in the presence of a temperature gradient, etc.). The use of these techniques in the growth of single crystals of nonstoichiometric compounds employing in congruent melting creates textured samples and in the case of some systems it is possible to separate single crystals from such samples.

In the simplest case the directional crystallization of a small volume of a liquid of compositions within the limits of the peritectic horizontal results in a continuous change in the composition of the liquid and solid phases: when a phase *A* crystallizes, the composition of the liquid phase becomes richer in a component *B* so that when the solution reaches the peritectic point, crystallization of the phase *AB* begins and this in turn results in enrichment of the melt with the component *A* and its subsequent crystallization. The resultant ingot then consists of several phases.[64]

The method of a floating zone or directional solidification of nonstoichiometric melts has been used in the case of the La–Sr–Cu–*O* system and has produced oriented eutectoid structures composed of alternate Cu_2O and $La_{10.8}Sr_{0.2}CuO_4$ fibers.[65] The floating zone method with laser heating has been used successfully to grow Bi–Sr–Ca cuprate crystals.[66]

The molten solution method has been used, in its classical variant, most frequently in the crystallization of Bi–Ca superconductors. Good results have been obtained employing, as mineralizer solvents, alkali chlorides[5,67] or their eutectic (KCl + NaCl) mixtures[67,68,5] or Sr–Ca carbonates.[67] Fluoride solvents producing CuO crystals and stable fluoride complexes of Ba (or Sr) are retained in the liquid phase.[69] The binary KCl + NaCl system with the melting point of 658 °C is promising also for the preparation of $Ba(Pb,Bi)O_3$ single crystals.[70] The following solvents have also been tested but have failed to give positive results: Na_2MoO_4, KF, Bi_2O_3 (Ref. 71), lithium borates $Li_2B_4O_7$ and $Li_2B_2O_4$, barium borates BaB_4O_7 and BaB_2O_4, B_2O_3–PbO mixtures, etc.[79,72,73]

The hydrothermal method employing typical aqueous solvents has been found useful only for $BaPb_{1-x}Bi_xO_3$ bismuthates,[74] whereas cuprates decompose in the presence of water or aqueous solutions.[75] One of the possible ways of developing this method involves the use of nonaqueous (organic) solvents at moderate temperatures and pressures. In spite of the great similarity of high-temperature superconducting cuprates—one parent structure (pervoskite), presence of alkaline earth metals, nonstoichiometry of the compositions—each material will be shown to need an individual approach in the development of the method for preparing the materials in the form of single crystals. The main problems are then the characteristic features of the structure of these cuprates (layer nature of the structure, presence of a superstructure, tendency to twinning, presence of cleavage planes, phase transitions) and also the characteristic features of the chemical composition and behavior (oxygen nonstoichiometry, mixed valence of the main elements,

higher activity, incongruent melting). The *problem of an inert container* is of special importance. Practically all the currently used crucible materials—Ni, Pt, MgO (Ref. 69), Au, ZrO_2:Y, $MgAl_2O_4$, SiO_2 (Ref. 77), (Zr, Ti)–SnO_2 (Ref. 78), ZrO_2, ThO_2 (Ref. 76)—react in the molten state resulting in partial dissolution of the crucible materials, which lowers the quality of the resultant crystals and reduces T_c. The weakest interaction with the crucible material is reported for Au, Pt, MgO, ThO_2, and (Zr, Ti)–SnO_2. Attempts have also been made to use CuO (Ref. 79) and Y_2O_3 crucibles in the preparation of $YBa_2Cu_3O_{7-x}$ crystals by the partial melting method.

Microprobe x-ray spectroscopic investigations of the chemical composition of the regions of a melt adjoining the walls of a crucible made of an oxide material have revealed the presence of $BaAlO_2$, $BaZrO_3$, and $BaSnO_3$ with Y and Cu impurities. In the case of Pt crucibles the undesired result is the formation of platinate cuprates $Ba_4(Pt,Cu)O_6$ (Ref. 80), $Y_2Ba_3Cu_2PtO_{10}$ (Refs. 69, and 80–83), $Y_2Ba_2CuPtO_8$ (Ref. 84), Sr_4PtO_6 (Ref. 85), $Sr_{1.75}Ca_{1.5}Cu_{0.5}PtO_x$ (Ref. 86), and $Ca_{5.7}Sr_{2.2}CuPt_{0.7}O_x$ (Ref. 87). The refractory oxides based on Y_2O_3 (Ref. 88), are promising materials for the crucibles which would prevent contamination of the melt during growth of 123 single crystals.

3.1. Single crystals based on La_2CuO_4

3.1.1. Phase diagram of the La_2O_3–CuO system

Among the currently known structural types of high-temperature superconductors which exhibit the transition at $T_c > 30$ K the $(La,M)_2CuO_4$ (M = Ba, Sr) composition was the first to be prepared and it proved subsequently the easiest to grow in the form of single crystals. This is primarily due to the relative simplicity of its chemical composition, which is La_2CuO_4, where Ba and Sr are in fact dopants, and it is also related to the nature of the phase diagram of the La_2O_3–CuO system which makes it possible to crystallize La_2CuO_4 from a nonstoichiometric melt with an excess of CuO.

The very first reports of growth of $(La,Sr)_2CuO_4$ single crystals have resulted in identification of the ranges of the compositions with a section of the liquidus where stable crystallization of this compound is possible. Detailed investigations of the pseudobinary La_2CuO_4–CuO and $(La,Sr)_2CuO_4$–CuO systems are reported in Refs. 89–93: they were carried out employing a variety of methods, including differential thermal analysis, x-ray phase analysis, visual polythermal method, etc. These experiments have been carried out both in air and in an oxygen stream.

Figure 7 gives the phase diagram of the La_2CuO_4–CuO system based on the data of different authors[89,91,92] and reflecting most fully the chemical processes in this system. The compound La_2CuO_4 decomposes on melting at 1375 °C and the system is characterized by a eutectic with the coordinates 88 mol.% CuO and 1050 °C (Ref. 91). Somewhat different coordinates of the eutectic are however given in Refs. 93 and 94: 91 mol.% CuO, 1007 ± 5 °C and 94 mol.% CuO, 1047 ± 10 °C. In the region of primary crystallization of copper oxides the liquidus curve has an inflection at 1300 °C, corresponding to the CuO–Cu_2O transition.[93] The difference between the phase diagrams plotted on the basis of the experimental data obtained in air and those based on the results obtained in an oxygen atmosphere reduces to an increase in the temperature of the eutectic by about 35 °C and a shift of the eutectic point by about 1% in the direction of less CuO (Ref. 91). The addition of strontium oxide reduces the eutectic temperature by ~15 °C and this reduction is a linear function of the proportion of strontium (Fig. 7d).

This system always contains $LaCuO_3$, but usually this is not revealed by differential thermal analysis (it was discovered by this method only in the study reported in Ref. 89), and its crystallization is induced by slow cooling (< 1 °C/h), as demonstrated in Ref. 89. Therefore, the use of different methods in the construction of phase diagrams is the obvious reason for the discrepancies between the results obtained by different authors. One should stress also another feature associated with the real presence of monovalent copper in the system. The compound Cu_2O is absent from the diagrams in Fig. 7, although the results of many investigations including those reported in Refs. 89, 81, and 82 indicate that this oxide is always present in quenched droplets of the melt when they crystallize in air. Apparently, we cannot exclude the possibility of appearance of this compound also in an oxygen atmosphere at elevated temperatures, because in practice the La_2CuO_4–CuO phase diagram changes from pseudobinary to pseudoternary and the system is more complex requiring a special analysis. Attention has been given to this point in more recent papers (see, for example, Refs. 93 and 95). Figure 7e is the isobaric phase diagram of the La_2O_3–CuO–$CuO_{0.5}$ system at a partial pressure of 0.021 MPa (Ref. 95). The 1585 K isotherms correspond to the $La_2CuO_4 \rightarrow La_2O_3 + L$ reaction (L is the liquid phase) accompanied by partial dissociation of CuO in the melt. Invariant points (squares in Fig. 7e) have been found at 1278, 1298, and 1585 K under quaternary equilibrium (S + S + L + G) conditions, where S, L, and G represent the solid, liquid, and gaseous phases because of a reduction in the number of the degrees of freedom by one under isobaric conditions. The temperature 1585 K corresponds to the peritectic $La_2O_3 + L \rightarrow La_2CuO_4$, 1298 K corresponds to the eutectic formed from the CuO and Cu_2O phases, 1278 K to the eutectic of La_2CuO_4 and CuO, and 1263 K to the ternary eutectic formed from the phases La_2CuO_4, CuO, and Cu_2O observed when the CuO oxide content is below 50%.

The La–Sr–Cu–O system includes binary compounds $La_{n+1}Cu_nO_{3n+1-y}$, $n \leqslant 2$, $Sr_{14}Cu_{24}O_{41}$ and a ternary compound $La_{8-x}Sr_xCu_8O_{20-y}$, $1.28 \leqslant x \leqslant 1.92$ (Refs. 96 and 97).

The phase diagram was investigated[96] below the solidus line at 950 °C and the oxygen pressure 1 bar. A new ternary compound $La_{1+x}Sr_{2-x}Cu_2O_{5.5+\delta}$, $0.05 \leqslant x \leqslant 0.15$ was identified and its unit cell parameters were found to be $a = 3.80$ Å $= a_{per}$, $b = 11.48$ Å $= 3a_{per}$, and $c = 20.23$ Å $= 5a_{per}$. Similar structures are formed by rare-earth elements Sm, Eu, and Gd. The other ternary compounds $La_{8-x}Sr_xCu_8O_{20-\delta}$ and $La_{2-x}Sr_{1+x}Cu_2O_6$ are found in the intervals $1.6 \leqslant x \leqslant 2.0$ and $0.05 \leqslant x \leqslant 0.15$.

X-ray diffraction characteristics of the compounds which can be obtained in the La_2O_3–SrO–CuO (Cu_2O) system are listed in Table II.

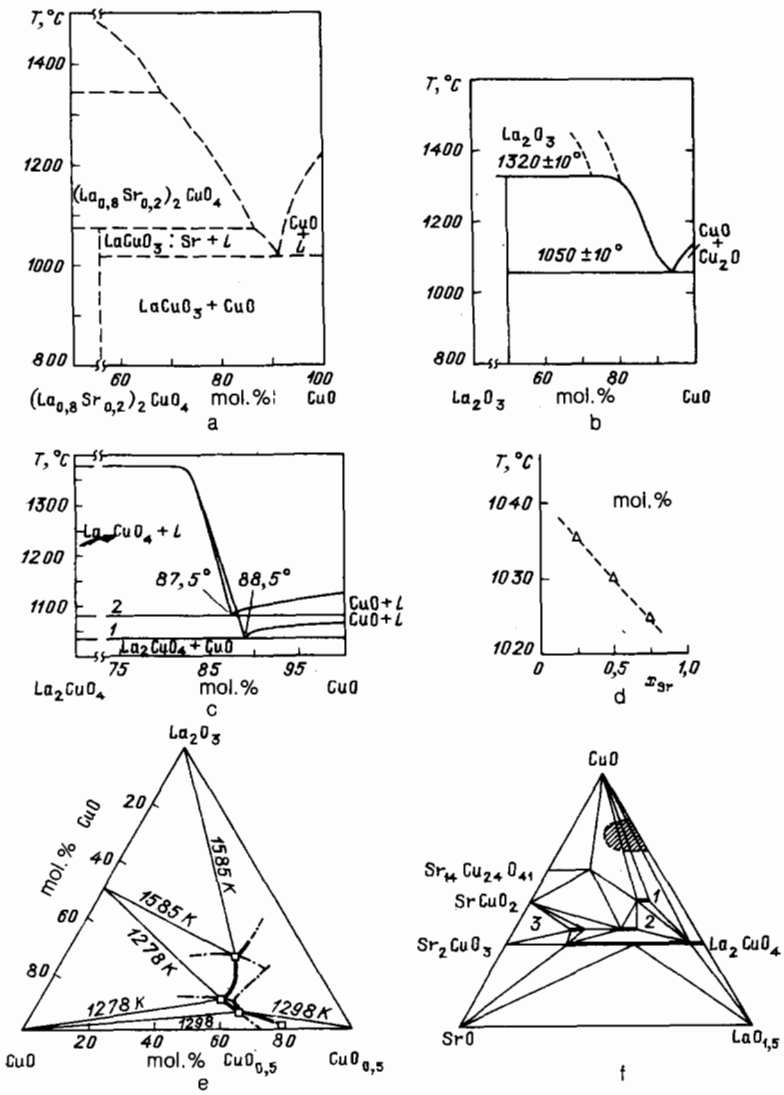

FIG. 7. Phase diagrams of the systems based on lanthanum and copper oxides: a) Ref. 89; b) Ref. 92; c) Ref. 91 (1–in air, 2–in oxygen); d) dependence of the eutectic temperature on the strontium content (Ref. 92); e) phase diagram of the La_2O_3–CuO–Cu_2O system (cf. 95); f) subsolidus phase diagram of the La_2O_3–SrO–CuO system at 950 °C and P_{O_2} = 1 bar (Ref. 96), where the thick lines identify the regions of formation of solid solutions (*1*–$La_{8-x}Sr_xCu_8O_{20-\delta}$, $1.6<x<2.0$; *2*–$La_{2-x}Sr_{1-x}Cu_2O_{6-\delta}$, $0.05<x<0.15$; *3*–$La_{1+x}Sr_{2-x}Cu_2O_{5.5+\delta}$, $0.05<x<0.15$; the shaded region in Fig. 7f shows the initial compositions used by the authors of Ref. 80 to grow $La_{2-x}Sr_xCuO_4$ single crystals.

3.1.2. Growth of $La_{2-x}Sr_xCuO_4$ single crystals

The La_2O_3–CuO and $La_{2-x}Sr_xCuO_4$–CuO phase diagrams[97,98] demonstrate decomposition of lanthanum cuprate of the peritectic type and formation of the eutectic lanthanum cuprate in the form of copper oxide. This is the reason for the use of copper-rich melts when lanthanum cuprates are grown.

Single crystals of lanthanum cuprate, both pure and

TABLE II. X-ray diffraction data for crystalline phases formed in the La_2O_3–SrO–CuO system.

Composition	Unit cell parameters, Å			Space group	Ref.
	a	*b*	*c*		
$SrCuO_2$	3,56	16,32	3,92	*Cmcm*	[98]
$SrCu_2O_2$	5,48	—	9,82	$I4_1/amd$	[99]
Sr_2CuO_3	12,68	3,91	3,48	*Immm*	[100]
$LaCuO_2$	6,11, α=36,50°	—	—	$R\bar{3}m$	[101]
$LaCuO_3$	5,431, α=60,51°	—	—	*R*3*c*	[102]
$La_4Sr_3O_9$	11,657	7,348, β=115,6°	13,471	*Cc*	[103]
La_2CuO_4	5,363	5,409	13,17	*Cmca*	[104]
				$I4/mmm$	[105]
$La_{1+x}Sr_{2-x}Cu_2O_{5,5+\delta}$ $(0,05<x\leqslant 0,15)$	3,80	11,48	20,23		[95]

those with partial La–Sr substitution, can be prepared quite readily either from nonstoichiometric melts of the La–Sr–Cu–O system or in the presence of typical solvents used in the method of crystallization from a molten solution (PbO, $Li_4B_2O_5$).[108–110] Single crystals are prepared either by slow cooling of the melts or by pulling a seed or by seeding with Pt rods or by other methods (Table III).

A typical process is as follows: a charge is prepared by sintering in air (600–1000 °C); if the charge is stoichiometric relative to the compound to be grown, a solvent is added to it (usually CuO); after mixing, the crucible (usually made of platinum) is heated to a temperature of the order of 1150 °C (in the case of La and La–Sr cuprates; or to 1350 °C (La–Ba cuprate). After holding this temperature for some time, the subsequent steps can vary: they may involve slow cooling,[110,112,113] quenching,[71] seeding with a platinum wire,[80,82,115,128] and pulling.[110,114,118]

The strontium (barium) concentration in the crystals is always less than in the original charge [$x_1 = 0.12$, $x_2 = 0.15$ (Ref. 114), $x_1 = 0.05$, $x_2 = 0.15$ (Ref. 90), where x_1 and x_2 are the concentrations of strontium in the solid and liquid phases, respectively] and it depends on the strontium content in the system. In the range $0 < x < 0.1$ the distribution coefficient is close to 0.75 (Ref. 123). Other data suggest that during growth of the Sr-substituted cuprate about ~30% of the strontium present in the melt is incorporated into the growing crystals[92] or it may be even as low as 10% in the crystal.[110]

Larger crystals are sometimes formed by seeding from above or "mechanically" by immersion of a Pt rod kept at a lower temperature or by introducing a seed consisting of, for example, the isostructural compound $LaSrFeO_4$ (Ref. 107) or a plate of a compound of similar composition formed from a molten solution.[111] Nucleation of crystals occurs on the melt surface at 1200 °C (Refs. 92 and 111). When a crystal becomes sufficiently large and can no longer be supported by the surface tension forces, it sinks to the bottom where it continues to grow. At ~1100 °C it is possible to separate crystals from the fairly viscous melt by means of a Pt grid.[92] In other investigations a solution has been decanted at a temperature of 1100 °C (Ref. 113).

Large La_2CuO_4 and $La_{2-x}Sr_xCuO_4$ single crystals

TABLE III. Growth of $La_{2-x}M_xCuO_{4-\delta}$ (M = Sr, Ba) single crystals.

Composition	Initial system	Maximum temperature, °C	Details of procedure	Dimensions of crystals, mm	T_c, K	Ref.
La_2CuO_4, $La_{1-x}Sr_xCuO_4$ (x = 0.025; 0.05; 0.075; 0.1; 0.2)	La–Sr–Cu–O (excess CuO)	1250	slow cooling to 1150 °C (4 °C/h)	25×20×5 40×40×5	12 (x = 0.075)	[71] [92]
$(La_{1-x}Sr_x)_2CuO_4$ ($0 \leq x \leq 0.15$)	La–Sr–Cu–O (10% La_2O_3, 90% CuO)	1250	slow cooling (2–3 °C/h), growth at bottom of crucible	10×10×2	5 – 25 (x = 0.05 – 0.1)	[111]
$La_{2-x}Sr_xCuO_{4-\delta}$ $La_{1.8}Sr_{0.2}CuO_{4-\delta}$ (x>0.2)	+ CuO(50 mass%)	1160	slow cooling with seeding from above (by introduction of thermocouple)	2.5×2.5×0.2	–	[112]
La_2CuO_4($La_{2-x}Sr_xCuO_4$) (x = 0.2)	$La_2CuO_4 + Li_2Co_3 +$ + B_2O_3($Li_4B_2O_3$)	1150	slow cooling	platelets	no high-temp. supercond.	[110] [113]
$La_{1.88}Sr_{0.12}CuO_4$	$La_{1.85}Sr_{0.15}CuO_{4+\delta}$ CuO(55–80 mol.%) 0.2 MPa O_2	–	floating zone method, growth rate 1–3 mm/h 1 – 3 MM	diameter 6 mm, length 15 mm	29	[114]
La_2CuO_4	La_2CuO_4 + CuO	1105 – 1060	slow cooling	9.5×5×2	no high-temp.	[115]
$La_{2-x}Sr_xCuO_4$ (x~0; 0.15)	La – Sr – Cu – O	1220–1060	slow cooling, 4 °C/h; seeding on Pt wire	4×8×2	supercond.	[115]
$La_{1.85}Sr_{0.15}CuO_4$	$La_{1.85}Sr_{0.15}CuO_4$	900–1100	hot pressing	1.5 mm on surface of ceramic	37.5	[116]
			solid-phase synthesis	1×1×0.5		[117]
$La_{2-x}Sr_xCuO_4$ (x~0.1)	$La_{2-x}Sr_xCuO_4$ (20 mol.%) + CuO (80 mol.%)	1300	slow cooling; 3 °C/h	8×8×2	3.8	[106]
La_2CuO_4	La – Sr – Cu – O		not given	3×4×0.5	14	[109]
$La_{1.85}Sr_{0.15}CuO_4$	$La_{1.85}Sr_{0.15}CuO_4$	1120	solid-phase synthesis	0.5		[117]
$La_{2-x}Sr_xCuO_4$	$La_{2-x}Sr_xCuO$		slow cooling (2–3 °C/h)	15×15×1.5	10 – 17	[113]
$La_{1.95}Sr_{0.05}Cu_{0.9}O_4$	$La_{2-x}Sr_xCuO_4$ (10 – 40 mol.%) + CuO (B_2O_3)	1276	slow cooling, seeding from above, pouring away solution at 1100 °C	4×8×2	8	[90]
$La_{1.85}Sr_{0.15}Cu_{0.94}O_x$	(x = 0.15 – 0.33)			9.5×5×2		
$La_{2-x}Sr_xCuO_4$ ($0 < x < 0.2$)	La_2O_3–SrO–CuO	1300	slow cooling (0.5–2 °C/h to 110 °C) seeding from above Czochralski method, V (rot.) = 20 rpm, $V_{(pull.)}$ = 0.1–0.2 mm/h	10×10×3 diameter of 10mm, length 15–20 mm	5	[80,118] [80,82]
$La_{2-x}Sr_xCuO_4$	La_2O_3 – $SrCO_3$–CuO–Cu_2O	1240	slow cooling, 46 °C/h	4×4×0.1 4×8×0.1	–	[119]
$La_{2-x}Sr_xCuO_4$ (x = 0.004)	La – Sr – Cu – O (80 mol.% CuO)	1300	slow cooling to 1150–1200 °C, 1–4 °C/h	2 cm^3	6 – 15	[120]
$La_{1.86}Sr_{0.14}Cu_{0.97}O_{3.89}$	$La_{2-x}Sr_xCuO_4$–CuO (> 78 mol.%)		moving solvent method, velocity 1 mm/h, P_{O_2} = 100–200 kPa	rod, diameter 8 mm, length 40 mm	37.5 (onset)	[121]
$La_{2-x}Sr_xCuO_4$	$La_{2-x}Sr_xCuO_4$ (50 mol.%) $Li_4B_2O_5$(50 mol.%) (x = 0 – 0.2)	1150	cooling to 1000 °C, 2 °C/h, nucleation on platinum rod	10×10×1	–	[122]
$La_{0.975}Ba_{0.025}CuO_4$	La – Ba – Cu – O (La:Ba:Cu = 0.277:0.1:1.0)	1350	quenching of melt	thin platelets	~10	[71]
$La_{1.984}Ba_{0.016}CuO_4$	La–Ba–Cu–O ($BaCO_3$:CuO = 15:85)	1350	seeding from above, pulling rate 0.3–0.5 mm/h	diameter 18 mm, length 4 mm	not high-temp. supercond. [semicond. $\rho(T)$]	[125]
			spontaneous crystallization	17×14×1		[126]
$La_{1.5}Ba_{1.5}Cu_3O_{7.11}$	La–Ba–Cu–O	–	crystallization of molten solution	1×1×1	–	[127]
$La_{2-x}Sr_xCuO_4$	$La_{2-z}Sr_zCuO_4$–y–CuO (z = 0.05–0.4, y = 3.5–7)	1240	cooling from 1240 to 1050 °C at 2 °C/h, from 1050 to 25 °C at 100 °C/h	10×10×1	10–21	[123,124]

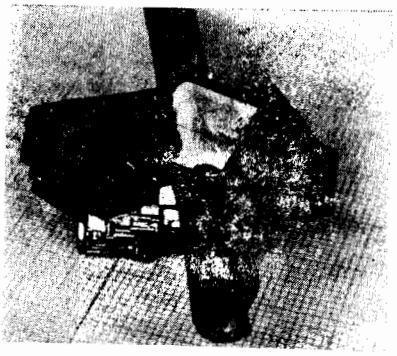

FIG. 8. Single crystals of $La_{2-x}Sr_xCuO_4$ grown by crystallization from a molten solution.

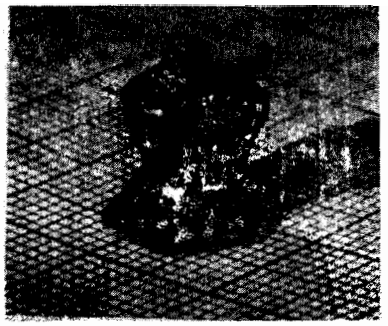

FIG. 9. Single crystal of $La_{2-x}Sr_xCuO_4$ grown by pulling from a nonstoichiometric melt by the Czochralski method.

have been prepared by pulling from the melt.[80,82] The composition of the melt is nonstoichiometric in relation to the crystal being grown (there is an excess of CuO) and the temperature of homogenization of the melt is 1300–1100 °C. Experiments show that heating even to 1400 °C results in crystallization of just one phase, $La_{2-x}Sr_xCuO_4$, from the molten solution. Figure 8 shows a crystal formed by slow cooling of a molten solution with localization of nucleation on a Pt rod.

The use of an oriented seed has made it possible to prepare large (10 mm in diameter and 15 mm long) single-crystal boules (Fig. 9) by pulling from the melt in accordance with the Czochralski method.[80] The rate of rotation of the seed was in this case 20 rpm and the pulling rate was 0.1–0.2 mm/h. The crystals grown in this way were either nonsuperconducting or had values of T_c (of the order of 5 K), which were very low compared with the corresponding values for the ceramic.[80]

The directional crystallization method involving the passage of a molten zone[65] has made it possible to prepare crystallographically oriented samples of eutectoid-type structures in the investigated La–Sr–Cu–O system. A molten zone was established between two polycrystalline rods of the $La_{1.8}Sr_{0.2}CuO_4$–CuO composition in the ratio 54–46 mol.% or 33–67 mol.%; the rates of rotation of the rods were 40 rpm, the pulling rate was 15 mm/h, and the height of the molten zone was 7 mm. This procedure produced ingots 7 mm in diameter and several centimeters long, which were oriented Cu_2O fibers in the matrix of the $La_{2-x}Sr_xCuO_4$ phase oriented along the [Ref. 111] axis. Samples of this type were much easier to prepare than single crystals and the preferred orientation made it possible to study the anisotropy of the electrical properties at right-angles and parallel to the (110) plane. The superconducting transition temperature T_c of these samples was close to T_c reported for polycrystalline materials and it amounted to 34–35.5 K; the magnetic anisotropy was $\Delta M_{\perp}/\Delta M_{\parallel} = 4.2 - 7.5$.

Floating-zone laser melting yielded polycrystalline boules in which thin single-crystal $(La_{1-x}Sr_x)_2CuO_4$ platelets of ~ 1 mm size were observed;[62] the initial composition of the melt had an excess of CuO.

The floating zone method gave the best results when infrared heating was employed.[114] Powders of La_2O_3, CuO, and $SrCO_3$ were subjected to the standard ceramic technology which yielded rods 6 mm in diameter and 50 mm long (at a sintering temperature of 1100–1200 °C); these rods had an excess of CuO (55–80 mol.%) relative to the La_2CuO_4 stoichiometry. The passage of a molten zone (at a velocity of 1–3 mm/h) in an O_2 atmosphere produced single-phase ingots with the exception of the end parts of the ingots where a mixture of $La_{2-x}Sr_xCuO_4$ and La_2O_3 was observed.

Large single crystals are frequently not superconducting and exhibit the semiconducting type of the temperature dependence of the electrical resistivity. In some cases (Table III) freshly grown crystals have exhibited a transition to the superconducting state but the value of T_c has been always less than for the ceramic samples.[80,90,104] The authors of Ref. 14 succeeded in growing a large single crystal in an atmosphere of O_2 and its value of the superconducting temperature was high: $T_c = 29$ K ($\rho = 0$).

Single crystals with the highest value of T_c (onset of the superconducting transition at 37.5 K and the width of the transition $\Delta T_c = 1.1$ K) have been prepared by the method of a moving solvent in a system rich in CuO (50–80 mol.%).

The rate of rotation of the feed and seed rods in these experiments was 30 rpm and the growth rate was 1 mm/h. The growth took place in an oxygen atmosphere at a pressure $P(O_2) = 100$–200 kPa (Ref. 121).

Single crystals of Ba-substituted lanthanum cuprate have been obtained, like those of Sr-substituted material, by crystallization from a molten solution with an excess of CuO (Table III). Freshly grown crystals showed no transition to the superconducting state and the semiconducting[126] type of the dependence $\rho(T)$ was observed. After annealing in O_2 the samples with a certain value of x became superconducting, but at fairly low temperatures (down to 10 K).

The unit cell parameters of the grown single crystals are listed in Table IV.

It is thus clear that large La_2CuO_4 and $La_{2-x}Sr_xCuO_4$ single crystals can be grown quite readily from molten solutions containing CuO both by spontaneous crystallization under slow cooling and by introducing a seed followed by pulling or by growth of a crystal in the bulk of the melt. In the latter case the crystals are faceted by the faces growing most slowly (in the case of La_2CuO_4 the faces of the orthorhombic bipyramid truncated by the basal plane).[93] The slower is the cooling of the molten solution, the larger are the crystals which are obtained (up to 2.5 cm in diameter[71] for the La–Sr composition and up to 1.7 cm for the La–Ba mate-

TABLE IV. Unit cell parameters of $La_{2-x}Sr_xCuO_4$ single crystals.

Value of x	Unit cell parameters, Å			Space group	T_c, K	Ref.
	a	b	c			
<0,025	5,360	5,391	13,190	—	—	[122]
≥0,025	3,794	—	13,15	$I4/mmm$		[122]
0,075	5,366	5,514	13,170	—	25	[126]
0	5,366	5,414	13,170	$Cmca$		[92]
0,14	3,793	—	13,19	$I4/mmm$	37,5 $\Delta T_c = 1,1$ K	[121]
—	3,7802	—	13,2139	$I4/mmm$	—	[129]

rial).[107] Crystals prepared by different methods are of satisfactory quality, but they are characterized by a very large scatter of the values of T_c. As a rule, the lower is the cooling rate of the system (and, consequently, the growth rate of a crystal) the lower is the temperature of the transition to the superconducting state, or alternatively a crystal does not exhibit any superconducting properties at all. The temperature dependence of the resistivity can be quite different for a ceramic sample of a given chemical composition and for crystals of the same composition prepared by different methods.

The lowering of T_c or the absence of T_c in the case of single crystals are either due to the specific distribution of the second component (Sr) in the main matrix or due to an oxygen deficit. An investigation of $La_{2-x}Sr_xCuO_4$ single crystals with different strontium concentrations has made it possible to establish that the nature of the distribution of Sr between the La sites can vary.[130] When the strontium content is low (as is true of $La_{1.94}Sr_{0.06}CuO_4$), the distribution of strontium is homogeneous throughout the sample, which facilitates diffusion of oxygen into the sample and appearance of superconductivity. When the distribution of the strontium atoms is homogeneous, an increase in their concentration increases the concentration of "holes" in the CuO_2 layers, which is important for the transition to the superconducting state. In ceramic and single-crystal samples prepared by fast crystallization the distribution of strontium between the La lattice sites is homogeneous and both crystals and the ceramic exhibit a transition to the superconducting state. At low growth rates it is found that the strontium distribution becomes ordered, so that atoms occupy only certain sites in the lattice and the higher is the strontium concentration the stronger is the ordering, which stimulates formation of O vacancies and results in the loss of superconductivity.

One of the reasons for the deficit of O may be the chemical reduction of CuO to Cu_2O; moreover, the longer is the crystallization process, the greater is the loss of oxygen because of the decomposition of CuO.

The difference between the unit cell parameters of the nonsuperconducting crystals, on the one hand, and of the superconducting ceramic, on the other, provides further confirmation of the fact that the superconducting properties of $La_{2-x}Sr_xCuO_4$ are largely determined by the fine structure of the material. The slight changes in the dependences $\rho(T)$ exhibited by the annealed and unannealed crystals demonstrate irreversibility of the process of formation of the fine structure during crystal growth. It is worth noting also that an oxygen deficit of single crystals lowers the value of the ratio c/a of crystals compared with the ceramic.[91]

3.2. $LnBa_2Cu_3O_{7-\delta}$ single crystals (Ln = rare earth)

3.2.1 Phase relationships and phase diagram of the Y_2O_3–BaO–CuO system

The very first reports of the crystallization of $YBa_2Cu_3O_{6.5+x}$ samples[77,131,132] revealed regions in the ternary $YO_{1.5}$–BaO–CuO diagram in which formation of small platelet $YBa_2Cu_3O_{6.5+x}$ crystals was accompanied by the appearance of other phases at certain temperatures. Numerous subsequent investigations have extended greatly a region of this kind which adjoins the CuO vertex, as demonstrated in Fig. 10. The thick lines in this figure are the tie-lines for which the phase diagrams have been constructed with different degrees of precision. However, there is still no reliable information on the conditions ensuring single-phase crystallization in this system. Obviously, an investigation of the phase diagram of the $YO_{1.5}$–BaO–CuO (or $YO_{1.5}$–$BaCuO_2$–CuO) system, including all possible isothermal and polythermal tie-lines should identify the optimal compositions, as well as the presence in nature of the liquidus curve and thus the optimal temperatures for such crystallization.

Quite extensive data are now available on the various subsystems containing Y, Ba, and Cu oxides.[132–139] Construction of isothermal and polythermal tie-lines for this sys-

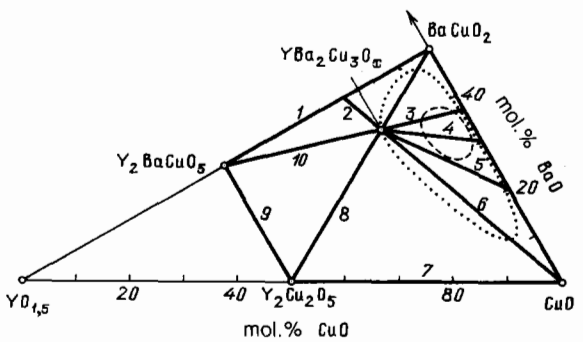

FIG. 10. Regions of formation of $YBa_2Cu_3O_{7-\delta}$ crystals. The numbers represent polythermal tie-lines investigated in detail as follows: *1*) Ref. 133; *2*) Ref. 132; *3*) refs. 132 and 34; *4*) Ref. 134; *5*) Ref. 134; *6*) Refs. 132 and 134; *7*) Refs. 133 and 135; *8*) Refs. 132 and 136; *9*) Ref. 133; *10*) Ref. 132. The dashed line surrounds a region of compositions used most frequentlyl in growing single crystals (Ref. 123); the larger dotted line surrounds the region of compositions from which single crystals were grown (Ref. 123).

tem by the traditional differential thermal and x-ray phase analyses frequently gives results that are not only different, but sometimes even directly contradictory. This is mainly due to the variable amount of oxygen in the system, because this amount depends on the nature of the atmosphere and on the kinetics of temperature changes. Moreover, the aggressive melt frequently interacts with the container material (Pt, Al_2O_3, etc.), which in the final analysis also complicates the processes of formation of various phases and affects the results.

In addition to $YBa_2Cu_3O_{6.5+x}$, the $YO_{1.5}$–BaO–CuO system includes, in the range of compositions adjoining the CuO vertex, a number of points corresponding to the following reliably identified compounds: Y_2BaCuO_5 (green phase), $BaCuO_2$ ($BaCu_2O_2$), CuO, and $Y_2Ba_2O_5$, usually with concomitant phases observed on crystallization of $YBa_2Cu_3O_{6.5+x}$. Obviously, the nature of the thermal stability of these phases plays an important role in identification of the conditions necessary to obtain the 123 crystals. The melting (decomposition) temperatures of these phases are listed in Table V.

The results obtained by different authors for the Y_2O_3–BaO–CuO system have indicated the existence of the following phases:

$Y_2Cu_2O_5$;
$BaCuO_2$, Ba_2CuO_3;
$Ba_4Y_2O_7$, $Ba_3Y_4O_9$, $Ba_2Y_2O_5$;
BaY_2CuO_5, $Ba_3YCu_2O_{6.5+\delta}$, $Ba_4YCu_2O_{7.5+\delta}$; $Ba_5YCu_2O_8$;
$Ba_8Y_3Cu_5O_{18}$; $Ba_4YCu_3O_9$, $Ba_2YCu_3O_{7-\delta}$.

The nature of the melting (or decomposition) of the compound $YBa_2Cu_3O_{6.5+x}$ has been considered on many occasions, but the conclusions reached diverge considerably. According to Ref. 142, the melting point of this compound in air is 925 °C, according to Ref. 131 it is 980 °C, whereas the value 993 °C is given in Ref. 143 and 1020 °C in Refs. 144 and 145. The most detailed study of the melting and nature of decomposition of all the compounds mentioned above can be found in Ref. 141. According to the authors of this paper, practically all the compounds in the $YO_{1.5}$–BaO–CuO system decompose on melting. The results obtained are used to conclude that there are four eutectic and three peritectic points in the investigated range of compositions. However, the results are only very approximate and in many cases they do not agree with the results of investigations of polythermal tie-lines.

As pointed out already, a study of polythermal tie-lines and the construction of pseudobinary phase diagrams is a far from simple task. This can be illustrated by considering the construction of the simplest of the phase diagrams, that for the $BaCuO_2$–CuO system. According to Refs. 80, 146, and 141, this diagram is of the eutectic type, but the reported temperatures of the eutectic and its position differ considerably from one report to another, and its coordinates given in the cited papers lie within the intervals 780–930 °C and 18–35 mol.% CuO. The coordinates adopted in most of the papers correspond to 28 mol.% BaO and 72 mol.% CuO.

In the case of other internal and more complex tie-lines of the system we cannot expect ideal agreement. We shall simply consider those tie-lines that govern the region of possible crystallization of the 123 phase in order to determine the existence and extent of the liquidus curve of this compound.

Studies of the $YBa_2Cu_3O_x$–$BaCuO_2$ system were reported in Refs. 79 and 136 (Fig. 11). An attempt to construct a detailed phase diagram of the system in a much wider range of compositions within the limits $\frac{1}{2}Y_2Cu_2O_5$–$BaCuO_2$ was made in Ref. 136. In Ref. 132 the diagram is very schematic, but in both cases there is one common feature: $YBa_2Cu_3O_x$ is located at ~1000 °C and at some stage there is an equilibrium between Y_2BaCuO_5 and the liquid phase. It should be pointed out that a whole range of solid-phase transitions and unknown phases reported in Ref. 136 is a clear demonstration of the complexity of the system and the need to invoke additional methods, apart from holding the sample at a given temperature in the course of the differential thermal and x-ray phase analyses. The method of holding at a given temperature makes it possible to determine quite accurately the phase composition under partial melting conditions, since the liquid becomes separated from the solid phase and we can exclude secondary formation of crystals in the interaction between the solid phase and the liquid in the course of cooling.

Studies of the $YBa_2Cu_3O_x$–CuO system were described in Refs. 132, 134, and 147 (Fig. 12). The more detailed dia-

TABLE V. Melting (decomposition) temperatures of compounds in the $YO_{1.5}$–BaO–CuO system[137,141,68].

Compound	Decomposition (melting) temperature, °C	Comments
$YBa_2Cu_3O_{6.5+x}$ (123)	1015	Y_2BaCuO_5+L
Y_2BaCuO_5 (211)	1270 (1125)	Y_2O_3+L
$Y_2Cu_2O_5$	1122 (1190)	Y_2O_3+L
$BaCuO_2$	1015 (1042)	L ($BaCu_2O_2$)
CuO	1026 (1080)	Cu_2O
	1120	congruent melting
Cu_2O	1230	
BaY_2O_4	1400	incongruent melting (peritectic)
$Ba_2Y_2O_5$	<800—1000	stable at T < 800 °C
$Ba_3Y_4O_9$	2160	congruent melting
$Ba_4Y_2O_7$	>1000(1140)	
$BaCu_2O_3$	>700	$BaCuO_2$+CuO

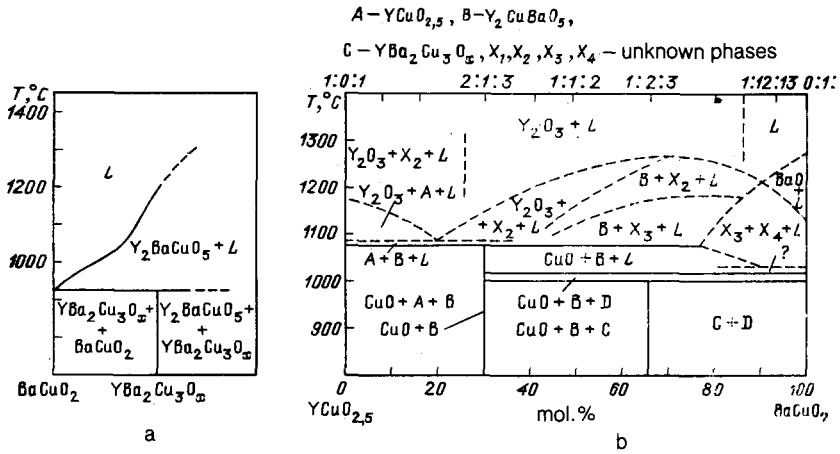

FIG. 11. Phase diagrams of the $YBa_2Cu_3O_x$–$BaCuO_2$ system: a) Ref. 132; b) Ref. 134.

gram based on Ref. 134 does not include the $YBa_2Cu_3O_x$ liquidus, whereas the authors of Ref. 132 identified it in a very narrow range of temperatures and compositions. Obviously, the results reported in Ref. 134 are more correct because the liquidus given in Ref. 132 does not even lie within the field of single-phase crystallization of $YBa_2Cu_3O_x$ identified in Fig. 10. Moreover, the results of Ref. 134 are in agreement with those reported in Ref. 147, where again a schematic diagram does not include a region of single-phase crystallization of the 123 phase. According to Ref. 147, an oxygen atmosphere simply increases slightly the temperature of the eutectic without altering significantly the nature of the diagram.

Information on the $YBa_2Cu_3O_x$–$Ba_3Cu_5O_8$ system is given in Refs. 132, 134, and 148 (Fig. 13). We can see that the results reported in Ref. 134 are more detailed: they include the $YBa_2Cu_3O_x$ liquidus which is very narrow along the composition axis, but reaches 50 °C along the temperature axis. The liquidus of $YBa_2Cu_3O_x$ extended on the composition scale is given in Ref. 141, so that these two parts of the diagram are quite similar and clearly we can use them to find experimentally the conditions for single-phase crystallization of 123.

According to Ref. 134 (Figs. 13d and 13e) the $YBa_2Cu_3O_x$–$Ba_3Cu_7O_{10}$ system is characterized by a more extended region of the $YBa_2Cu_3O_x$–liquid equilibrium with the liquidus extending over the temperature interval 920–995 °C in the range of concentrations 7–19 mol.% $YBa_2Cu_3O_x$. This part of the diagram is in good agreement with the results of the crystallization experiments. It is in this range of compositions that the best results are obtained on crystal growth.

The $YBa_2Cu_3O_x$–$Ba_3Cu_2O_5$ system is also characterized[134] by a small $YBa_2Cu_3O_x$ liquidus in a very narrow range of concentrations within a temperature interval ~50 °C.

The presence of a region where $YBa_2Cu_3O_x$ and the liquid phase are in equilibrium is supported also by investigations of the isothermal liquidus sections reported for this system. For example, according to Ref. 149, this region is indeed located near the eutectic point of the $BaCuO_2$–CuO system (according to Ref. 149, this point corresponds to 76 mol.% CuO + 24 mol.% BaO) with few percent Y_2O_3. The results of Ref. 149 agree also with those reported in later papers[150,151] on the determination of the field of primary crystallization of $YBa_2Cu_3O_{7-x}$.

The authors of Ref. 150 carried out a detailed investigation of the various tie-lines of the $YO_{1.5}$–BaO–CuO system and proposed a three-dimensional model shown in Fig. 14, where the liquidus surface of the 123 phase is identified.

It therefore follows from the results of investigations of pseudobinary polythermal tie-lines that in a certain range of temperatures and compositions of the $LnO_{1.5}$–BaO–CuO system we can expect single-phase crystallization of compounds with the formula $LnBa_2Cu_3O_x$. This is supported also by investigations of the crystallization of cuprates of other rare-earth elements, for example the results of a comprehensive investigation[150,151] of the phase diagrams of the $NdBa_2Cu_3O_x$–$Ba_3Cu_5O_8$ system, and of a study of the conditions for crystallization of $NdBa_2Cu_3O_{7-\delta}$, which had made it possible to achieve crystallization of this compound using seeds in the surface layer of the melt.

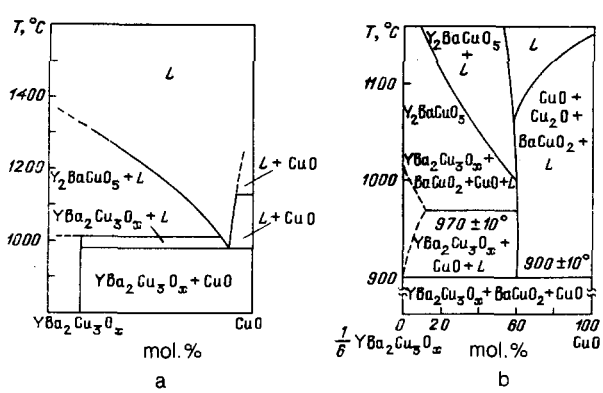

FIG. 12. Phase diagrams of the $YBa_2Cu_3O_x$–CuO system: a) Ref. 132; b) Ref. 134.

3.2.2. Growth of $LnBa_2Cu_3O_{7-\delta}$ (123 phase) single crystals

The partial melting method of growing single crystals was proposed in Refs. 76 and used subsequently by various authors.[63,77,78,9,152–156] Partial rather than complete melting is used because the range of compositions where single crys-

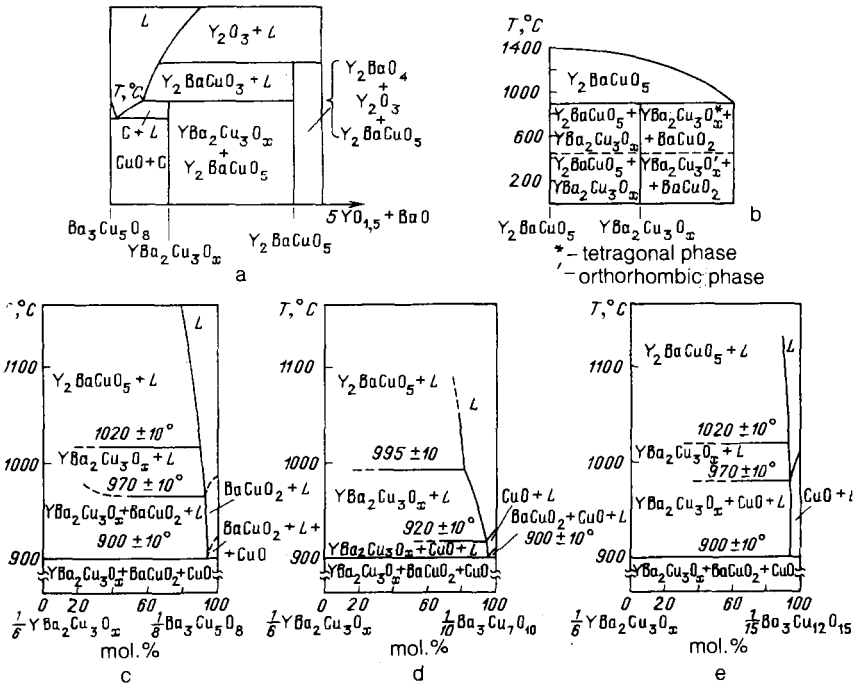

FIG. 13. Phase diagrams of the $YBa_2Cu_3O_x$–$Ba_3Cu_5O_8$ (a–c), $YBa_2Cu_3O_x$–$Ba_3Cu_7O_{10}$ (d), and $YBa_2Cu_3O_x$–$Ba_7Cu_7O_{10}$ (e) systems: a) Ref. 140; b) Ref. 132; c) Ref. 134; d) Ref. 134; e) Ref. 134.

tals of the 123 phase are formed is very narrow (0.25–1.23 at.% *Y*, whereas the content of *Y* in $YBa_2Cu_3O_{7-\delta}$ is 7.7 at.%) and it follows from an analysis of the phase diagrams discussed above that the 123 phase is formed by a peritectic reaction at the boundary separating the solid Y_2BaCuO_5 (211) phase and the liquid. According to Ref. 157, this reaction can be written in the form

$$Y_2BaCuO_5 + 3BaCu_2O_2 + O_2 = 2YBa_2Cu_3O_6 + CuO$$

or

$$2Y_2BaCuO_5 + 2BaCuO_2 + 4BaCu_2O_2 + O_2 = 4YBa_2Cu_3O_6.$$

Under the conditions of oxygen deficit (due to reduction during melting of some proportion of CuO to Cu_2O) in the barium cuprate system a special role in the crystallization of Y-123 is played by the gaseous phase.[157] Consequently, growth of large single crystals is possible only near the surface of the melt which is in contact with an oxidizing atmosphere or in the bulk of the melt at the boundaries with gas-filled bubbles containing an oxidant (O_2).

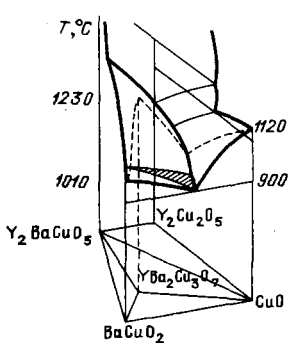

FIG. 14. Three-dimensional phase diagram of the $YO_{1.5}$–BaO–CuO system.[138] The shaded surface represents the liquidus of the 123 phase. The dashed lines represent intersections of the liquidus surfaces of compounds with the $YBa_2Cu_3O_7$–$BaCuO_2$–CuO composition.

In general, the reaction of formation of the Y-123 phase can be divided into two stages:[157]

1) the process of oxidation of Cu^{1+} ions at the gas–liquid interface:

$$4Cu^{1+} + O_2 \rightarrow 4Cu^{2+} + 2O^{2-};$$

2) the process of formation of Y-123 at the interface between the Y-211 solid phase and the liquid:

$$Y_2BaCuO_5 + 3Ba^{2+} + 5Cu^{2+} + (9 - 2\delta)\,O^{2-} \rightarrow YBa_2Cu_3O_{7-\delta}.$$

Since the growth of Y-123 crystals occurs on the surface of the Y-211 phase, the rate of growth is governed by the rate of diffusion of the main components across the layer of the new phase.[143] This accounts for the low rates of growth of Y-123 in accordance with the peritectic reaction. The extended temperature range of the crystallization process (~300 °C) makes it impossible to grow crystals of the Y-123 phase from the supercooled melt by passing the peritectic transformation even at very high cooling rates right up to 10^6 °C/s (Refs. 64, 158, 159).

Crystals are grown by the *partial melting* method in accordance with the following procedure. A mechanical mixture of Y, Ba, and Cu oxides (or carbonates) of composition which is nonstoichiometric relative to the 123 phase is heated to temperatures of the order of 900 °C (Ref. 76) or 1000 °C (Ref. 155). The excess content of BaO and/or CuO results in partial melting of the original material [the melting point of $BaCuO_2$ is 800 °C, that of CuO (Cu_2O) is 1230 °C, the melting points of BaO_2 and BaO are ~450 °C and ~1900 °C, respectively, and the melting of

$YBa_2Cu_3O_{7-\delta}$ in air at 925 °C is accompanied by decomposition]. Platelet $YBa_2Cu_3O_{7-\delta}$ crystals grow during slow cooling in the interior of the original material. Nucleation and growth of these crystals takes place in closed cavities formed as a result of evolution of oxygen due to partial reduction of CuO ($2CuO = Cu_2O + O$);[63,77] crystals thus grow in a medium which is rich in oxygen.

An analysis of the compositions used by different authors to prepare $YBa_2Cu_3O_x$ single crystals was reported in Ref. 89 (see Fig. 10). The range of compositions in which partial melting takes place[76] is identified by a dashed curve in Fig. 10. The freshly grown crystals have tetragonal structure and their superconducting transition temperature is $T_c \sim 55$ K; after annealing it rises to $T_c \sim 86$ K (Ref. 76). According to Ref. 76, the crystals prepared from melts richer in copper have lower superconducting transition temperatures.

The temperatures, durations of heating, durations of maintenance of a given temperature, and cooling rates vary somewhat from one report to another. In some investigations the initial material was either the 123 ceramic[156] containing CuO and BaO additives or a quenched sintered material. For example, in the experiments reported in Refs. 63 and 9 a nonstoichiometric mixture of oxides and carbonates was brought to the melting point (1180–1150 °C); it was then quenched at room temperature, heated again to 900 °C (Ref. 9) or 970 °C (Ref. 63), and kept at this temperature for 4–7 days; it was next cooled slowly to room temperature. Crystals obtained in this way were up to 1–2 mm in size; they were very thin tetragonal plates.

Another variant of the partial melting method was proposed in Ref. 160. The initial charge was the 123 ceramic and the flux was a mixture of BaO_2 and CuO in the molar ratio 1:3 or 2:5. The content of the charge in the flux was 0.6–1.2%. Seeds were introduced into the charge–flux mixture by adding 2 mass% of the 123 powder. This mixture was heated in a platinum crucible to 1000 °C after preliminary maintenance of heat at 800 °C; the former temperature was maintained for 2–4 h and this was followed by slow (20–10°/h) cooling until full solidification took place (850 °C); the crucible was then cooled inside the furnace. Crystals of maximum $2 \times 2 \times 0.3$ mm size grew in the cavities at the bottom and at the walls of the crucible.

A further development of the method of partial melting is a technique of *partial melting of a multilayer ceramic* proposed in Ref. 152. Direct sintering at 950 °C produced samples with the nominal compositions $YBa_2Cu_3O_x$, $YBa_8Cu_9O_x$ and $YBa_8Cu_9F_wO_z$. These substances were used in the preparation of multilayer pellets in which a layer of the 123 composition was in contact with the layers enriched with Ba and Cu. These pellets were subjected to multistage heating to 960 °C; this temperature was maintained for up to 20 h and the pellets were then cooled at a rate of 3 °C/h to 935 °C and then faster at 30 °C/h to room temperature. The whole process took place in an oxygen atmosphere. The melting points of the Ba- and Cu-rich layers were less than that of the 123 layer so that an increase in temperature resulted in partial melting of a Y–Ba–Cu–F–O layer and the result was formation of Y-123 platelet crystals with edges of the order of 1 mm and 0.03 mm thick at the interfaces and in cavities formed within the Cu- and Ba-rich layers. The main advantage of this technique was the absence of a crucible and the consequent avoidance of the problem of contamination of the Y-123 crystals with the products of the interaction between the melt and the crucible.

The temperatures used in the partial melting method can be lowered by adding In_2O_3 as the solvent in amounts proportional to the ratio $In/(Y + In) = 0.05$–0.07 (Ref. 161).

In the case of the Ln_2O_3–BaO–CuO system the methods of partial melting, crystallization of nonstoichiometric compositions, and crystallization from a molten solution are qualitatively the same: the composition of the system is the same and the conditions during growth are the same. The main difference is in the quantitative ratio of the original components (an increase in the fraction of CuO–BaO in the case of the molten solution methods) and in the corresponding change in temperature. Table VI summarizes the data on the preparation of 123 single crystals. This table lists mainly the results reported in 1988–1989. This was done because later investigations have been essentially repetitions using the methods of the first studies and with the attention concentrated mainly on variations in the temperature regimes (they are different because of different crucible materials and different purities of the initial reagents) and in the treatment of the crystals after growth.[178–186]

At high concentrations of the refractory components the process of heating to a temperature of the order of 900–1000 °C results in partial melting, so that an increase in the proportion of the low-melting-point components and use of the eutectic compositions of the flux (BaO + CuO) makes it possible to follow the procedure analogous to the conventional method of crystallization from a molten solution. In this method the critical factors are the temperature—time crystallization regime, the presence of impurities, and the Y:Ba:Cu composition of the original charge. The general procedure is as follows: heating to temperatures usually of the order of 1000–1100 °C is followed by maintenance of this temperature for the purpose of homogenization of the melt and by slow cooling until Y-123 crystallizes (depending on the composition, the presence of impurities may alter this temperature within the range 960–900 °C). After completion of the crystallization process, which occurs during slow cooling of the melt until final stratification of the whole volume of the original mixture, it is desirable to remove the liquid phase and then to cool the system slowly to room temperature. Specific examples of the crystallization procedure are given in Table VI.

The need for *removal of the liquid phase* at high temperatures after the formation of the Y-123 crystals arises from the fact that it is not possible to separate the grown crystals from the solidified flux by dissolving the latter (for example by boiling in water or in various solutions) and it is difficult to extract the required crystals mechanically.

The problems encountered in decantation of the melt are as follows: a crucible has to be taken out rapidly from a furnace which is at a high temperature and this results in thermal shock that can fracture crystals. Moreover, droplets of the melt may still remain on the surfaces of crystals. It is then necessary to follow a well-tried heat treatment, in which such droplets are melted again in order to ensure free flow of the melt from the surfaces of solidified crystals.

TABLE VI. Conditions for growing $YBa_2Cu_3O_{6.5+x}$ (123) single crystals.

Method	Composition	Details of procedure, maximum temperature	Crucible material	Dimensions of crystals, mm	T_c, K after annealing	Ref.
Partial melting	(123) + CuO 78–22%	second heating of melt quenched from 1150 °C, maintenance of 900 °C for 4 days cooling at 1 °C/min	Pt	1×1×0.2	89	[10]
do.	Y:Ba:Cu = 1:4:10	~1000 °C, slow cooling (4–15 °C/h) down to 880 °C	Pt, Ni, Al_2O_3, MgO, ZrO_2, ThO_2	1.2×0.8×0.5 (up to 4 mm)	55 (before annealing), 86	[76]
do.	(123) + CuO (140 – 250% excess)	quenching of melt from 1180 °C after maintenance for 1.5 h	Al_2O_3	5×5×0.3	–	[63]
do.	(123) + CuO + $BaCuO_2$	1000–950 °C, slow cooling (25 °C/h)	Au	2.5×2.5 ×(0.01–0.08)		[155]
do.	(123) + CuO 1:3–3:1	1200–1050 °C, cooling at 15 °C/h to 700 °C	Pt, Al_2O_3	5	91.3	[153]
do.	Y_2O_3,$BaCO_3$,CuO,In_2O_3 In/(Y + In) = 0.05–0.07	960–930 °C, maintenance for 70 h, growth under isothermal conditions; 1025 °C, slow cooling to 970 °C	Al_2O_3	(2 – 5)×(2–5) ×(0.2–0.5)	76–90	[161]
do.	Y:Ba:Cu = 1:4:10	multistage heating (780–980 °C), slow cooling to 830 °C	ZrO_2:Y	2×2×0.5	60	[162]
Partial melting of multilayer ceramic	$YBa_2Cu_3O_x$, $YBa_nCu_nO_y$, $YBa_nCu_nO_yF_z$	multistage heating to 960 °C, cooling to 935 °C at 3 °C/h	–	1×1×0.03	91.5	[152]
Crystallization of nonstoichiometric melt	BaO–Y_2O_3–CuO 15:5:65	1060 °C, cooling at 3 °C/h to 850 °C	Pt	2×2×(0.01–0.03) (tetragon.)	no transition	[131]
do.	Y_2O_3–$BaCO_3$–CuO 0.5:4:10	1000 °C (2–36 h), cooling at 6 °C/h to 840 °C in oxygen atmosphere	MgO	10×10	80	[163]
Crystallization of nonstoichiometric melt	Y:Ba-Cu = 1:4:10	1000 °C, cooling at 6 °C/h, maintenance of 910 °C for 3 days, cooling at 12 °C/h	Al_2O_3,Pt	2×2×0.1	70 92.4	[164]
do.	(123) + excess BaO–CuO	1000–1200 °C, slow cooling, $P(O_2)$ = 100–2800 bar	Al_2O_3	6×4×0.1	40–70	[17]
Crystallization from molten solution	(123) + eutectic Bao–CuO in ratio 1:3	1010–1040 °C, slow cooling, 4–10 °C/h	Al_2O_3,Pt	8×6 1.5×0.1	–	[69]
Crystallization of nonstoichiometric melt	Y_2O_3–BaO–CuO 1:2:3	sintering at 930 °C, melting at 1350 °C, slow cooling	Pt	1.5×1.5×0.04	90	[156]
do.	(123) + (BaO_2 + CuO) (2%) 1:3 2:5	1000 °C maintained for 2–4 h, slow cooling	–	2×2×0.3	65	[160]
do.	(123) + 3CuO	1236 °C, cooling to 700 °C at 1 °C/h	Pt	1.5×1.0×0.2		[165]
do.	Y–Ba–Cu–O			1×2×0.1	60	[166]
do.	$YO_{1.5}$–$BaCO_3$–CuO 1:4:10	1060 °C, cooling to 800 °C at 1–4 °C/h	Al_2O_3	platelet area 40 mm^2, thickness 10–30 μm	82	[167]
do.	Y–Ba–Cu–O	slow cooling		1×0.5×0.2	90	[168]
				1×1×0.3	93	[169]
				2×2(0.03–0.05)	90	[170]
Crystallization from molten solution	Y_2O_3–$BaCO_3$–CuO–(Cu_2O)	1060–1150 °C, slow cooling (1 °C/h) in air or in O_2	Al_2O_3	1.4×1.4×0.3	58–88	[171]
do.	(123) + eutectic BaO–CuO	multistage cooling		4×2×5×0.1	92	[172,152]
Crystallization from molten solution	(123) + (28%$BaCO_3$ + 72% CuO) 1:19	1010 °C (15 min), multistage cooling to 900 °C, 7–10 °C/h to 930 °C; introduction of porous ceramic at 930 °C for 1 h to remove melt	Al_2O_3	up to 3 mm	not given	[173]
do.	(123) 6.7% + eutectic BaO + CuO	1020 °C (28 h), cooling to 920 °C at 1 °C/h, decantation of melt	Pt, ZrO_2	15×11×0.4 8×3×1		[174]
do.	$YBa_2Cu_3O_{7-\delta}$ + KCl + NaCl (weight ratio 100:11.2:8.8)	1000 °C maintained for 1 h, cooling to 680 °C at 1–3 °C/h fast cooling outside the furnace in air	Al_2O_3	up to 4 mm along edge of plate	54 (before annealing), δ = 0.5)	[175]
do.	Y_2O_3–BaO–CuO (4 at.% Y, 30% Ba, 66% Cu)	1010 °C, cooling at 0.1–0.5 °C/h, decantation at 970–900 °C; temperature fluctuations to reduce number of nuclei	Al_2O_3	5×5×2 mm^3 (cooling at 0.1 °C/h)	82–88 ΔT = 2K	[176]
do.	sintered 123 phase Y:Ba:Cu = 4:27:69 (I) 6.6:26.6:66.6 (II)	12 h at 980 °C (I) or 1050 °C (II), cooling at 2–4 °C/h	–	1×1×0.7 (I) 2.5×2.5×0.1 (II)		[177]
Temperature gradient in thin molten layer	123 + (1BaO + 3CuO)	980 °C, temperature gradient 2–5 °C/cm, maintenance of 980 or 960 °C (crystallization temperature) for 70 h	–	4×3×0.5		[177]
Crystallization from molten solution	Y_2O_3–$BaCO_3$–CuO (3–5%) + (BaO + CuO) eutectic ratio	1000–1100 °C, slow cooling to 960–900 °C, melt decantation	Pt	10×10×0.03	93 ΔT = 0.2 K	[80,82]
do.	Y_2O_3–CuO–$BaCuO_2$ 0.012–0.268–0.707	1050 °C maintained for 5–15 h, cooling to 900 °C at 1–6 °C/h, decantation of solution, cooling at 20–50 °C/h to 400 °C	Al_2O_3 ZrO_2	5×5×0.1	–	[180]

Crystallization on a Pt grid inserted in the melt[187] can facilitate extraction of crystals from the crystallization zone. The grid with the grown crystals is raised at some specific temperature and taken out of the melt to a colder zone.

It is possible to separate the melt when growing $YBa_2Cu_3O_{7-\delta}$ single crystals by introducing a porous ceramic which absorbs the melt. After ~1 h at 930 °C the ceramic is removed and the cooling of the crucible to room temperature is continued.[173]

This method has a number of advantages: it makes it easier to separate the crystals from the solidified melt, tends to reduce the amount of the melt on the crystals, and makes possible *in situ* annealing of the grown single crystals. However, there are also a number of shortcomings. They include possible damage to a crystal in the central part of the crucible when a ceramic is introduced. Contamination due to partial corrosion of the ceramic is important in crystals growing in the peripheral parts of the crucible and at its bottom.

The melt can also be removed from the surfaces of crystals by utilizing the ability of the melt to "climb" along a wetted surface. This method was used[177] during growth in a wedge-shaped gap between the bottom of a crucible and a spacer placed inside it. A temperature gradient of 2–5 °C/cm was established in this gap; prolonged (~70 h) maintenance of 980 °C (or 960 °C) gradually removed the melt, which "climbed out" along the wetted surface. Larger crystals were obtained at higher temperatures.

Usually the "climb" of the melt along the crucible walls hinders stable crystal growth. The authors of Ref. 184 prevented "climb" of the melt by inserting an Al_2O_3 rod into the melt: this established a temperature gradient along the rod and a cold zone was formed above the melt, the crust of the solidified part of the melt covered the surface, and it prevented further "climb" of the melt.

The best results were obtained by *crystallization of a solution in the molten* BaO–CuO (28–72 mol.%) *eutectic.* The 123: (BaO + CuO) ratio varied from one investigation to another. According to Ref. 69 the results are obtained by heating one part of the 123 phase and three parts of the eutectic BaO–CuO mixture to 1010–1040 °C and slow cooling at a rate of 4–10 °C/h. The size of the individual platelets grown in this way could reach 8×6 mm. When the ratio of Y-123 to the BaO–CuO eutectic mixture was (6–25%):(94–75%) complete melting was not observed[146] and there were many signs of partial melting, including formation of large cavities where crystals grew.

The 123 single crystals can also be grown successfully by slow cooling of the complete melt when the Y_2O_3 concentration mixture is less than 5 mol.%. Homogenization of the melt can be ensured by raising its temperature to 1100–1200 °C (Refs. 80, 82, 169).

The *temperature regime* in growing $YBa_2Cu_3O_{6.5+x}$ single crystals depends greatly on the initial reagent. For example, if the source of barium is $BaCO_3$, the melt should be heated to ~1200 °C and without additional exposure at this temperature it is then cooled to ~910 °C (at 200 °C/h). When the rate of cooling is less, a large amount of Pt accumulates in the melt and enters a growing crystal greatly reducing T_c. If BaO, BaO_2, or $Ba(NO_3)_2$ are used, the optimal conditions involved maintaining the melt at 950 °C for a day and subsequent cooling to 900 °C at a rate of 1 °C/h or less. In this case the thickness of the 123 crystalline plates is several times greater. In this way we were able to prepare Y-123 single crystals needed for different physical investigations.

The temperature regime during heating depends also on the characteristics of the barium source. If this source is $BaCO_3$, it is necessary to heat it slowly (50 °C/h—see Ref. 176) from 800 to 1000 °C in order to decompose barium carbonate completely. There is no need for such slow heating if the source of barium is BaO, BaO_2, $Ba(NO_3)_2$, or $BaCuO_2$.

It is pointed out in Ref. 163 that the duration of holding the melt at a high temperature is important. Large crystals cannot be obtained without maintenance of such a high temperature for the purpose of homogenization. If 1000 °C is maintained for 4 h, the result is in the form of very tiny (up to 1 mm) 123 crystals on the surface of the melt. An increase in the duration of maintenance of this high temperature to 36 h can produce platelets with the edge size up to 10 mm, as reported in Ref. 163.

The thickness of the resultant plates depends strongly on the *rate of cooling of the system.*[174–176] If the cooling rate is $v = 5$–10 °C/h, the thickness of the plates is only a few microns, for $v = 2$–5 °C/h it is 0.05–0.2 mm, and for $v = 0.5$ °C/h the thickness is in excess of 1 mm. The largest dimensions of the platelets obtained in this way are 15×11×0.4 mm and 8×3×1 mm (low cooling rates). The crystallization conditions are listed in Table VI.

According to Ref. 176 in the region of optimal concentrations of the components the thickness of the platelet 123 crystals can be 500 μm, 1 mm, and 2 mm when the cooling rates are 0.5, 0.3, and 0.1 °C/h. When the cooling rate is less than 0.5 °C/h, additional {101} and {011} faces appear in the crystals. Rapid cooling (>30 °C/h) creates signs of a nonequilibrium morphology in the form of dendrites and zigzag-shaped edges of the {001} faces.

The thickness of these plates increases on increase in the ratio $BaO/YO_{1.5}$, on increase in the duration of maintenance of the maximum temperature, and on reduction in the rate of cooling of the system. Single crystals with a clear faceting grow from a charge containing Cu_2O as the additive.[120]

The value of T_c and the crystal habit are influenced also by the *presence of impurities.* According to Ref. 174 the growth in a crucible made of ZrO_2 or the presence of In, Sn, and Nb impurities tended to produce thin platelets; larger crystals were obtained in the presence of K or Li, but these impurities increased the tendency for the capture of melt drops by the surfaces of crystals. Separation of the melt from the grown crystals occurs more readily in the presence of Ti, Mo, and V (Ref. 157).

Typical $YBa_2Cu_3O_{7-\delta}$ crystals are shown in Fig. 15. The superconducting characteristics of the 123 phase can be improved, according to Ref. 188, by crystallization from a molten solution in an electrochemical cell. A distinguishing feature of this approach is the saturation of the melt (70% CuO, 25% BaO, 5% Y_2O_3) with oxygen by introduction of a platinum electrode (T~950 °C) into the melt and the application of a potential of −250 mV to the surface of the melt. This increases the "activity" of O_2 in the melt from 10^{-6} atm to $\gtrsim 1$ atm. This approach makes it possible to grow superconducting crystals without the need for subsequent annealing.

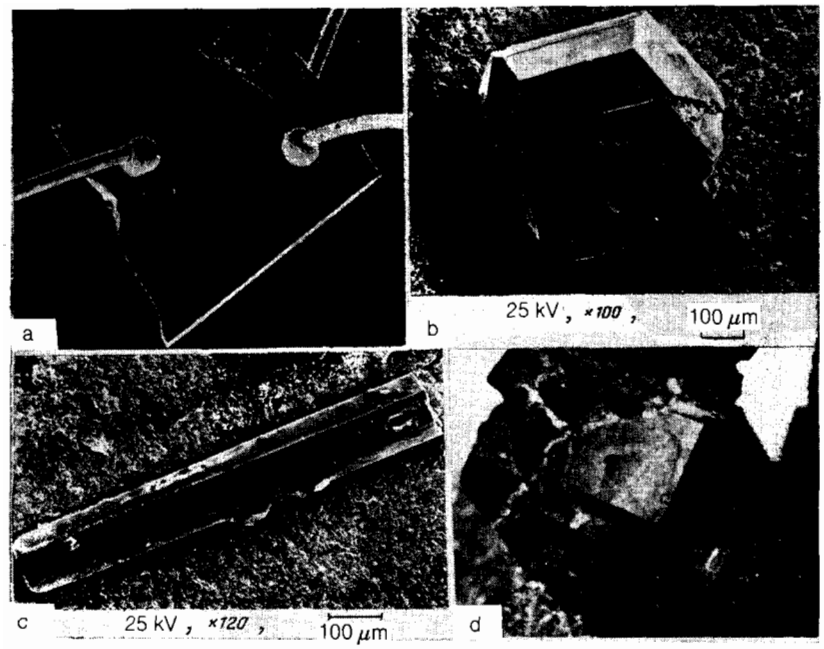

FIG. 15. Typical appearance of $YBa_2Cu_3O_{7-\delta}$ single crystals and concomitant phases crystallizing in the Y–Ba–Cu–O system:[80,82] a) $YBa_2Cu_3O_{7-\delta}$; b) $Y_2Ba_3Cu_2PtO_{10}$; c) $Ba_4(Pt,Cu)O_6$; d) $BaCuO_2$.

A detailed analysis of the composition of Y-123 has been made only in a few cases; usually the attribution to the 123 family has been made on the basis of x-ray diffraction investigations. It follows from the available data that the usually obtained crystals are close to the 123 stoichiometry, but in some cases there is a systematic deficit of the Cu(1) copper amounting to 1–10% (Refs. 163 and 189), the Pt impurity may be present when crystals are grown in a Pt crucible,[80,92,190] and Al may be present if an Al_2O_3 crucible is used.[92]

Single crystals containing other rare-earth elements (Table VII—see Refs. 151 and 191–210) could be grown under similar conditions. The thermal stability of $LnBa_2Cu_3O_{7-\delta}$ compounds in the rare-earth series of elements and the corresponding peritectic reaction temperature increase on increase in the size of the Ln^{3+} ions.[193] The highest thermal stability is exhibited by neodymium cuprate $NdBa_2Cu_3O_{7-\delta}$. An increase in temperature should also increase the solubility of the Ln-123 compounds in eutectic $BaCuO_2$–CuO melts, creating more favorable conditions for the growth of Nd-123 single crystals. The Nd content of the liquid phase, which is in equilibrium with Nd-123, is higher than that of Y-123 and it amounts to ~1.6 at.% Nd (which is almost 30% higher than in the Y-123 case), so that it is possible to grow quite readily Nd-123 single crystals.[150,193,194] The value of T_c for nonstoichiometric crystals is less than that for those with the stoichiometric composition: in the case of $Nd_{1.2}B_{1.8}Cu_3O_x$ this temperature is approximately 40 K less than for $NdBa_2Cu_3O_x$ (Ref. 209). A considerable amount of Pt in an $Nd_{1-x}Ba_{2-x}Cu_{3-z}Pt_zO_y$ plate with $x = 0.45$, 0.54, and 0.66 suppresses the transition to the superconducting state.[194] The superconducting phase grows on the surface of the semiconducting $Nd_{1.5}Ba_{1.5}Cu_3O_x$ phase. The melting point of this phase is approximately 10 °C higher than that of $NdBa_2Cu_3O_x$, so that the 1.5–1.5–3 phase crystallizes first when the melt is cooled. Single crystals of Ln-123 compounds are usually thin plates with twin and polydomain structures. The twinning tendency differs somewhat for compounds containing different rare-earth elements. According to Ref. 208, the Tm–Ba–Cu–O system is most likely to produce samples of Ln-123 single crystals with fairly large single-domain regions. The largest single-domain region in such single crystals can reach the dimensions of ~0.7×0.5 mm. Such single crystals are obtained by crystallization from a molten solution in CuO and their superconducting transition temperature is $T_c = 91$–93 K. Single-domain regions in Y-123 crystals are usually of 100×100 μm dimensions; it is reported in Refs. 211 and 186 that single-domain single crystals of up to 1 mm size can be prepared.

The morphology of the growth surfaces of Ln-123 single crystals indicates that the growth occurs from the solution;[79] the growth mechanism clearly involves dislocations. Irrespective of the crucible material, polygonal spirals have been observed on the surfaces of crystals grown from a molten solution. The shape of these spirals depends on the crucible material: it is octagonal for crystals grown in CuO and ZrO_2 crucibles, square for Al_2O_3 crucibles,[179] and circular in the case of Pt containers. This change in the shape of the spirals is clearly associated with the influence of impurities which are transferred to the melt as a result of partial dissolution of the crucible material. In the case of side {010} surfaces there is a characteristic funnel-shaped morphology, the nucleation begins at the corners and edges of the crystal, and growth is in accordance with the two-dimensional nucleation mechanism. The differences between the growth mechanisms observed for different faces is due to the different atomic structures of these faces and the different degrees of anisotropy of the bonds on the surfaces.[79,179,212,213] The unit cell parameters of Ln-123 single crystals that have been

TABLE VII. Conditions for growth of single crystals of rare-earth cuprates $RBa_2Cu_3O_{6.5+x}$ (R is a rare-earth element).

R	Dimension of crystals, mm	Grotwh method, composition of system	Maximum temperature, details of procedure	T_c,K	Ref.
Pr	≲1 mm	molten solution, stoichiometric $Pr_2CuO_4 + BaO_2 + CuO$ mixture	1000 °C, slow cooling at 5 °C/h to 200 °C	no transition down to 4.2 K	[191]
Nd,Gd,Yb	2×2×0.03	solution in molten BaO (28%)–CuO(72%)	1300 °C, slow cooling (25 °C/h) and intermediate quenching from 1250–1300 °C followed by heating to 1040 °C	not determined	[192]
Nd	4×5 (0.5–1) mm platelets; cubes with 1 mm edge	solution in molten Nd_2O_3–$BaCO_3$—CuO (excess of CuO)	1050–1200 °C, slow cooling, 1.5–5 °C/h to 950 °C		[193]
Nd	1.2×1.2×0.06 mm platelets, 1.25×1.25×0.87 mm cubes	solution in molten $BaCO_3$–Nd_2O_3–CuO 1) Ba:Nd:Cu = 2:1:3 2) Ba:Nd:Cu = 2:1:10	similar to preceding (Ref. 193)	~75 ($\rho = 0$)	[194]
Nd	3×3×0.5 mm platelets, rods 1 mm in diameter, 5–6 mm long	solution in molten $NdBa_2Cu_3O_7$(25%) + $Ba_2Cu_3O_8$(75%)	a) 1100 °C, slow cooling, 10 °C/h to 900 °C b) seeding from above (Pt wire), 1080 °C, cooling at 5–10 °C/h, wire with seed rotated at 20–30 rpm	53 ($\rho = 0$)	[150]
Nd Gd		solution in molten PbO,Gd_2O_3(10%)–BaO(30%)–CuO(60%)	slow cooling		[195]
Gd	3×2×0.2	solution in molten 20%(123) + (28% BAO–72% CuO)80%	1080 °C, slow cooling, annealing) 2 °C/h to 650 °C	90 (after annealing)	[196]
Gd	2×3×6	sintered 123 pellet, 20 mm in diameter and 2–3 mm thick	multistage cooling from 1005 °C (2h)–980 °C (48 h)–940 °C (8 h)–900 °C (8 h)–850 °C (8h)–750 °C (24 h)–550 °C (24 h)	92 ($\rho = 0$, after annealing)	[197]
Eu	0.5×0.5×0.05	solid-phase synthesis	900–950 °C in O_2 atmos-	90–95	[198]
Eu	1.1×0.56×0.022	solution in melt based on BaO	phere slow cooling	90–93	[199]
Eu	2×2×0.5	solution in molten (123)–CuO in ratios 1:1 or 1:2	1150 °C, slow cooling		[171]
Dy	3×3	solution in molten (123)–CuO in ratios 1:2 or 1:3 (123–CuO–BaO in ratio 1:6:1.3	970–1157 °C, maintained for 12 h, cooled at 17 °C/h	not determined 93, $\Delta T = 0.4$ K	[200] [201]
Er	1×1×0.3	partial melting of $RBa_4Cu_{8.5}O_y$	930 °C, slow cooling	81	[202]
Er	1×1×0.3	solution in molten (123) + 3CuO + BaO	1150 °C, slow cooling to 1000 °C, fast cooling to room temperature, second heating to 900 °C, cooling with furnace	86.5 ($\rho = 0$)	[203]
Y, Gd, Dy Er, Tm, Eu, Yb, Lu	2.5×2.5×1 (Y) 4×4×1 (Gd) 5×1.5×1.5(Eu)	solution in molten (123) + 6CuO	1160 °C for 4h, cooling to 900 °C at 2–4 °C/h	91(Y,Gd,Er) 90.5(Yb) 65(Dy) 80(Eu,Ho) 78(Lu) 89(Tm)	[204]
Er	1×1×0.3	solution in molten, Er:Ba:Cu = 1:5:10	900 °C for 17 h, 1000 °C for 17 h, cooling at 3–10 °C/h to 400 °C, maintained for 10 days	92 (onset)	[205]
Nd	1×1×0.4	solution in molten Nd_2O_3–$BaCO_3$–CuO. 0.5:2:8, 0.5:4:8.5, 0.5:4:8.5	1100 °C, cooling at 3 °C/h in air	no transition	[205]
Gd	3×3×0.4	solution in melt, hf melting in cold (Cu) container, $BaCO_3$ + 2CuO + (2–5 mol.%)$GdBa_2Cu_3O_7$	1200 °C, cooling at 1000 °C/h	93 (onset)	[206]

TABLE VIII. Unit cell parameters of $RBa_2Cu_3O_x$ single crystals.

Composition	Unit cell parameters, Å			T_c, K	Comments	Ref.
	a	b	c			
$YBa_2Cu_3O_7$	3,8193	3,8852	11,6873		*Pmmm*	[50]
$YBa_2Cu_3O_6$	3,857	—	11,8194		*P4/mmm*	[50]
$YBa_2Cu_3O_{6,5+x}$	3,863	—	11,837	—	no transition	[169]
	3,826 (2)	3,890 (2)	11,705 (3)	~93	after annealing	[169]
$YBa_2Cu_3O_x$	3,897	3,824	11,714	92,4		[164]
$YBa_2Cu_3O_x$	3,8605	3,8613	11,718	~55		[76]
	3,854	3,861	11,675	88 (ρ=0)		[76]
$Y_{0,92}(Ln)_{0,03}Ba_2Cu_{2,95}O_x$	3,857	—	11,828	~60	before annealing	[190]
	3,823	3,879	11,735	~93	after annealing	[190]
$Y_{0,94}(Ln)_{0,02}Ba_2Cu_{2,88}O_x$	3,865	—	11,704	—	before annealing	[190]
	3,368	—	11,604	60—80	after annealing	[190]
$YBa_2Cu_3O_x$	3,8605	3,8613	11,718		before annealing	[78]
	3,854	3,861	11,675		after annealing	[78]
$YBa_2Cu_3O_x$	3,857 (1)	3,876 (1)	11,692 (5)	~65 (ρ=0)		[160]
$YBa_2Cu_3O_x$	3,855	3,864	11,740	54	before annealing	[175]
	3,842	3,877	11,603	—	after annealing	[175]
$PrBa_2Cu_3O_7$ ($Ba_2Pr_3^{4+}Pr_{0.3}^{3+}Cu_{0.7}^{3+}Cu_{2.3}^{2+}O_7$)	3,8918	—	11,6484	—	no transition even after annealing in oxygen, P4/mmm	[191]
$NdBa_2Cu_3O_7$	3,888	3,873	11,67	—	platelets	[193]
	3,890	3,877	11,67		cubes	[193]
$GdBa_2Cu_3O_7$	3,859 (1)	3,885 (2)	11,759 (3)		*Pmmm*	[192]
	3,8410	3,9007	11,7104			[197]
$DyBa_2Cu_3O_x$	3,857 (1)	3,859 (1)	11,708 (5)		freshly grown	[76]
	3,856 (1)	3,858 (1)	11,704 (4)		after annealing	[76]
	3,846 (2)	3,856 (2)	11,664 (7)		after annealing under different conditions	[76]
$EuBa_2Cu_3O_x$	3,866	—	11,735	90—95		[198]
$ErBa_2Cu_3O_x$	3,822	3,887	11,63			[202]
$LuBa_2Cu_3O_x$	3,90	3,75	11,67			[204]

TABLE IX. Unit cell parameters of phases formed in the Ln_2O_3–BaO–CuO systems.

Composition	Cell structure	Unit cell parameters, Å			Ref.
		a	b, β	c	
$BaCuO_2$	cubic	18,277	—	—	[210]
$BaCuO_2$	orthorhombic	9,780 9,624	5,627 5,641	4,758 4,746	[214] [210]
$Y_2Ba_2O_5$	tetragonal	4,386	—	11,856	[215]
$Y_2Ba_4O_7$	tetragonal	4,361	—	28,68	[215]
Y_2BaCuO_5	orthorhombic	12,161	7,121	5,664	
$Ba_4Pt_{2-x}Cu_{1-x}O_y$	tetragonal	5,81	—	8,46	[204]
$Y_2Ba_3Cu_2PtO_{10}$	monoclinic	12,333	5,751, β = 105°40′	7,274	[81]
$Y_2Ba_2CuPtO_8$	orthorhombic	13,207	10,321	5,680	[84, 216]
$ErBa(Cu_{1,1}Pt_{0,9})O_y$	orthorhombic	10,287	5,659	13,157	[217]
$Ba_{0,25}Cu_3Cl_{2,5}O_y$	tetragonal	5,515	—	13,808	[218]
$BaCu_2O_3$	orthorhombic	3,785	8,627	6,720	[137]
$Ba_{41}Cu_{44}O_{84}Cl_2$	cubic	18,27	—	—	
$Ba_8Y_3Cu_5O_{18}$	tetragonal	5,787	—	8,014	[219]
$Ba_5YCu_2O_9$	orthorhombic	4,030	4,090	12,160	[219]
$Ba_4YCu_2O_{7,5+\delta}$ [221]	low-temperature tetragonal	5,811	—	8,017	[221, 215] [220]
($Ba_3YCu_2O_{6,5+\delta}$ [220])	high-temperature tetragonal, pseudocubic	8,06	—	4,035	[219]

grown are listed in Table VIII; the parameters of the compounds which are formed together with these crystals are listed in Table IX.

3.2.3. Growth of $Y_2Ba_4Cu_8O_{16-x}$ single crystals

This compound was first separated in epitaxial films[222–224] and was later reported in polycrystalline ingots.[225] Single crystals of $Y_2Ba_4Cu_8O_{16-x}$ were grown[226] by the method of zone melting with optical radiation heating in the presence of an excess oxygen pressure. This Y-248 phase melted incongruently, excess pressures up to 50 atm did not prevent decomposition of the Y-248 phase (which occurred in accordance with the peritectic reaction), and attempts to prepare crystals from billets of stoichiometric composition were unsuccessful. It is known that the zone melting method can be used to prepare crystals of incongruently melting compounds if the initial liquid compositions of the compound to be crystallized are nonstoichiometric. Crystallization of the 248 compound was attempted from compositions rich in CuO and BaO using ceramic billets 7–8 mm in diameter and ~90 mm long. This process took place under an oxygen pressure of at least 30 atm because otherwise a strong evolution of O_2 from the melt was observed.[226] The results were in the form of textured ingots consisting of single-crystal lamellas of $2\times0.3\times0.2$ mm dimensions. These crystals had the orthorhombic cell with the parameters $a = 3.853$ Å, $b = 3.861$ Å, $c = 27.04$ Å; the superconducting transition temperature was $T_c = 81$ K. Prolonged annealing in air followed by cooling at a rate of 20 °C/h caused decomposition of the 248 phase producing $YBa_2Cu_3O_{7-\delta}$ and CuO.

3.3. Single crystals of superconducting phases in the Bi–Sr–Ca–Cu–O system

3.3.1. Phase relationships in the Bi–Sr–Ca–Cu–O system

The compounds with the formula $Bi_2Sr_2Ca_{n-1}Cu_nO_y$ ($n = 1$, 2, or 3) represent the third class of cuprate superconductors with four members (Table I): they are distinguished by a large number of components participating in the formation of these chemical compounds. Crystals can be grown from the four-component Bi_2O_3–SrO–CaO–CuO system or a more complex one if it is necessary to use mineralizers or stabilizers of the high-T_c phase.

An increase in the number of the components of the system increases the number of their allowed combinations and the possibility of stacking errors in the metal–oxygen layers, variations of numbers of such layers, and the probability of formation of phases with similar (or identical) parameters in the (a, b) plane, but with a different value of the parameter c. This is exactly the situation in the case of the Bi–Sr–Ca–Cu–O system, which makes it more difficult to prepare single crystals of the individual phases and to identify them. The cuprate with the nominal 1112 composition,

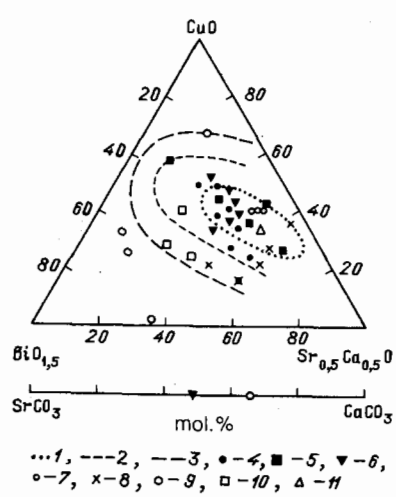

FIG. 16. Regions of crystallization of complex cuprates in the $BiO_{1,5}$–(Sr, Ca)O–CuO system: *1*) region of obtaining compounds exhibiting superconductivity (Ref. 229); *2*) region where compounds with resistivity of 10^3 Ω cm are obtained; *3*) region where compounds with resistivity of 10^5 Ω cm are obtained. High-temperature superconducting cyrstals: *4*) Ref. 230; *5*) Ref. 229; *6*) 110 K phase (Ref. 231); *7*) 110 K phase (Ref. 232); *8*) crystals with metallic conduction (Ref. 229); *9*) semiconducting crystals (Ref. 230); *10*) no high-temperature superconductors (Ref. 230); *11*) no crystals (Ref. 230).

initially described as a superconducting compound, has been found to be a mixture of several phases[227,228] whose compositions given by various authors can differ quite considerably. The $Bi_2Sr_2CuO_y$ cuprate is characterized by $T_c < 10$ K (Ref. 228), whereas according to Ref. 23 this temperature is 20 K. Partial replacement of Sr with Ca increases T_c. In the composition triangle with the Sr:Ca equiatomic ratio the authors of Ref. 229 have picked out regions with different behavior of complex cuprates: they exhibit different types of the temperature dependence of the electrical resistivity (Fig. 16). Clearly, a slight change in the composition can result in loss of superconductivity.[229-232]

In view of the complexity of the system under consideration, the phase relationships and diagrams have been plotted for the individual tie-lines and subsystems. Such subsystems reveal that there are many binary and ternary compounds in the Bi–Sr–Ca–Ca–O systems.

The phase relationships for the $BiO_{1.5}$–SrO–CuO, $BiO_{1.5}$–CaO–CuO, SrO–CaO–CuO, and CaO–SrO–$BiO_{1.5}$ systems have been investigated at temperatures 500–800 °C in air.[233] In the case of the binary subsystems it has been found that the following compounds are formed:[233,234] Bi_2CuO_4, $Bi_{1-x}Sr_xO_y$, $(0.2 \leqslant x \leqslant 0.3)$, $BiSr_3O_y$, Sr_2CuO_3, $SrCuO_2$, $Sr_3Cu_5O_{8+\delta}$, and $CaCuO_3$. The following compounds have been reported for the ternary subsystems:

Bi–Sr cuprates:

$Bi_2Sr_2CuO_x$,
$Bi_7Sr_7Cu_6O_x$,
$Bi_7Sr_8Cu_5O_x$,
$Bi_4Sr_8Cu_5O_x$;

Bi–Ca cuprates:

$Bi_{1-x}Ca_xCuO_3$ $(x = 0{,}1;\ 0{,}25;\ 0{,}41;\ 0{,}54)$;

Sr–Ca cuprates:

$(Sr_{1-x}Ca_x)_2CuO_3$; $0 \leqslant x \leqslant 0{,}7$

(initial ratio (Sr + Ca)/Cu = 1)

$Sr_{1-x}Ca_xCuO_2$; $0 \leqslant x \leqslant 0{,}7$

(initital ratio (Sr + Ca)/Cu = 1);

$(Sr_{1-x}Ca_x)Cu_5O_6$, $0 \leqslant x \leqslant 0{,}5$

(initial ratio (Sr + Ca/Cu = 1);

ternary oxides Bi, Sr, and Ca with the formula $Bi_{1-x}(Sr, Ca)_xO_y$:

$Bi_{0.55}Sr_{0.45-x}Ca_xO_y$, $0 \leqslant x \leqslant 0{,}1$,
$Bi_{0.4}Sr_{0.6-x}Ca_xO_y$, $0 \leqslant x \leqslant 0{,}3$,
$Bi_{0.25}Sr_{0.75-x}Ca_xO_y$, $0 \leqslant x \leqslant 2$,
$Bi_{0.46}Ca_{0.54}Sr_xO_y$, $0{,}1 \leqslant x \leqslant 0{,}2$,
$Bi_3Sr_4Ca_3O_y$.

There is also practical interest in the part of the phase diagram representing the $BiSrCaCu_2O_y$–$BiSrCaCuO_y$ subsystem (Fig. 17a).[235] According to the published data, the liquidus curve of the 2212 phase lies within the range $1.5 < n < 1.875$. Such compositions are recommended for single crystal growth.

Figure 17b shows schematically the phase diagram of the pseudobinary system $Bi_2(Sr, Ca)O_4$–$(Sr, Ca)CuO_2$ based on the data of Ref. 236. The 85 K phase melts incongruently at a temperature above 900 °C; the primary crystallization region of $Bi_2Sr_2CaCu_2O_8$ is characterized by a very narrow range of compositions and temperatures (the latter of the order of 20 °C). The crystallization temperature of Bi-2212 lies within the interval 840–860 °C; at lower temperatures 840–780 °C the compound $Bi_2Sr_2CuO_6$ crystallizes.

The complexity of the crystallization processes in the Bi–Sr–Ca–Cu–O system is demonstrated by the fact that the crystallization of superconducting phases of different compositions is accompanied by precipitation of a whole series of concomitant (in some cases predominant in respect of the mass) crystalline products. For example, various authors have reported that a solidified ingot may contain the following:

solid solutions based on calcium cuprate $(Ca, Sr)_2CuO_3$;

solid solutions based on strontium cuprate: $(Sr, Ca)CuO_2$ (Ref. 23) or $SrCu_{1.7}O_x$ (Ref. 85);

Bi–Sr–Ca oxides with the formulas $Bi_6(Ca, Sr)_5O_{14}$ (Ref. 23) and $Ca_7Bi_{10}O_{22}$ (Ref. 237);

cuprates $Bi_3Sr_5Cu_3O_y$ (Ref. 238) and $Bi_7Ca_4Sr_1Cu_{0.56}O_{16}$ (Ref. 239);

copper oxides CuO or Cu_2O.

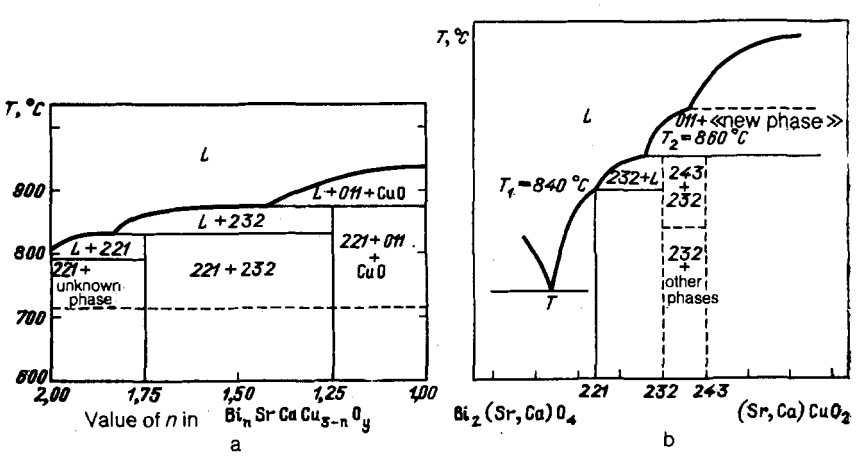

FIG. 17. Phase diagrams of the systems $Bi_nSrCaCu_{3-n}O_y$, $1<n<2$ (*a*, Ref. 235) and $Bi_2(Sr, Ca)O_4$–$(Sr, Ca)CuO_2$ (*b*, Ref. 236). The three-figure index gives the values of the indices *a*, *b*, and *c* in the formula $Bi_a(Sr, Ca)_bCu_cO_x$.

The quaternary system Bi_2O_3–SrO–CaO–CuO includes homologous phases in the form of the compounds Bi-2212, Bi-2223, and Bi-2234 (containing the 30, 37, and 42 Å phases, respectively). Attempts to obtain these phases from stoichiometric mixtures have produced multiphase samples even in the case of solid-phase synthesis. A review of the main problems encountered in solid-phase synthesis and heat treatment of superconducting Bi–Sr–Ca cuprates can be found in Ref. 240.

The identical initial compositions and different conditions during synthesis produced mixtures with different ratios of the Bi–Sr–Ca–Cu phases. The Bi-2212 phase with 85 K appears most easily, but "purer" samples are obtained from the 4334 and not from the 4424 composition,[241] the Bi-2223 phase with the higher T_c (110 K) forms in a small amount together with the other Bi phases.[242-244] Introduction of Pb as an isomorphous impurity (Bi–Pb substitution) can stabilize, depending on the Pb content and the conditions during heat treatment, the formation of the 2212 phase and increase the proportion of the 2223 phase in the final product. The optimal content of Pb should not exceed ~30% because a higher proportion of lead gives rise to an independent Ca_2PbO_4 phase.[245]

Moreover, in the case of the Bi–Sr–Ca cuprates it was found that compounds with different degrees of the Sr–Ca substitution are formed with the same structure type; the structure of these compounds is such that, depending on the conditions during their preparation, all three elements Bi, Sr, and Ca can occur in the same layers. The compound with the structure of the Bi-2212 type exists, according to Ref. 246, in the following ranges of the compositions: 28–35.7 mol.% $BiO_{1.5}$; 16.5–35.5 mol.% SrO; 8.5–17.5 mol.% CaO; 27–32 mol.% CuO. The 2201, 2212, and 2223 phases have homogeneity regions in the range of the Ca/Sr ratios from 1:1 to 0:2, from 1:1 to 1:5, and for 1:1 (Ref. 247). For a fixed optimal Bi/Pb ratio ($Bi_{1.84}Pb_{0.34}Sr_xCa_yCu_zO_w$) the change in the ratio of the other components gives rise to crystalline phases with different values of T_c in the range 86–104 K (Ref. 245). Phases with higher values of T_c are formed for higher values of the ratio Sr/Ca. The authors of Ref. 245 have suggested that the optimal composition is $Bi_{1.84}Pb_{0.34}Sr_{1.91}Ca_{2.0}Cu_{3.0}O_w$, because then the samples have high values of T_c and consist of a single phase. Electron microscopic examination has shown that the phases with different values of the c lattice period are intergrown.[248-249]

When Pt or Al_2O_3 crucibles are used, the final products may contain crystalline phases with the compositions of Sr and Ca aluminates and complex Bi–Cu–Sr–Ca–Al oxides.[23] A solidified melt of the 2224 composition was found[87] to contain black crystals in the form of hexagonal prisms, the phase is nonconducting, a recalculation of the results of the analysis of these authors gave the composition $Ca_{5.7}Sr_{2.2}CuPt_{0.7}O_x$. The authors of Ref. 85 pointed out that the platinate Sr_4PtO_6 formed on interaction of Bi–Sr–Cu–O melts with the crucible material (Pt); at $T = 1000$ °C the hexagonal cuprate platinate was found to have the composition $Ca_{1.75}Sr_{1.5}Cu_{0.75}PtO_6$. The crystallographic characteristics of nonsuperconducting phases in the Bi–Sr–Ca–Cu–O–(Pt) system are listed in Table X.

3.3.2. Growth of single crystals of Bi superconductors in the Bi–Sr–Ca–Cu–O system

Single crystals of Bi superconductors belonging to this system were grown by the methods of crystallization from the melt with different degrees of deviation from stoichiometry or by slow cooling of the melt, as well as employing different variants of the vertical and horizontal zone melting methods, and also by crystallization from a molten solution using mineralizers (Table XI, based on Refs. 5, 6, 33, 34, 66–68, 230, 236–238, 250–273).

All the methods found successful in growing single crystals belonging to the La–Sr–Cu–O and Y–Ba–Cu–O systems were applied also to the Bi system.

The existence of four homologous $Bi_2Sr_2Ca_{n-1}Cu_{2n}O_x$ phases with similar parameters a and b, but with different values of the parameter c, and incongru-

TABLE X. Crystallographic data for concomitant phases in the Bi–Sr–Ca–Cu–O system.

Compound	Crystal structure	Unit cell parameters, Å			Ref.
		a	b	c	
Bi_2CuO_4	tetragonal	8,510	—	5,814	[233]
$BiSr_3O_y$	orthorhombic	16,98	17,04	16,74	[233]
$Bi_2Sr_2CuO_y$	orthorhombic	5,39	24,05	34,03	[233]
$Bi_7Sr_7Cu_6O_y$	orthorhombic	4,89	5,40	24,83	[233]
$Bi_7Sr_8Cu_5O_y$	tetragonal	5,37	—	24,61	[233]
$SrCu_{1,7}O_y$	hexagonal	3,77	—	24,34	[87]
Sr_2CuO_3	orthorhombic	12,695	3,923	3,501	[234]
$SrCuO_2$	orthorhombic	3,574	16,33	3,920	[234]
$(Sr_{0,79}Ca_{0,21})_{1,01}CuO_{2+\delta}$	orthorhombic	3,509	16,23	3,895	[237]
$Sr_{0,54}Ca_{0,45}Bi_{0,01}Cu_{3,12}O_y$	orthorhombic	11,41	13,09	3,91 (c_1) 2,74 (c_2)	[237]
Ca_2CuO_3	orthorhombic	12,240	3,778	3,256	[234]
$(Ca_{0,9}Sr_{0,1})_{2,25}CuO_{3+\delta}$	orthorhombic	12,299	3,291	3,795	[237]
$(Ca_{0,85}Sr_{0,15})_{1,04}CuO_{2+\delta}$	tetragonal	3,865	—	3,215	[237]
$Ca_{5,7}Sr_{2,2}CuPt_{0,7}O_y$	hexagonal	16,8	—	11,7	[87]
Sr_4PtO_6	hexagonal	9,74	—	11,90	[85]
$Ca_{1,75}Sr_{1,5}Cu_{0,75}PtO_6$	hexagonal	9,442	—	11,125	[86]
$Sr_{1,5}Ca_{1,4}Cu_{0,7}Pt_{0,5}O_y$	hexagonal	17,30	—	12,17	[87]
$(Bi_{0,97}Sr_{0,03})_{1,06}\cdot(Cu_{0,87}Al_{0,13})_3O_y$	monoclinic	5,375	23,955	17,175	[237]
$Bi_3Sr_5Cu_3O_y$	orthorhombic	5,375	23,955	17,176	[237]

TABLE XI. Conditions for growth of single crystals of Bi compound superconductors.

Initial composition, ratio of components	Composition of single crystals	Crucible material	Maximum temperature, °C	Details of procedure	Dimensions of crystals, mm³	T_c, K	Ref.
Bi:(Sr + Ca):Cu 4:3:2	$Bi_4(Bi_{0.42}Sr_{3.20}Ca_{0.42})Cu_2O_y$ $Bi_4(Bi_{0.33}Sr_{3.22}Ca_{2.16})Cu_4O_y$	Al_2O_3 Au	840–960	slow cooling	5×7×(0.02–0.06)	78–84	[23]
4334 + Bi_2O_3 + CuO (2112,8336,10336)	4334 $Bi_{2.2}(Sr,Ca)_{2.6}Cu_2O_y$	Al_2O_3	1000	slow cooling to 500 °C at 10 °C/h	7×5×1	81.5	[251]
Bi–Sr–Ca–Cu–O 1112 + 3 CuO	2212 22(0.8)2	Al_2O_3	1200	maintained for 5 h, cooling to 800 °C at 5 °C/h	1×1×0.1	80.6	[252]
Bi:(Sr + Ca):Cu 4:6:4 1112,1111	464 $Bi_4(Sr,Ca)_6Cu_4O_y$ $Bi_4Sr_{3.9}Ca_{1.5}Cu_{3.8}O_y$	Al_2O_3 Al_2O_3	1150	1150 and 875 °C maintained for some time, slow cooling at 25 °C/h (1150–875 °C) and 5 °C/h (875–755 °C)	edge of platelet 4 mm	84	[253]
1111; (1.4)11(3.3) (2.29):1:1:(1.45) Bi:Sr:Ca:Cu	$Bi_{4+x}Sr_{6-x-y}Ca_yCu_4O_z$ $x = 0.4, y = 2; 1,4$ $Bi_{4+x}Sr_{4-x-y}Ca_yCu_2O_x$ $x = 0.6, y = 1$	Pt	950	slow cooling to 700 °C at 5 °C/h	edge of platelet up to 10 mm	80 no supercond.	[6]
1112	$Bi_{3.6}Sr_{3.1}Ca_{1.4}Cu_4O_x$	Al_2O_3	1065	slow cooling at 15 °C/h or 5 °C/h	1.2×1.0×0.5	93	[254]
Bi_2O_3:(Cao,SrO):CuO 23:46:31	$Bi_4Sr_{3.1}Ca_3Cu_{4\pm0.3}O_y$	Al_2O_3	850	slow cooling to 600 °C at 4–6 °C/h	10×10×1	85 (onset)	[237]
Bi–Sr–Ca–Cu–O ()	2212	–	1025	cooling to 925 °C at 80 °C/h, maintained for 10 h, cooling to 835 °C at 1 °C/h	3×5×0.05	86	[255]
1112 + Bi_2O_3 + CuO	4(0.5)22	–	1000 – 900 (O_2)	slow cooling at 10 °C/h	2×2×1	0.66	[256]
2212 1.8 1.8 1.2 1.2	$Bi_{1.7}Sr_{1.9}Ca_{1.0}Cu_{2.3}O_y$ (main phase)	floating zone method	900	laser heating, pedestal method			[33]
$(1+u)Bi_2O_3$ $+ (2+u)\{(1-x)SrCO_3$ $+ xCaCO_3\}$ $+ (2+w)CuO$ $(0 \leq u,v,w \leq 0.3)(0 \leq x \leq 1)$ $Bi_2O_3 \cdot 2SrCO_3 \cdot 2CuO$ $- 1.3Bi_2O_3 \cdot 2.3CaCO_3$ $\times 2.3CuO$	2111 (Ca,Sr)(Cu,Bi)$O_{2+\delta}$ 2212 (platelets) 3503 (needles)		1400	cooling to 800 °C at 7 °C/h	1×1×0.2 0.5×0.5×0.05 0.2 0.2 1	–	[238]
Bi-Sr-Ca-Cu-O	mixture of cuprates $Bi_2(Bi_{0.2}Sr_{1.8}Ca_{1.0})Cu_2O_8$	zone melting	T_{mp}	molten zone moving at 1 mm/h, O_2 0.6 liter/h	8×3	29	[257]
Bi_2O_3:$SrCO_3$:$CaCO_3$:CuO 1:1.5:1.5:2	$Bi_2Sr_1Ca_{1.2}Cu_{1.7}O_y$ $Bi_{2.3}Sr_{1.2}Ca_{1.4}Cu_2O_y$	Al_2O_3	1100	multistage cooling to 970 °C, 5 cycles with temperature difference 20 °C	platelets	80	[258]
2212	2212,2223	Al_2O_3	1200	fast cooling to 910 °C, slow cooling to 760 °C (3–4 °C/h)	8×5×1	89 (onset, after annealing)	[230]
Bi_2O_3—SrO— CaO—CuO 2212, 2122, 1112	2212,2112		950	multistage heating to 900 °C for 4 h, cooling at 1 °C/min to 600 °C, and 20 °C/min to 25 °C		92 (onset) 78–80	[34]
4334 + (Bi_2O_3 + CuO) (excess)	2201 2212 2223	Al_2O_3	1140	cooling to 890 °C, maintained for several days (7 days for 2223 phase)	platelets	10 85 110	[240]
1112 (feed rod)	1112	floating zone method	950–900	floating zone method, laser heating, cooling rate 0.017–10 mm/min	whisker crystals, diameter 0.5–1.5 mm	85	[66]
2 1.3 1 2	$Bi_{2.1}Sr_{1.2}Ca_{1.0}Cu_2O_{7+\delta}$	Pt	900	zone recrystallization method, molten zone velocity 0.5–2 mm/h	5×20×0.3	85–87	[239]
Bi_2O_3:SrO:CaO:CuO 4:3:3:4	2212		875 878	partial melting complete melting cooling rate 5 °C/h to 750 °C	2×2×1 (intergrowths) 1×1×0.02	90 ($\rho = 0$)	[259]
$\{1.1Bi_2O_3$—$2SrCO_3$— $0.8CaCO_3 \cdot 2CuO\}(50\%)$- $\{0.54KCl\text{-}0.46KF\}$ (50%)	$BiSr_{0.8}Ca_{0.6}CuO_4$ (2212) $Bi_{2.1}Sr_{1.4}Ca_{0.3}CuO_x$	Pt	600	slow cooling, evaporation of solvent		80	[61, 260]
2212 + KCl (30 mass %)	$Bi_{2.2}Sr_{3-x}Ca_xCu_2O_y$ $(x - 1.1 - 1.2)(2212)$		900	heating to 900 °C at 300 °C/h, maintained for 3 h, cooling to 776 °C at 5 °C/h	3×3×0.03	89	[261]
4334 + (KCl + NaCl) 1112 + (KCl + NaCl)	two phases with $c = 30.80–30.93$ $c = 24.51$ Å		960	slow cooling, 5 °C/h	10×5×0.5	80	[67]
1112 + KCl (1:10 by weight)	1112	Pt	850	slow cooling to 700 °C	10×10×0.05	80	[68]
1112 + KCl (80 mass %)	$Bi_2(Sr,Ca)_3Cu_3O_y$	Pt	910	heating at 100 °C/h, maintained for 0.5 h, fast cooling to 25 °C	1×1×0.5	86	
Pb:Bi:Sr:Ca:Cu 1:4:3:2:3	$Pb_{0.6}Bi_3Sr_2Cu_3O_x$	Al_2O_3	1030	maintained for 6 h, slow cooling to 800 °C at 2–10 °C/h	10×4×3	82 ($\rho = 0$)	[263]
2212 + KCl (1:4 by weight)	2212 $Bi_{2.2}Sr_{2.1}Ca_{0.8}Cu_2O_y$ $Bi_{1.6}Sr_{0.7}Ca_{0.2}Cu_2O_y$	Pt	950	heating at 14 h, cooling to 740 °C at 3 °C/h, fast cooling to 25 °C	10 mm²	85–87	[264]
1113 1115	$Bi_{2.2}Sr_2Ca_{0.7}Cu_2O_y$ $Bi_{2.2}Sr_2Ca_{0.7}Cu_2O_y$	Al_2O_3	960	cooling to 760 °C at 6 °C/h, quenching in liquid nitrogen	5×7 ×(0.005 – 0.01)	50	[265]

TABLE XI. (Continued)

Initial composition, ratio of components	Composition of single crystals	Crucible material	Maximum temperature, °C	Details of procedure	Dimensions of crystals, mm³	T_c, K	Ref.
1112 + KCl(NaCl) (1:4 by weight)	2212		875	cooling to 760 °C/h at 10 °C/h	–	84	[5]
$BiO_{1.5}$—SrO—CaO—CuO 33 – 24 – 18 – 25 at.%	2212	Al_2O_3	870–820	slow cooling, growth on seed in surface layer	1×0.5×0.1 5×2	85	[236]
$Bi_{2.2}Sr_{1.8}Ca_{0.75}Cu_{1.8}O_y$ + $SrCaCu_4O_6$	$Bi_{2.2}Sr_{1.63}Ca_{0.65}Cu_{1.8}O_y$ $Bi_{2.2}Sr_{1.8}Ca_{0.75}Cu_{1.89}O_y$ (at bottom below $SrCaCu_4O_6$ layer) $Sr_{0.3}Ca_{1.8}Cu_2O_y$	Al_2O_3	1020	1020 °C maintained for 12 h, cooling at 60 °C/h to 920 °C, maintained for 10 h, cooling at 1 °C/h to 820 °C, and at 10 °C/h to 100 °C	1.5×1×0.1 3×1.5×0.7	77	[266]
$BiO_{1.5}$—$SrCO_3$—$CaCO_3$—CuO (22 – 34) – (20 – 23) – (11 – 15) – (31 – 34)%	$Bi_2(Sr,Ca)_3Cu_3O_{8+\delta}$ 2223 2201	Pt	930	930 °C maintained for 12 h, cooling at 2 °C/h to 800–820 °C, temperature gradient 5–10 °C/cm	12×8×0.1 0.15×0.1×0.05	70–96 (midpoint) 110 (midpoint) 10–25 (midpoint)	[267]
$Bi_6Sr_3Ca_3Cu_4O_y$	2212	Al_2O_3 Pt	880	cooling to 880–800 °C at 0.4–2.2 °C/h, followed by cooling in a furnace	5×3×1	84	[268]
2212	3.3 – 2.6 – 1.1 – 2		1200	cooling in 2 h to 910 °C, cooling at 10 °C/h to 500 °C	12	83	[269]
Bi—Sr(La)—Ca(Y)—Cu—O $Bi_{2.4}Sr_{2-x}La_xCa_{1-y}(Na,Y)_yCu_2O_z$ (10% excess relative to 2212) 2.4:2:0.95:2	Bi—Sr—Ca—Cu 2.1 – 1.94 – 0.88 – 2.07	Al_2O_3	1010	cooling to 900 °C maintained for 1 h, cooling to 775 °C at 30 °C/h, and to 20 °C at 50 °C/h	2 cm², thickness 20–100 μm	90	[270]

ent melting of the phases were the reasons why layer epitaxial configurations composed of different Bi–(Sr, Ca) phases were formed from molten solutions. When the composition of the liquid in equilibrium with solid phases did not differ too much, it was found that precipitation of one solid phase, or even a slight segregation at the crystallization front, could alter the composition of the adjoining liquid which reached equilibrium with a different solid phase and this resulted in crystallization of that phase.[271] The growth of the new phase then altered the composition of the liquid so that the first phase or some new phase was precipitated. For example, when as a result of crystallization of the Bi-2212 phase the liquid became richer in Ca and Cu, the conditions could become favorable[271,64] for the crystallization of the Bi-2223 phase, which could reduce the Ca and Cu content in the melt and result in precipitation of either the 2212 phase or of the 2201 phase.

It was found that the easiest to grow are the Bi-2212 and Bi-2201 crystals. Cooling of a homogenized melt resulted first in the crystallization of the Bi-2201 phase, which began at 875–880 °C and was complete at 840–835 °C (Refs. 236 and 267). Cooling enriched the liquid with bismuth and depleted it of copper and, to a lesser extent, also of calcium. In the temperature range 840–780 °C it was found that single crystals of $Bi_2Sr_2CuO_6$ (Bi-2201) were grown. In turn this phase could react with (Sr, Ca)CuO_2 producing Bi-2212.

One of the important factors governing the composition of the final crystallization products was the selection of the initial composition of the mixture.

In the case of a calcium-free system it was found that slow cooling (5 °C/h) of the melt kept at a temperature not exceeding 920 °C resulted in growth of platelet crystals of the layer Bi-Sr cuprate with $T_c = 10$ K and the areas of the platelets were 5×5 mm² (Ref. 85). The composition of these crystals was $(Bi, Sr)_4CuO_4$ (structure type 2201); the ratio of strontium to bismuth was $0.8 < Sr/Bi < 0.9$. Single crystals of the Bi-2201 phase with dimensions up to several millimeters were obtained as a result of slow cooling of the melt (with compositions along the 221–232 tie-line) after crystallization of the Bi-2212 phase (at temperatures below 840 °C).[236] The authors of Ref. 258 assert that their crystalline products contained also a phase with $n_{Cu} = 2$, similar to the (Bi, Sr, Ca) cuprate with $T_c = 85$ K and with the lattice parameter $c = 30.6$ Å. This phase could not be separated because it was intergrown with the $n_{Cu} = 1$ phase. The two phases were characterized by the composition ratio $(Bi + Sr)/Cu < 2.75$ ($n_{Cu} = 2$) or > 3.59 ($n_{Cu} = 1$).

Crystallization of the Bi phases from the melts rich in Cu and Bi usually produced visually indistinguishable phases with the platelet habit. It was reported in Ref. 261 that a bismuth-rich mixture yielded platelet crystals whose composition included an excess of Bi relative to the 4(6)4 or 4(4)2 stoichiometry. These were the following phases:

$$Bi_4(Bi_{0.33}Sr_{3.22}Ca_{2.16})Cu_4O_y \quad (\text{or} \quad 4{,}3—3{,}2—2{,}2—4),$$
$$Bi_4(Bi_{0.42}Sr_{0.20}Ca_{0.42})Cu_2O_y \quad (\text{or} \quad 4{,}4—3{,}2—0{,}4—2).$$

These crystals were very thin (20–60 μm) plates with the dimensions of the order of 5–7 mm at right-angles to the c axis.[21] These crystals were formed by slow cooling of the melt (860–940 °C) starting with a mixture with the composition Bi:(Sr + Ca):Cu = 4:3:2. Single crystals of similar composition with the formula $Bi_2(Sr, Ca)_{2.6}Cu_2O_x$ were obtained also using initial mixtures of different compositions such as 2112, 8336, and $\overline{10}336$ (i.e., 4334 + excess of Bi_2O_3 and CuO).[251] In the case of these crystals the Sr/Ca ratio was unstable and varied along a crystal between 1.05 and 1.13.

A charge with a low bismuth content and with the formula $Bi_2Sr_3Ca_3Cu_4O_y$ produced no single crystals,[230] whereas a mixture slightly richer in Bi yielded only nonconducting crystals. When the ratio of bismuth to copper was Bi/Cu ~ 4, the result was in the form of nonsuperconducting crystals characterized by the lattice parameter $c = 24.53$ Å (Ref. 92) with the formula $Bi_2(Sr,Ca)_2CuO_x$. In the range Bi/Cu ≫ 4 the yield consisted of crystals characterized by $T_c \sim 85$ K and $c = 30.69$ Å. The composition of these crystals corresponded to the formula $Bi_2(Sr,Ca)_3Cu_2O_x$. The phases much richer in Bi (Ref. 21), for example $Bi_4Sr_{2.4}CaCu_2O_y$ (Ref. 6) or $Bi_{4.84}Sr_{3.20}Ca_{0.42}Cu_2O_y$ (Ref. 21), or conversely the phases practically free of Bi [including the (Sr, Ca) cuprate depleted of Bi (Ref. 254) when the formula would be $Bi_{0.04}Sr_{0.6}Ca_{0.7}Cu_2O_x$] were not superconductors and the temperature dependence of the electrical resistivity $\rho(T)$ was typical of semiconductors. These phases had lower values of the parameter c amounting to 19.54 Å according to Ref. 254, and 24.3 Å according to Ref. 21.

It was concluded in Ref. 230 that the optimal composition for the preparation of (Bi, Sr, Ca) superconducting crystals is $Bi_2Sr_2CaCu_2O_x$. The authors prepared crystals with $T_c = 89$ K (this was the temperature at the onset of the transition) and with dimensions $8\times5\times1$ mm. The size of these crystals was increased by the following procedure: a crucible made of Al_2O_3 was used to heat the 2212 phase to 1200°C, this temperature was maintained for 2 h; this was followed by rapid cooling to 910 °C (this was the temperature at the bottom of the crucible whereas at the top of the crucible it was 950 °C) and then slow cooling at a rate of 3–4 °C/h to 760 °C (at the bottom of the crucible) and finally at a rate of 10 °C/h to 500 °C. The size of the crystals obtained in this way was up to $12\times5\times1$ mm when the transition began at $T_c = 109$ K and was completed at 83 K.

The initial 2212 composition yielded two phases: the 85 K phase with the parameter $c = 30.7$ Å (2212 phase) and the 110 K phase where $c = 36.4$ Å (2223 phase). The two phases formed intergrown structures.[230]

The optimal ratio of the initial oxides needed for the growth of Bi-2212 crystals was, according to Ref. 236, 33% $BiO_{1.5}$, 24% SrO, 18% CaO, and 25% CuO.

The initial compositions were selected in Ref. 237 along the line between the 4334 composition and the 90% Bi_2O_3–10% CuO eutectic, melting at $T \sim 600$ °C. When the initial compositions were 2122, 2212, 1112 (Ref. 34), the maximum heating temperature was 950–900 °C because heating below 900 °C did not result in crystal growth, whereas higher temperatures provided no advantages. The authors of Ref. 34 employed fairly fast cooling (60 °C/h in the interval 900–600 °C, 120 °C/h in the interval 600–25 °C). A tenfold reduction in the cooling rate did not increase the yield or the size of the crystals. The composition of the platelet Bi cuprates was in general the same as that of the original charge.

The method of *cyclic temperature variation* was used by the authors of Ref. 257 to grow single crystals of Bi high-temperature superconductors. Cycling of the temperature of a melt with the initial composition $Bi_2O_3:SrCO_3:CaCO_3:CuO = 1:1.5:1.5:2$ produced platelet $Bi_2Sr_{1.2}CaCu_{1.7}O_{6.9+\delta}$ crystals. Maintenance of 1100 °C for 20 h was followed by cooling to ~970 °C (100 °C/h) and then by short heating–cooling cycles such that in each cycle the maximum temperature was 20 °C lower than in the preceding one. After the fifth cycle the temperature was lowered at a rate of 10 °C/h to 700 °C. X-ray diffraction patterns revealed two phases (with 24 and 30 Å). The freshly grown crystals exhibited a wide transition to the superconducting state with the temperature at the onset of the transition 115–80 K. Annealing in air at 810 °C for 24 h increased T_c (the onset of the transition occurred at 115 K) and the temperature dependence of the resistivity $\rho(T)$ acquired a step. Among the Bi phases, the maximum T_c (105 K) was obtained for the ideal composition $Bi_2(Sr,Ca)_4Cu_3O_{10}$, which would be called the 2(4)3 phase if no distinction were made between Sr and Ca. Crystals of this phase were reported in Ref. 274 and their dimensions were $0.5\times0.5\times0.025$ mm.

The ratio of the main components of the solid phases grown from molten solutions of different stoichiometry was quite different from the ratio in the liquid phase. For example, when the original charge had the composition Bi:Sr:Ca:Cu = 2:2:1:2, the formula of the resultant crystals was $Bi_2Sr_{1.48}Ca_{0.6}Cu_{1.56}O_x$ (Ref. 275), whereas for the initial ratio 2.4:2:0.95:2 the crystals were $Bi_{2.10}Sr_{1.94}Ca_{0.88}Cu_{2.07}O_x$ (Ref. 270). The authors of Ref. 265 noted the following change in the cation composition relative to the initial one: 2.4 Bi in the original charge and 2 in the crystal, whereas the corresponding changes in the case of the other components were $2\to1.9$ for Sr, $0.95\to0.8$ for Ca, and $2\to2.1$ for Cu. Some deficit of Ca and Sr could be due to possible Bi–Cu, Bi–Sr, and Bi–Ca substitutions or due to the characteristic structure of the Bi phases manifested by an incommensurate periodicity along the b axis. A deficit of Ca and Sr was practically always found in the final crystals, although according to Ref. 246 in the case of the compositions close to Bi-2212 normalized to CuO the distribution coefficients were $K_{Bi_2O_3} = 0.99$–1.09, $K_{SrO} = 0.86$–0.96, and $K_{CaO} = 0.5$–0.95, i.e., the compositions of the liquid and solid phases which were in equilibrium differed only slightly.[246]

The crystallization temperature was lowered by different authors employing an excess of a component with the lower melting point and this component was Bi_2O_3 (Ref. 270), CuO (Refs. 252 and 265), or Bi_2O_3 and CuO together (Ref. 251).

Single crystals with the Sr/Ca > 1 ratio were reported in Ref. 252: when the original composition was 1112 + CuO (with the 1:3 ratio), the resultant crystals had the formula $Bi_2Sr_2CaCu_2O_8$ and their dimensions were $1\times1\times0.1$ mm. According to the data reported by different authors, the composition of the superconducting samples varied within certain limits: $Bi_{2.66-8}Sr_{1-4.2}Ca_{1.6-4}Cu_4O_y$. In the case of these compounds the lattice parameter was $c = 30.7$ Å. Single crystals of the superconducting Bi phases had been grown using extensively the directional crystallization method.[267–270,265] The simplest way of inducing directional crystallization involved establishment of a temperature gradient along a container. It was reported in Ref. 267 that a temperature gradient 5–10 °C/cm was established in a Pt container. Homogenization of the melt and removal of CO_2 was ensured by maintaining a mixture of oxides and carbonates (Table XI) at 930 °C for 12 h and then cooling it to 820-

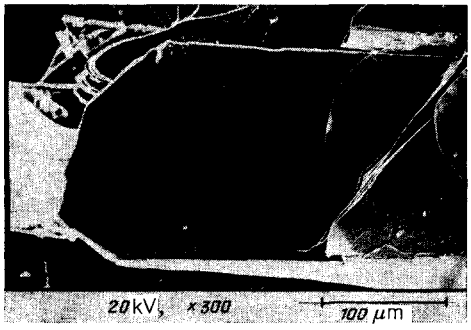

FIG. 18. Typical appearance of Bi-2212 single crystals grown by zone recrystallization.

800 °C at a rate of 2 °C/h. Crystallization of the 2212 phase began at 875–880 °C; the parts of the ingot formed at lower temperatures contained Bi-2201 ($c = 24.4$–24.6 Å, $T_{c,\mathrm{mid}} = 10$–25 K), CuO, $Ca_2SrBi_4O_9$, Bi_2CuO_4, and (Pt, Cu) $(Ca,Sr)_2O_x$ phases. In the high-temperature part of the ingot there were also very small ($0.15\times0.10\times0.05$ mm) crystals of the Bi-2223 phase.

The method of horizontal zone recrystallization was used[239] to grow single crystals of Bi superconductors. A boat with a charge (sintered sample of the 2–1.3–1–2 composition) was moved at a rate of 0.5–2 mm/h across a molten zone with the temperature 900 °C and the width of this zone was up to 10 mm. Experiments lasting 5–10 days produced textured samples consisting of Bi–Sr–Ca cuprate platelets packed at right-angles to the surface of the melt and readily split off from the bulk of a sample along cleavage planes oriented at right-angles to the (001) plane. The size of these platelets was up to $5\times20\times0.3$ mm. A typical form of this phase is shown in Fig. 18. The platelet packets were interleaved by polycrystalline $Ca_2Cu_3O_5$ and $Bi_7Ca_4Sr\cdot Cu_{0.56}O_x$ phases. X-ray diffraction investigations revealed traces of these phases in the bulk of the sample. Annealing in oxygen showed that the resistivity fell to zero at 85–87 K. A small kink at 110 K exhibited by the temperature dependence of the resistivity demonstrated that there was a certain amount of a phase with a higher superconducting temperature in the textured sample.

Single crystals of the superconducting phase in the form of thin platelets mixed with other phases were also prepared by the vertical zone melting method in a stream of O_2 (flowing at a rate of 0.6 liter/h). A molten zone several millimeters wide was formed by heating with a 1.5 kW halogen lamp.[256] An attempt to prepare single crystals of the 2212 composition by the laser-heating pedestal method was reported in Ref. 28. The floating zone method (with laser heating) was used later[66] to prepare textured crystalline samples. The nominal composition of these Bi–Sr–Ca–Cu–O samples was 1112 and they were grown using seed and feed rods formed by the usual solid-phase synthesis method. Crystals grew at pulling rates of 0.17–10 mm/min when the temperature was 900–950 °C. The resultant samples with a diameter of 0.5–1.5 mm were textured and contained single crystal parts.

The floating zone method was also used[276,277] in directional crystallization of $Bi_2Sr_2CaCu_2O_8$. A charge had the stoichiometric composition[277] and the growth took place on a $Bi_2Sr_2CaCu_2O_8$ seed in air. The resultant ingots had a layer structure in which single-crystal platelets or lamellas with dimensions up to $10\times2\times0.03$ mm were elongated along the ingot axis. As pointed out earlier, introduction of lead into this system promoted formation of high-temperature superconducting phases and in most of the investigations carried out more recently use was made of the more complex Pb–Bi–Sr–Ca–Cu–O system to prepare both lead-doped and pure Bi cuprates (see, for example, Refs. 178 and 278–280), retaining the procedure used also in the absence of lead.

In the presence of Pb the yield of the Bi-2212 crystals was higher and the crystallization temperature was somewhat lower. Lead was not always incorporated in the lattice of the crystalline compounds: in all cases it evaporated rapidly during crystallization. The stoichiometry of the crystals differed, as in the case of samples not doped with Pb, from the stoichiometry of the melt: a charge with the Bi:Sr:Ca:Cu:Pb = 4:3:2:3:1 composition yielded crystals with the cation ratio 3:2:1:3:0.6 (Ref. 178).

The authors of Ref. 280 noted that lead influenced the structure of the crystallizing phases. For example, in the case of the calcium-free Bi–Sr–Cu–O system it was found that crystallization of melts of the 223 composition produced Bi-2201 single crystals with the monoclinic structure, whereas a charge of the $Pb_{0.2}Bi_2Sr_2CaCu_2O_y$ composition yielded Bi-2201 crystals with the orthorhombic ($a = 5.41$ Å, $b = 5.42$ Å, $c = 24.03$ Å) lattice and an additional modulation in the (a, b) plane due to the presence of lead.

In addition to the methods used to grow Bi-system single crystals from nonstoichiometric melts, where the solvents were CuO, Bi_2O_3, or PbO taken in excess, or their mixtures, it was found that single crystals could also be grown by the traditional molten solution methods employing chloride fluxes.[5,67,68,260,261,264,281] A solution in a molten mixture of chlorides or a solution in molten KCl (Ref. 261) was used to grow $Bi_{2.2}Sr_2Ca_{0.8}Cu_2O_{8+\delta}$ single crystals. The authors of Ref. 261 used also nitrate solutions to produce a precipitate with the composition Bi:Sr:Ca:Cu = 2:2:1:2, which was heated at 500 °C, mixed with KCl (70 mass.%), and heated at a rate of 300 °C/h to 900 °C. After three hours at this temperature, the melt was cooled slowly to the melting point of KCl (776 °C) and then KCl was removed from the platelets produced in this way by dissolving it in water. The composition of the resultant crystals was $Bi_{2.2}Sr_{3-x}Ca_xCu_2O_y$ ($x = 1.1$–1.2). It was reported in Ref. 258 that single crystals of two phases, $BiSr_{0.8}Ca_{0.6}CuO_x$ ($T_c = 80$ K) and $Bi_{2.1}Sr_{1.4}Ca_{0.3}Cu_2O_y$, were obtained from a solution molten in 0.54 KCl–0.46 KF (eutectic, 600 °C) by evaporating the solvent (at a temperature of the order of 900 °C). It was reported there that the process of evaporation could be described by a first-order kinetic equation and that at constant temperature the relative amount of the evaporated solvent was directly proportional to the evaporation time. In general, KCl was not an ideal solvent for Bi cuprates because of the gravitational stratification of the melt: two liquid phases coexisting in the bulk of the melt, one of which was molten Bi–Sr–Ca cuprate at the bottom and the other was molten KCl saturated with the Bi–2212 phase above it.[264] Slow cooling of the solidified melt revealed the presence of two phases:

$$Bi_{2.2}Sr_{2.1}Ca_{0.8}Cu_2O_x \text{ and } Bi_{1.6}Sr_{0.7}Ca_{0.2}Cu_2O_x.$$

The composition of these crystals and their morphology depended on the 2212/KCl ratio in the original mixture. Sintered samples of the 1112 and 2212 composition were heated in a different experiment[281] together with an equimolar KCl + NaCl mixture to 890 °C and, after holding this temperature for 2 h in a Pt crucible, it was cooled at a rate of 4 °C/h to 630 °C and this was followed by cooling at a rate of 30–40 °C/h to room temperature. Good crystals were found in the regions above cavities. When a molten solution contained $<6\%$ of the dissolved Bi-1112 phase, it was found that Bi-2201 crystals were produced, if the proportion was $\sim 10\%$, then crystals of Bi-2212 were produced. Crystals of the Bi-2212 phase were readily formed in a KCl + NaCl melt containing 18–20% of the Bi-2212 phase. An increase in the concentration of the dissolved substance produced platelet instead of prismatic Bi-2201 crystals.

It was reported in Ref. 281 that crystals of the Bi-2212 phase could be formed only when the molten solution was rich in Cu and Ca, because this suppressed the reaction of decomposition of Bi-2212:

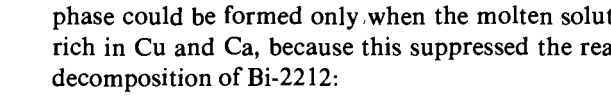

$$Bi_2Sr_2CaCu_2O_8 \rightarrow Bi_2Sr_2CuO_6 + CaCuO_2.$$

The main advantage of the molten solution method involving the use of molten halides was the ability to separate subsequently the Bi phases by washing in water or in weak electrolytes. Such washing removed the halides but did not cause deterioration of the superconducting characteristics of the crystals.

The reported results demonstrate that Bi-2212 single crystals with $T_c \sim 85$ K can be produced in a fairly reproducible manner in systems of different compositions and under different growth conditions. On the other hand, it has been found that single crystals of the 110 K phase Bi-2223 cannot be obtained in their "pure" form: only samples with both phases intergrown were obtained. Attempts have been made to prepare phases with a higher value of T_c by prolonged annealing (for 7 or more days). It has been assumed that such annealing should convert the disordered phase to the Bi-2223 phase on its own. However, the structural differences between the 2212 and the 2223 phases are very small, so that the difference between their free energies of formation is also very small, which prevents reliable separation of the conditions which would yield the two phases separately.[282] The temperature of formation of the Bi-2223 phase reported in Ref. 283 is 872–877 °C. The addition of lead reduces these temperatures to 835–869 °C. The unit cell parameters determined for single crystals of the superconducting phases, obtained in systems based on bismuth oxides, are listed in Table XII. Crystals grown by different investigators differ considerably in respect of the ratio of the main components, but in the majority of the reported cases the superconducting transition temperature is $T_c \sim 80$ K (after annealing in oxygen), i.e., it belongs to the Bi-2212 structure type. Crystals of the superconducting phases grow in the form of thin platelets; a ready cleavage, which follows from the structure of these compounds, makes it easy to split them off. It is assumed that this can be done most readily along the Bi layers, because of the anomalously large interatomic distances in the Bi layers.[260] The morphology of the growth surfaces demonstrates that the growth takes place from a solution[286] and the growth mechanism is evidently of the

TABLE XII. Unit cell parameters and values of T_c of Bi–Sr–Ca–Cu–O crystals.

Composition	Shape and dimensions of crystals, mm	Unit cell parameters, Å			T_c, K	Ref.
		a	b	c		
$Bi_4(Bi_{0,33}Sr_{3,22}Ca_{2,16})Cu_4O_y$ (2212)	5×7×(0,02—0,06)	5,3988	5,3934	30,73	78—84	[23]
$Bi_{4,4}Sr_{4,2}Ca_{1,4}Cu_4O_y$ (1112)	platelets with edge up to 10 mm	5,403	3,395	24,5	80	[6]
$Bi_{4,4}Sr_4Ca_2Cu_4O_y$ (2212)	platelets with edge up to 10 mm	5,403	3,395	30,70	80	[6]
$Bi_{4,0}Sr_{3,91}Ca_{1,51}Cu_{3,80}O_{15,97}$ (2212)	platelets with edge up to 4 mm	5,40	5,40	30,6	90	[253]
$BiSr(Ca_{0,35}Sr_{0,25}Bi_{0,40})_2Cu_2O_y$ (2212)	1,2×1,0×0,5	5,42	5,44	30,78	93	[254]
$Bi_2Sr_{0,5}Ca_2Cu_2O_x$	2×2×1	5,42	27,18	30,67	79	[256]
$Bi_4(Bi_{0,42}Sr_{3,20}Ca_{0,42})Cu_2O_y$	platelets	5,382	5,376	24,384	—	[23]
$Bi_{3,0}(Bi_{0,2}Sr_{1,8}Ca_{1,0})Cu_2O_8$	platelets	5,43	5,43	30,63	92	[257]
$Bi_2Sr_2CaCu_2O_8$	3×3×0,1	5,421	24,45	30,87	83 (midpoint of transition)	[284]
$Bi_2Sr_{3-x}Ca_xCu_2O_8$	platelets	5,399	5,414	30,90		[28]
$Pb_{0,6}Bi_2Sr_2CaCu_3O_x$	10×4×3	5,375	12,202	30,550	82	[263]
$Bi_{2,21}(Sr_{0,68}Ca_{0,32})_{2,85}Cu_2O_z$	—	5,410	—	30,87	80	[285]
$Bi_{2,09}(Sr_{0,56}Ca_{0,44})_{3,06}Cu_2O_z$		5,406	—	30,74	83	[285]
$(Bi_{0,85}Pb_{0,15})(Sr_{0,70}Ca_{0,30})_{2,69}Cu_2O_z$		5,411	—	30,76	86	[285]
$Bi_2Sr_2CaCu_2O_z$	platelets (before annealing)	5,446	5,463	30,819	75	[277]
	(after annealing)	5,417	5,419	30,746	86	[277]
$Bi_2Sr_2CaCu_2O_8$	» (before annealing)	5,413	5,421 ($xb_0 = 4,8$)	30,81	90	[270]
	(after annealing)	5,408	5,413 ($xb_0 = 4,7$)	30,81	77	[270]
$Bi_{2,01}Sr_{1,89}Ca_{0,77}Y_{0,28}Cu_{2,07}O_{8+\delta}$	—	5,406	5,409 ($xb_0 = 4,6$)	30,83	<77	[270]
$Bi_{2,06}Sr_{2,15}Y_{0,71}Cu_{2,08}O_{8+\delta}$		5,432	5,467 ($xb_0 = 4,1$)	30,23		[270]
$Bi_{2,01}Sr_{1,78}La_{0,30}Ca_{0,82}Cu_{2,10}O_{8+\delta}$		5,416	5,425 ($xb_0 = 4,6$)	30,71		[270]
$Bi_{1,99}Sr_{1,70}La_{0,43}Ca_{0,78}Cu_{2,10}O_{8+\delta}$		5,435	5,440 ($xb_0 = 4,7$)	30,55		[270]

The superstructure periodicity along the b axis, xb_0, is given in parentheses.

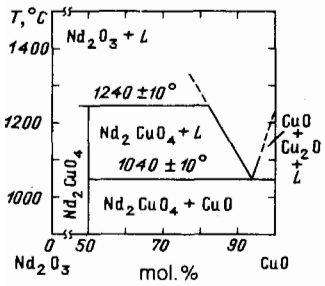

FIG. 19. Phase diagram of the Nd_2O_3–CuO system.[287]

dislocation type, because etching of the growth surfaces reveals the presence of dislocations.[288]

3.4. $M_{2-x}Ce_xCuO_{4+d}$ single crystals (M=Nd, Sm, Eu)

3.4.1. Phase diagram of the Nd_2O_3–(CeO_2)–CuO system

The phase diagrams of the Nd_2O_3–CuO and (0.85 Nd_2O_3 + 0.3CeO_2)–CuO systems were reported in Refs. 287 and 288. Neodymium cuprate Nd_2CuO_4 melts incongruently at 1240 °C and a liquidus curve below 1240 °C lies in the range of compositions between 82 and 93 mol.% CuO (Ref. 287). The systems have simple eutectics with the coordinates 1060 °C, 7.5% Nd_2O_3, 92.5% CuO (Nd_2O_3–CuO system), and 1150 °C, 6% Nd_2O_3, 94% CuO (Nd_2O_3–CeO_2–CuO system), as shown in Fig. 19, confirming that it should be possible to grow crystals of the pure and Ce-substituted neodymium cuprates from compositions of the Nd_2O_3–CeO_2–CuO system rich in copper oxide.

3.4.2. Growth of $M_{2-x}Ce_xCuO_{4+d}$ (M=Nd, Sm, Eu) single crystals

Single crystals of the Ce substituted neodymium cuprate were grown from nonstoichiometric melts with an excess of CuO and in some cases with an excess of CuO and CeO_2 (Table XIII) by the methods of slow cooling of a molten solution and spontaneous nucleation[15,287,288] or by slow cooling with a seed introduced from above,[289] or by the methods of a moving solvent[287] or partial melting.[290] Crystals formed quite readily, but the superconducting characteristics of $Nd_{2-x}Ce_xCuO_4$ single crystals were inferior to

TABLE XIII. Conditions for crystallization of $M_{2-x}Ce_xCuO_4$ (M = Nd, Sm, Eu) compound.

Compound	Composition	Method, crystallization conditions	Crucible material	Dimensions of crystals, mm³	T_c, K	Ref.
$(Nd,Ce)_2CuO_4$	15 mol.% (92.5% Nd_2O_3 + 7.5% CeO_2)–85 mol.% CuO	slow cooling in air from 1260 to 1040 °C at 15 °C/h	Pt	2×2×0.5		[287]
$Nd_{1.85}Ce_{0.15}CuO_{4-y}$	{(2 − x)Nd_2O_3 + 2xCeO_2} − CuO(50%), {(2 − x)Nd_2O_3 + 2xCeO_2} − CuO(85%)	moving solvent method, Ar + O_2 (9:1) flowing at 0.3 liters/min, rotation 30 rpm, growth rate 0.5–1 mm/h	Pt	6 mm diameter 22 mm length	10	[287]
$Nd_{1.84}Ce_{0.16}CuO_{4-y}$	Nd_2O_3 − CeO_2 − CuO Nd:Ce:Cu 35:10:55	Slow cooling from 1300 °C to 700 °C at 1.2 °C/h		10×10×0.3	21	[15]
$Nd_{2-x}Ce_xCuO_{4-y}$ (x = 0; 0.15; 0.18)	18%(Nd_2O_3 + CeO_2) − 82% CuO, 15% (Nd_2O_3 + CeO_2) − 85% CuO (mol.%)	slow cooling and seeding from above 1060 °C at 0.2–0.5 °C/h, pulling rate 0.1 mm/h	Pt	20×15×1		[289]
$Nd_{2-x}Ce_xCuO_{4+d}$ x<0.12 x≥0.12	(2 − y)/2 $Nd_2O_{3-y}CeO_2$ − CuO y = 0.29 (x = 0.14) y = 0.33 (x = 0.16)	fast (180°/h) heating to 1500 °C cooling to 1110 °C at 6 °C/h	Al_2O_3, Pt		no high-temp. supercond. (x = 0.12) 16(x = 0.14),	[291]
		fast heating to 1300 °C (160 °C/h), maintained for 6 h, cooling to 1000 °C at 6 °C/h		2×2×0.05	21(x = 0.14), ΔT_c = 5 K	
$Nd_{2-x}Ce_xCuO_4$ (x = 0.13 − 0.20)	(30 − z) $Nd_2O_{3-z}CeO_2$ − 70% CuO, 0<z<5.5 (optimal z = 4.05)	slow cooling from 1250 °C to 800 °C (5 °C/h)	Al_2O_3	3×3×0.2 10×10×0.3	23, ΔT_c = 2 K	[288]
$M_{2-z}Ce_zCuO_{4+d}$ M = Nd, z = 0.08 − 0.16, M = Sm, z = 0.04 − 0.13 M = Eu, z = 0.01 − 0.10	M_2O_3 − CeO_2 − CuO 8.21 − 1.78 − 90.01 (mol.%)	melting at 1150 °C, maintained for 6 h, cooling to 950 °C at 2.5 °C/h	Al_2O_3	2×2×0.005	4.2	[292]
	15.22 − 2.47 − 82.31 (mol.%)	melting at 1250 °C, cooling to 1050 °C at 2 °C/h, pumping out of melt through Al_2O_3	Pt	1×1×0.1 3×3×0.2		
$Nd_{2-x}Ce_xCuO_4$ (0<x<0.18)	Nd_2O_3 − CeO_2 − CuO 3.8 − 0.63 − 7.9 (g)	heating at 160 °C/h to 1320–1330 °C, cooling to 1100 °C, maintained for 50 h, and then to 25 °C, maintained for 3 h	Al_2O_3 (double crucible)	2×2.5×0.06	20	[290]

TABLE XIV. Unit cell parameters of M_2O_3–CeO_2–CuO single crystals.

Composition	a, Å	b, Å	Ref.
$Nd_{1,85}Ce_{0,15}CuO_4$	3,9479	12,039	[292]
$Sm_{1,85}Ce_{0,15}CuO_4$	3,9219	11,8086	[292]
$Eu_{1,85}Ce_{0,15}CuO_4$	3,9169	11,897	[292]
Nd_2CuO_4	3,94	12,15	[15]

those of the ceramic samples, exactly as in the case of $La_{2-x}Sr_xCuO_4$. Moreover, crystals grown in different parts of a crucible had different Ce concentrations. The limit of isomorphous incorporation of Ce in the Nd_2CuO_4 lattice was close to $x = 0.2$ (0.19 according to Ref. 291 and 0.24 according to Ref. 15). The distribution coefficient was not determined reliably: according to some data[289] it was higher than 1, whereas according to others[291] it was lower than 1.

Use of nonstoichiometric mixtures with relatively low melting points (1150 °C)[292] made it possible to grow these cuprate crystals in cavities that formed in the melt as a result of gas evolution (as in the partial melting method used to grow 123 single crystals).

These crystals were very thin platelets (Table XIII). Larger and thicker single crystals formed at higher melt temperatures (up to 1500 °C) after fast cooling. These single crystals were usually separated mechanically from the melt. It was reported in Ref. 292 that the melt was pumped out after the end of the crystallization process, which occurred between 1250 and 1050 °C, and at 1050 °C only about 30% of the initial volume remained in the molten state. This residual melt was removed from the crucible using a porous Al_2O_3 ceramic.[292] The crystals were then separated from the melt in dilute nitric acid. The result was in the form of single crystals with the tetragonal crystal lattice and the lattice parameters listed in Table XIV. According to Ref. 291, superconductivity was exhibited only by $Nd_{2-x}Ce_xCuO_{4+d}$ crystals with the Ce content 0.14–0.17 and the maximum value of T_c was obtained for $x = 0.14$. The superconducting transition appeared only after annealing in an inert (nitrogen) atmosphere at temperatures of the order of 950 °C (Ref. 288), which—according to some data (Ref. 291)—reduced the oxygen content per unit cell (the composition of the freshly prepared crystal was $Nd_{1.84}Ce_{0.16}CuO_{4.01}$, whereas after annealing in nitrogen it became $Nd_{1.84}Ce_{0.16}CuO_{3.97}$).[291]

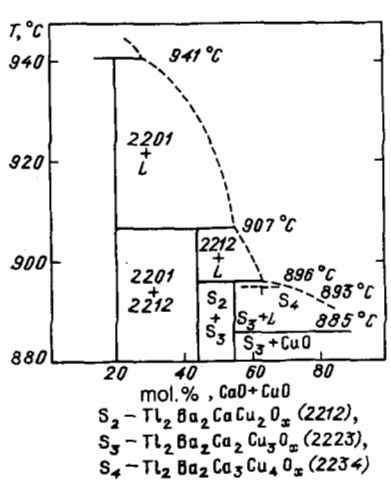

FIG. 20. Schematic phase diagram of the Tl system showing compounds with double TlO layers and the formula $Tl_2Ba_2Ca_{n-1}Cu_nO_{2n+4}$ (Ref. 297).

3.5. Single crystals of Tl cuprates

The Tl system is in many respects similar to the Ti system (Fig. 20), but because of the high toxicity of thallium, the procedures used to grow single crystals and to synthesize ceramic samples were somewhat different from those described above. It was usual to start not with a mixture of oxides or carbonates of the main elements, but with a prepared sinter material containing all the necessary components with the exception of thallium, which was added in the next stage. Eleven different structure types had been reported for the Tl–Ba–Ca–Cu–O system (Table I). Crystalline samples were usually quasisingle crystals consisting of intergrowths of two or more phases with a similar crystal structure.

Direct melting of a mixture of the oxides Tl_2O_3, BaO, CaO, and CuO in an oxygen atmosphere produced a porous dark sample with thin black platelets of $0.1 \times 0.1 \times 0.01$ mm dimensions.[35] The composition of these crystals was close to 5526 and the structure type was close to Bi-2212. It was assumed that the original thallium oxide decomposed at 850 °C yielding Tl_2O, which melted at low temperatures (of the order of 300 °C) forming a liquid phase reacting rapidly with the remaining components. Vaporization of thallium could be minimized by introducing oxygen and employing a closed crucible. The lattice parameters of single crystals obtained in this way were close to those of the Bi–2212 phase (Tables XV and XVI). The crystals were paramagnetic at room temperature and at 110 K there was a transition to the superconducting state.

The same research group later[34] produced single crystals of other Tl phases (Table XV). The initial charge was a mixture of oxides with different ratios of the components (compositions with the ratio $1 \leqslant Cu/Tl \leqslant 3$), which was placed in a Pt crucible with an internal diameter 2 mm, suspended in a vertical furnace. This crucible was heated rapidly (in 5 min) to 950 °C by moving it to the hot zone of the furnace, where it was kept for 1 h in an oxygen atmosphere. The temperature was then lowered to 700 °C in a period of 12.5 h and to 25 °C in 5–6 h. No crystals were formed when the initial temperature was below 900 °C. The solidified ingot consisted of platelets with an edge of 1–3 mm size and thickness 0.01 mm or less. Depending on the initial composition, crystals of three types were formed: their compositions were close to those of the 2223, 2212, and 1212 phases. The dominant composition was Tl-2212 and all three phases

TABLE XV. Conditions of growth of single crystals of Ti-compound superconductors.

Initial composition	Composition of single crystals	Crucible material	Maximum temperature, °C	Details of procedure	Dimensions of crystals, mm³	T_c, K	Ref.
Tl_2O_3—BaO—CaO—CuO	5526	Pt	950	cooling to 900 °C, maintained for 1 h, cooling to 750 °C at 10 °C/h	0.1×0.1×0.1	110 (onset)	[35]
$Tl_{1.8}Pb_{0.2}Ca_2Ba_2Cu_3O_x$	Tl–18, Pb–5, Ca–10, Ba–31,Cu–36%			slow cooling	1.5×1.5×0.075	60–70 (onset)	[271]
Tl_2O_3—BaO—CaO—CuO Tl:Ba:Ca:Cu 1112, 2223, 2212, 1212, 2512, 2132, 2112	2223 2122 1212	Pt	950	cooling of melt to 700 °C at 20 °C/h, to 25 °C at 120 °C/h, O_2 atmosphere	(1 – 3)×(1 – 3)×0.01	111 – 114 106 – 108 103 (before annealing)	[34]
Tl:Ba:Ca:Cu, 1346	1223			slow cooling	–	117	[293]
Tl_2O_3—BaO—CaO—CuO 2:1:1:2	2223 phase with 1223 intergrowths	Au	950	maintenance of 950 °C for 30 min, fast cooling to 900 °C, maintenance for 1 h cooling to 700 °C at 15 °C/h	0.5×0.5×0.05	105 (onset)	[294]
Tl_2O_3—BaO—CaO—CuO Tl:Ba:Ca:Cu, 1122	$TlBa_2(Ca_{0.87}Tl_{0.13})Cu_2O_7$	Al_2O_3	1250	cooling from 1250 to 1050 °C at 50 °C/h, 1050 to 700 °C at 150 °C/h, 700 to 300 °C at 250 °C/h			[295]
Tl—Ba—Ca—Cu—O	1212 2212		950	cooling 950–700 °C (5 °C/h), 700–400 °C (100 °C/h), 400–20 °C (150 °C/h), O_2 (0.8–1 liter/min)	5×3×0.3	80 105	[296]
2:1.5:2:2.5 2:(2 – 2.5):2:(3 – 3.5) 2:(3 – 7):2:(3.75 – 6.75) 2:4:24.5 = Tl:Ca:Ba:Cu	2021 2122 2223 2324		950	maintenance of 900–950 °C for 1 h, cooling to 745 °C at 10 °C/h	2×2×(0.05 – 0.2) 2×2.5×(0.05 – 0.2) 1×0.8×(0.05 – 0.2) 0.8×0.8×(0.05 – 0.2)	84 106 115–120 115 115	[297]
Tl:Ba:Ca:Cu = 2:2:1:2	2212			slow cooling in O_2 atmosphere	3×3×0.2		[298]

were present in the crystallization products of all the initial compositions investigated by this research group.[34] There was a tendency for the amount of the 2223 phase to increase when the melts contained an excess of calcium. A characteristic feature of the crystallization of Tl cuprates was the formation of syntactic intergrowths, when different phases grew epitaxially on one another. All the thallium cuprates obtained were superconductors and annealing in oxygen increased T_c by several kelvin.

Stabilization of the individual structure types was achieved by introducing other elements. For example, lead stabilized the Tl-1212 structure.[299]

3.6. Single crystals of complex cuprates

Attempts to modify the familiar structure types of superconducting cuprates have led to the discovery of a number of new cuprates with a more complex chemical composition and usually forming new types of structure. They include the following complex cuprates

$$Pb_2Sr_2(Y_{0.75}Ca_{0.25})Cu_3O_{8+\delta},$$

$$(Y_{1-x}Ca_x)Sr_2(Cu_{3-y}Pb_y)O_z,$$

$$Bi_2(Sr_{1-x}Ln_x)_2(Gd_{1-y}Ce_y)_2Cu_2O_{10+\delta},$$

TABLE XVI. Unit cell parameters of single crystals belonging to the Tl system.

Composition	Unit cell parameters, Å			Ref.
	a	b	c	
5526 (close in structure to Bi-2212)	5,467	—	29,306	[35]
1112 (Pb)	3,863	3,863	12,741	[271]
2212	5,458	5,467	29,306	[34]
1212	5,452	—	29,75	[34]
1112	3,8472	—	12,721	[294]
2212	3,856	—	29,34	[298]

whose single crystals were obtained in the investigations reported in Refs. 38, 42, 300, and 301.

Single crystals of $Pb_2Sr_2Y_{0.75}Ca_{0.25}Cu_3O_{8+\delta}$ were grown by immersion in molten PbO—CuO using the method of preparation of "precursors" described in Ref. 39. Platelet crystals of $2.5\times2.5\times0.5$ mm dimensions with the lattice parameters $a = 5.371(6)$ Å, $b = 5.457(6)$ Å, $c = 15.708$ Å were reported in Ref. 300. Twin boundaries were readily visible in these platelets when they were examined in polarized light. The temperature of the transition to the superconducting state was 21 K.

Compounds with the formula $(Y_{1-x}Ca_x)Sr_2(Cu_{3-y}Pb_y)O_{7-\delta}$ could be regarded as of the Y-123 structure type in which some of the Y and Cu atoms were replaced with Ca and Pb. Single crystals with $x = 0.13$ or 0.15 and $y = 0.69$ or 0.71 did not undergo the transition to the superconducting state.[42,301,302] This provided a further confirmation that isomorphous impurities in Y-123 caused deterioration of the superconducting characteristics of this compound. The superconducting compositions were identified in Ref. 42 as those with $c = 0.25$, 0.30, or 0.35 and $y = 0.65$.

Crystals with $x = 0.46$ and $y = 0.25$ were prepared by the floating zone method using optical heating.[303] The linear recrystallization rate was 30 mm/h. Textured ingots contained single crystals of $0.5\times0.5\times0.1$ mm dimensions with $T_c < 40$ K and the structure of the single-crystal phase was of the Y-123 or Tl-1212 type.

Single crystals of the third new cuprate, $Bi_2(Sr_{1-x}Ln_x)_2(Gd_{1-y}Ce_y)_2Cu_2O_{10+\delta}$, were prepared by crystallization from a molten CuO solution (melting at 1150 °C, slow cooling at a rate of 3 °C/min to 1000 °C, and then cooling in air). The size of Bi-2222 single crystals was $0.425\times0.07\times0.003$ mm and the chemical composition corresponded to

$$Bi_{1,931}Sr_{1,802}Gd_{1,720}Ce_{0,455}Cu_{2,00}O_{10,16},$$

or, in the idealized form,

$$Bi_2(Sr_{0,9}Ce_{0,1})_2(Gd_{0,87}Ce_{0,13})_2Cu_2O_{10+\delta}.$$

These crystals had orthorhombic symmetry, the space group was *Cmmb*, and the unit cell parameters were $a = 5.435$ Å, $b = 5.446$ Å, $c = 17.826$ Å. Superstructural reflections were observed along the b and c axes: $b = 9b_0 = 49.06$ Å, $c = 2c_0 = 35.66$ Å (Ref. 38).

3.7. Single crystals of $Ba_{1-x}K_xBiO_3$

The transition to the superconducting state in the Ba–K–Bi–O system has been observed in the compound $Ba_{1-x}K_xCuO_3$ with the primitive cubic lattice of perovskite type and compositions in the range $0.25\leqslant x\leqslant0.4$ (Refs. 7, 8, and 239). Direct fusion of the oxides Bi_2O_3, BaO, and K_2O usually produces a multiphase polycrystalline sample; this procedure is carried out in evacuated Ag tubes. Bulk single-phase polycrystalline Ba–K–Bi–O samples with $T_c \sim 30$ K were reported in Ref. 308 and they were grown from a specially treated mixture of oxides.

Single crystals of $Ba_{1-x}K_xBiO_3$ ($x = 0.37$) of 0.03–0.3 mm size were formed[8] by dehydration of the melt $KOH\cdot nH_2O$, containing $Ba(OH)_2Bi_2O_3$; the growth took place at 400–475 °C in air or in oxygen. Crystals with $x = 0.37$ had the primitive cubic lattice with $a = 4.2869$ Å and at $x\sim0.25$ the lattice exhibited orthorhombic distortions.[8] The maximum value of $T_c = 30.5$ K was obtained for $x\sim0.4$.

Microcrystals of $Ba_{1-x}K_xBiO_3$ were also prepared[305] by heating a mixture of $Ba(OH)_2\cdot8H_2O$, Bi_2O_3, and KOH in air at 360 °C. These crystals had the cubic lattice parameter $a = 4.3223$ Å and the space group was $Pm3m$. The compounds with the parameter $a\sim4.3$ Å exhibited superconductivity in the Ba–K–Bi–O system.[304,305]

3.8. Single crystals of $BaPb_{1-x}M_xO_3$ (M = Bi, Sb)

The Ba–Pb–(Bi)–O system has been known for some time: the first single crystals were prepared by crystallization from a molten solution using the following solvents: KCl (Refs. 241 and 70), PbO_2, and PbO_2–Bi_2O_3 (Refs. 306 and 307); the relevant data are given in Table XVII.

When PbO_2–Bi_2O_3 mixtures were used as the flux, it was found that crystals grew on the surface of the melt[307] because of the similarity of the densities of the crystallizing $Ba(Pb, Bi)O_3$ and PbO_2–Bi_2O_3 materials and because of

TABLE XVII. Conditions for growth of $BaPb_{1-x}M_xO_3$ (M = Bi, Sb) single crystals.

Composition	Details of procedure, composition of system	Maximum temperature, crystallization method	Dimensions of crystals, mm	T_c, K	Ref.
$BaPb_{1-x}Bi_xO_3$ ($x = 0.3$; 0.38)	crystallization from solution in molten BaO–PbO_2–Bi_2O_3, 15–70–15 mol.% ($x = 0.3$), 20–60–20 mol.% ($x = 0.38$)	1050 °C (10 h), slow cooling (30 h) to 780–860 °C; decantation of melt; $\Delta T = 10$ °C	platelets, 15×15	10.4 (onset) ($x = 0.3$), semicond. up to 4.3 K ($x = 0.38$)	[307]
$BaPb_{1-x}Bi_xO_3$ ($0<x<0.3$)	hydrothermal synthesis, 4.5 mol KCl	400–450 °C, $\Delta T = 20$–30°, (3–5 °C/cm), $P = 1000$ kg/cm^2	$3\times3\times1$	11.7 (onset) ($x = 0.24$), $\Delta T_c = 1.8$	[308] [309]
$BaPb_{1-x}Bi_xO_3$ ($x = 0.2$; 0.25; 0.3)	hydrothermal synthesis, 3 mol NaOH	400–450 °C, $\Delta T = 30$ °C, 100 MPa	$2\times2\times2$ ($x = 0.2$), $5\times5\times4$ ($x = 0.25$; 0.3)	9.8($x = 0.2$), 11.7($x = 0.25$), $\Delta T_c = 1.6$ K, 9.2($x = 0.3$)	[74]
$BaPb_{0.75}Sb_{0.25}O_3$	crystallization from solution in molten PbO, PbO–$BaCO_3$–Sb_2O_3, 48.080–13.515–1.456 (g)	1150 °C (3 h), cooling at 4 °C/h to 750 °C, maintained for 24 h, cooling with furnace	1–2 mm	3.5	[43]

the low viscosity of the melt. It was found that this process occurred during slow cooling of the molten solution (Table XVII) when a vertical temperature gradient was maintained (the temperature at the bottom of the crucible was higher by 10 °C than on the surface). After cooling to temperatures of the order of 780–860 °C (depending on the Pb/Bi ratio in the original charge) the melt was decanted. The lower the decantation temperature, the larger the resultant crystals (plates of 12×12 mm^2 area were obtained at 840 °C and this area increased to 15×15 mm^2 at 820 °C). Crystals of $BaPb_{1-x}Bi_xO_3$ were prepared under these conditions.

The crystals with $x = 0.3$ exhibited the superconducting transition at 10.4 K, whereas those with $x = 0.38$ showed no transition when they were cooled right down to 4.3 K (Ref. 243).

The compound $BaPb_xBi_{1-x}O_3$ was practically the only one among the high-temperature superconductors, and could be obtained in the form of single crystals by crystallization from aqueous media, i.e., by the hydrothermal crystallization method. These crystals were formed in near-neutral or alkaline solutions of KCl or NaCl (Refs. 308 and 309), or NaOH (Ref. 67). The crystallization occurred in sealed Au ampoules at temperatures of the order of 400 °C in the solution zone. The necessary temperature was determined by the value of x: the higher the x for the original $BaPb_{1-x}Bi_xO_3$ charge, the higher the temperature needed to obtain single crystals. The distribution coefficient was less than unity (0.8) for the crystallization from chloride solutions,[308] but it was unity for alkaline solutions.[67] The chloride solutions yielded crystals with $x < 0.3$, whereas the solutions in NaOH produced crystals with $0\leqslant x\leqslant 1$.

According to Ref. 67, crystals grown by the hydrothermal method were of higher quality than those grown from molten solutions and were characterized by narrower $\Delta T\approx 1.8$ K) transition to the superconducting state.

A typical form of $Ba(Pb,Bi)O_3$ single crystals obtained by us from alkaline hydrothermal solutions is shown in Fig. 21. The perovskite structure was retained after partial replacement of lead with antimony, but the temperature of the transition to the superconducting state fell strongly (down to 3.5 K). Single crystals of the Sb modification of the perovskite structure were obtained by crystallization from a molten solution (Table XVII, Ref. 43). These crystals formed on deviation of the composition of the system being grown from the intended one within the limits of $\pm$ 15% Sb.

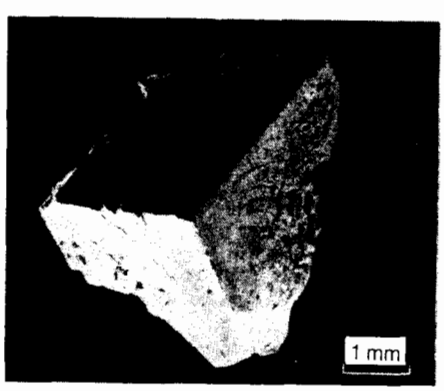

FIG. 21. Typical $Ba(Pb, Bi)O_3$ single crystals.

Samples with $x\geqslant 0.35$ showed no superconducting transition.

4. CONCLUSIONS

In spite of the great variety of the methods used to grow single crystals of high-temperature superconductors, the range of optimal crystal growth methods is very limited. The similarity of these structural and chemical properties (because the majority of the high-temperature superconductors are complex tetragonal and pseudotetragonal cuprates) is responsible for the similarity of the technology used in growth of single crystals of high-temperature superconductors. The incongruent nature of melting of high-temperature superconductors determines *a priori* the advantages of the molten solution crystallization method. The negative influence of impurities on the superconducting characteristics (with the exception of the Pb impurity in the Bi systems) has made it necessary to search for solvents among the compounds of the investigated systems with the lowest melting points. These compounds are copper and bismuth oxides and barium cuprates. In the case of the ternary La_2O_3–(SrO)–CuO system a suitable solvent is copper oxide. In the case of more complex systems this oxide is no longer the optimal solvent. For example, the eutectic with the BaO–CuO 72/28 mol.% composition, with the lowest melting point, is optimal for the Y_2O_3–BaO–CuO system.

At lower temperatures the probability of contamination of single crystals by partial dissolution of the crucible materials is less, which—together with the high solubility—means that eutectic mixtures are preferred as solvents.

More complex systems with four or more components, such as

$$Bi_2O_3—SrO—CaO—CuO,\ Tl_2O_3—BaO—CaO—CuO,$$
$$Bi_2O_3—PbO—SrO—CaO—CuO$$

and others follow the same general rule. In their case the best method for growing single crystals is again crystallization from a molten solution containing excess (relative to the stoichiometry of the compound being grown) low-melting-point components of the problem. To distinguish this method from the standard method of crystallization from a solution in a melt of a low-melting-point substance it is more logical to describe the method of crystallization of HTSC as the method of crystallization from component nonstoichiometric melts.

Growth of crystals from nonstoichiometric melts has been studied along two directions: crystallization with partial melting and that with complete melting; in the former case the growth of crystals occurs in local parts of the volume of a charge and it usually occurs in cavities that form as a result of evolution of gas bubbles. In the latter case, depending on the experimental method, growth of crystals may occur on the surface of the melt, at the bottom of a crucible, or on one of the side walls of a crucible (depending on the direction of the temperature gradient).

The general approach to the process of crystallization from nonstoichiometric melts applies equally to different cuprates: the procedure involves heating until the charge melts, maintenance of a selected temperature for a certain time (usually several hours) in order to homogenize the

melt, and slow cooling of the melt to the spontaneous crystallization temperature.

Beyond this general scheme there are possible variants.

One can lower the temperature to the room value rather slowly (sometimes in stages) or be removed by decantation or pumping out. The advantages and shortcomings of these techniques have been discussed above in the case of specific systems of compounds.

The growth process may be initiated in a variety of ways: one can introduce rods of a foreign material (for example, Pt) into the melt or seeds made of structurally similar compounds or seeds of the compound being crystallized or one can create deliberately cavities in the interior of the melt (double crucible method). In the case of complex systems it has not yet been possible to localize single-crystal growth in this way, in contrast to the usual refractory compounds. Seeds are, however, promising in the case of simpler systems (La–Sr–Cu–O, Nd–Ce–Cu–O) and they have been used to grow large single crystals of the (La, Sr) and (Nd, Ce) cuprates.

Naturally, the apparent simplicity of the general approach to the process of crystallization fails to make clear all the difficulties that await experimentalists trying to grow single crystals of high-temperature superconductors. Each compound requires the development of individual growth methods, which sometimes have to be very precise, and this includes the temperature profile of the process (both in time and space), the duration of each stage, the composition of the growth atmosphere and of the original charge, etc.

The kinetic features of the process crystallization of high-temperature superconductors (low growth rates at right-angles to the c axis) mean that the process of growth has to be prolonged, but an increase in the duration of contact between high-temperature strongly reactive melts with crucibles results in the accumulation of impurities in the melt because of partial dissolution of the crucible material. Such impurities are captured by a growing crystal and cause deterioration of its characteristics. It is then necessary to adopt a reasonable compromise and select moderate durations [for example several days in the case of the (Y, Ba) cuprate]. The search for solvents suitable for growing single crystals of ternary systems

$$La_2O_3—SrO—CuO,\ Ln_2O_3—BaO—CuO$$

has proved largely fruitless and excess amounts of the component oxides are used. On the other hand, in the case of systems with four or five components such as

$$Bi_2O_3—SrO—CaO—CuO,\quad Bi_2O_3—PbO—SrO—CaO—CuO$$

another method of growing single crystals has proved effective: it involves the standard crystallization from a molten solution using low-melting-point salts (for example, alkali halides) as the flux materials.

Fast methods for growing single crystals of high-temperature superconductors (fast heating to the melting point by optical radiation and rapid cooling, growth rates of the order of 10^{-3}–10^{-2} cm/s)[64] suffer from high temperature gradients at the crystallization front. The result is a polycrystalline ingot from which separate crystals of small dimensions can be separated.

The traditional method of gas-flame crystallization

FIG. 22. Single crystals of $Bi_2Sr_2CaCuO_4$ grown by the Verneuil method.

(Verneuil method) has not proved popular in the preparation of high-quality single crystals, although polycrystalline boules of high-temperature superconducting cuprates have been grown successfully by this method.[310] As in the case of the fast crystallization from droplets of the melt, the Verneuil method can readily yield small crystals (of <1 mm size) on the surface of a boule (Fig. 22).[310]

These methods of fast crystallization of the melt droplets by optical heating and the Verneuil method of gas-flame heating are similar in their results to the method of laser pulling from a pedestal.[28,311] Once again the high temperature gradient at the growth front makes it possible to increase greatly the growth rate compared with the growth of bulk single crystals and the increase is by about two orders of magnitude. However, the high uncontrolled temperature gradients are responsible for the fact that the samples are textured.

The high crystallization rates attainable in the last three methods are important from the point of view of possible quenching of metastable phases needed in detailed studies.

The methods of directional crystallization (zone melting) usually produce textured samples of the investigated cuprate systems and single crystals can be cleaved from these samples. This method gives the best results in the case of the Bi system, which may be due to the fact that the nature of melting of (Bi, Sr, Ca) cuprates is less incongruent than that of (Y, Ba) cuprates. In principle, in the case of a smooth crystallization front and controlled motion of this front it should be possible to grow a single crystal or several large single-crystal blocks, as indeed is found in the case of the La–Sr–Cu–O system.

A special place among the high-temperature superconductors is occupied by the noncuprate compounds based on barium bismuthate. In the case of one of them, barium bismuthate plumbate, good results have been obtained by the hydrothermal method of single crystal growth. In the case of the remaining high-temperature superconducting materials the degradation of compounds due to prolonged contact with water excludes the traditional method of hydrothermal synthesis with aqueous solvents.

It follows that intensive investigations of physicochemical properties of multicomponent systems and the search for methods of growing single crystals have led to identification

of a number of methods which are promising for growing single crystals of high-temperature superconductors of different compositions.

We are now at the stage where detailed work will be needed on determination and refinement of the phase diagrams, modernization of the known methods, search of ways of altering in a deliberate manner the morphology of single crystals without deterioration of the superconducting properties, and methods for preparation of high-quality single crystals.

The author is deeply grateful to his colleagues at the Institute of Crystallography of the USSR Academy of Sciences, S. M. Stishov, A. B. Bykov, and G. D. Ilyushin for their constant interest and help in writing this review.

[1]J. G. Bednorz and K. A. Muller, Z. Phys. B **64**, 189 (1986).
[2]M. K. Wu, *et al.* Phys. Rev. Lett. **58**, 908 (1987).
[3]P. M. Lambert, *et al.*, J. Solid State Chem. **75**, 332 (1988).
[4]A. W. Sleight, *et al.*, Solid State Commun. **17**, 27 (1975).
[5]L. F. Schneemeyer, *et al.*, Nature (London) **332**, 422 (1988).
[6]M. Hikita, *et al.*, J. Cryst. Growth **91**, 282 (1988).
[7]D. G. Hinks, *et al.*, Nature (London) **333**, 836 (1988).
[8]L. F. Schneemeyer, *et al.*, Nature (London) **335**, 421 (1988).
[9]M. A. Damento, *et al.*, Appl. Phys. Lett. **51**, 690 (1987).
[10]J. D. Jorgensen, *et al.*, Phys. Rev. B **38**, 11337 (1988).
[11]M. Onoda, *et al.*, Jpn. J. Appl. Phys. Part 2 **26**, L363 (1987).
[12]Y. Tokura, *et al.*, Nature (London) **337**, 345 (1989).
[13]H. Sawa, *et al.*, Nature (London) **337**, 347 (1989).
[14]M. Kosuge, Jpn. J. Appl. Phys. Part 2 **28**, L49 (1989).
[15]Y. Hidaka and M. Suzuki, Nature (London) **338**, 635 (1989).
[16]J. E. Greedan, *et al.*, Phys. Rev. B **35**, 8770 (1987).
[17]J. Karpinski, *et al.*, Physica C (Utrecht) **153–155**, 830 (1988).
[18]P. Marsh, *et al.*, Nature (London) **334**, 141 (1988).
[19]S. Kemmler-Sack, *et al.*, J. Less-Common Met. **144**, L1 (1988).
[20]C. Michel, *et al.*, Z. Phys. B **68**, 421 (1987).
[21]J. Akimitsu, *et al.*, Jpn. J. Appl. Phys. Part 1 **26**, 2080 (1987).
[22]H. Maeda, *et al.*, Jpn. J. Appl. Phys. Part 2 **27**, L209 (1988).
[23]A. Ono, *et al.*, Jpn. J. Appl. Phys. Part 2 **27**, L786 (1988).
[24]C. W. Chu, *et al.*, Phys. Rev. Lett. **60**, 941 (1988).
[25]S. Sueno, *et al.*, Jpn. J. Appl. Phys. Part 2 **27**, L1463 (1988).
[26]H. W. Zandbergen, *et al.*, Nature (London) **332**, 620 (1988).
[27]S. Adachi, *et al.*, Jpn. J. Appl. Phys. Part 2 **28**, L209 (1989).
[28]D. Gazit and R. S. Feigelson, J. Cryst. Growth **91**, 318 (1988).
[29]Z. Z. Sheng and A. M. Hermann, Nature (London) **332**, 55 (1988).
[30]D. Dem-Haughes, Met. Mater. **14**, 741 (1988).
[31]H. Kusuhara, *et al.*, Jpn. J. Appl. Phys. Part 2 **28**, L1772 (1989).
[32]T. Mochiku, *et al.*, Jpn. J. Appl. Phys. Part 2 **29**, L588 (1990).
[33]T. Itoh, *et al.*, Jpn. J. Appl. Phys. Part 2 **27**, L559 (1988).
[34]D. S. Ginley, *et al.*, J. Cryst. Growth **91**, 456 (1988).
[35]B. Morosin, *et al.*, Physica C (Utrecht) **152**, 222 (1988).
[36]Z. Z. Sheng, *et al.*, Phys. Rev. Lett. **60**, 937 (1988).
[37]Y. Tokura, *et al.*, Nature (London) **342**, 890 (1989).
[38]I. Nakai, *et al.*, Jpn. J. Appl. Phys. Part 2 **29**, L572 (1990).
[39]R. J. Cava, *et al.*, Nature (London) **336**, 211 (1988).
[40]N. W. Zandbergen, *et al.*, Physica C (Utrecht) **159**, 81 (1989).
[41]H. Sawa, *et al.*, J. Phys. Soc. Jpn. **58**, 2259 (1989).
[42]A. Ono and Y. Uchida, Jpn. J. Appl. Phys. Part 2 **29**, L586 (1990).
[43]R. J. Cava, *et al.*, Nature (London) **339**, 291 (1989).
[44]V. I. Simonov, *et al.*, Pis'ma Zh. Eksp. Teor. Fiz. **48**, 290 (1988) [JETP Lett. **48**, 323 (1988)].
[45]K. Yamada, *et al.*, Jpn. J. Appl. Phys. Part 1 **27**, 1132 (1988).
[46]B. Dabrowski, *et al.*, Physica C (Utrecht) **162–164**, 99 (1989).
[47]C. Chaillout, *et al.*, Physica C (Utrecht) **162–164**, 57 (1989).
[48]J. D. Jorgensen, *et al.*, Phys. Rev. B **36**, 3608 (1987).
[49]S. Sueno, *et al.*, Jpn. J. Appl. Phys. Part 2 **26**, L842 (1987).
[50]M. A. Alario-Framo, *et al.* Physica C (Utrecht) **156**, 455 (1988).
[51]J. Narayan, *et al.*, J. Opt. Microsc. **1**, 18 (1989).
[52]J. P. Zhang, *et al.*, Supercond. Sci. Technol. **1**, 132 (1988).
[53]S. Nakajima, *et al.*, Physica C (Utrecht) **158**, 471 (1989).
[54]M. Verwerft, *et al.*, Physica C (Utrecht) **156**, 607 (1988).
[55]D. E. Cox, *et al.*, Phys. Rev. B **38**, 6624 (1988).
[56]R. V. Kasowski, Phys. Rev. B **38**, 6470 (1988).
[57]M. Kikuchi, *et al.*, Physica C (Utrecht) **158**, 79 (1989).
[58]R. Hull, *et al.*, Phys. Rev. B **39**, 9685 (1989).
[59]H. W. Zandbergen, *et al.*, J. Cryst. Growth **96**, 716 (1989).
[60]A. R. Yavari, *et al.*, J. Cryst. Growth, **91**, 290 (1988).
[61]T. Hakada, *et al.*, Mon. J. Inst. Ind. Sci. Univ. Tokyo **40**, 279 (1988).
[62]T. R. Dinger, *et al.*, Phys. Rev. Lett. **58**, 2687 (1987).
[63]H. Katayama-Yoshida, *et al.*, Jpn. J. Appl. Phys. Part 1 **26**, 2007 (1987).
[64]I. P. Kazakov, Preprint No. 167 [in Russian], Lebedev Physics Institute, Academy of Sciences of the USSR, Moscow (1989).
[65]L. Trovilleux, *et al.*, J. Cryst. Growth **91**, 268 (1988).
[66]J. E. Zhang, *et al.*, Mater. Lett. **8**, 46 (1989).
[67]A. Katsui, Jpn. J. Appl. Phys. Part 2 **27**, L844 (1988).
[68]A. Katsui and H. Ohtsuka, J. Cryst. Growth **91**, 261 (1988).
[69]H. J. Shell and F. Licci, J. Cryst. Growth **85**, 607 (1987).
[70]A. Katsui and M. Suzuki, Jpn. J. Appl. Phys. Part 2 **21**, L157 (1982).
[71]S. Shamoto, *et al.*, Solid State Commun. **66**, 195 (1988).
[72]B. M. Wanklyn, *et al.*, Solid State Commun. **66**, 441 (1988).
[73]K. Watanabe, J. Cryst. Growth **100**, 393 (1990).
[74]S. Hirano, J. Cryst. Growth **85**, 602 (1987).
[75]R. A. Laudise, *et al.*, J. Cryst. Growth **85**, 569 (1987).
[76]L. F. Schneemeyer, *et al.*, Nature (London) **328**, 601 (1987).
[77]D. L. Kaiser, *et al.*, Appl. Phys. Lett. **51**, 1040 (1987).
[78]C. Thomsen, *et al.*, Phys. Rev. B **37**, 9860 (1988).
[79]B. N. Sun, *et al.*, Physica C (Utrecht) **157**, 189 (1989).
[80]A. B. Bykov, *et al.*, J. Cryst. Growth **91**, 30 (1988).
[81]T. Hibiya *et al.*, Jpn. J. Appl. Phys. Part 2 **28**, L63 (1989).
[82]L. N. Dem'yanets, *et al.*, *Extended Abstracts of Papers presented at Sixth All-Union Conf. on Crystal Growth*, Moscow, 1988 [in Russian], Vol. 2, p. 364.
[83]G. Calestani, *et al.*, Solid State Commun. **66**, 223 (1988).
[84]Y. Laligant, *et al.*, Europhys. Lett. **4**, 1023 (1987).
[85]P. Ströbel, *et al.*, Physica C (Utrecht) **156**, 434 (1988).
[86]A. B. Bykov, *et al.*, Kristallografiya **35**, 869 (1990) [Sov. Phys. Crystallogr. **35**, 511 (1990)].
[87]M. B. Kosmyna, *et al.*, *Abstracts of Papers presented at First All-Union Conf. on High-Temperature Superconductivity*, Kharkov, 1988 [in Russian], Vol. 3, p. 82.
[88]H. J. Shell, W. Sadowski, *et al.*, Supercond. Sci. Technol. **2**, 17 (1989).
[89]H. J. Shell and F. Licci, Mater. Res. Bull. **13**, 56 (1988).
[90]C. Chen, *et al.*, J. Cryst. Growth **91**, 659 (1988).
[91]P. J. Picone, *et al.*, J. Cryst. Growth **91**, 463 (1988).
[92]Y. Hidaka, *et al.*, Rev. Electr. Commun. Lab. **36**, 567 (1988).
[93]G. A. Emel'chenko, *et al.*, Izv. Akad. Nauk SSSR Neorg. Mater. **26**, 1560 (1990).
[94]K. Oka and M. Unoki, Jpn. J. Appl. Phys. Part 2 **26**, L1590 (1987).
[95]G. A. Emel'chenko, *et al.*, Sverkhprovodimost' (KIAE) **3**, 140 (1990) [Superconductivity **3**, 134 (1990)].
[96]D. M. De Leeuw, *et al.*, J. Solid State Chem. **80**, 276 (1989).
[97]L. Er. Rakho, *et al.*, J. Solid State Chem. **73**, 514 (1988).
[98]Chr. L. Teske and H. M. Müller-Buschbaum, Z. Anorg. Allg. Chem. **379**, 234 (1970).
[99]Chr. L. Teske and H. M. Müller-Buschbaum, Z. Anorg. Allg. Chem. **371**, 325 (1969).
[100]Chr. L. Teske and H. M. Müller-Buschbaum, Z. Anorg. Allg. Chem. **379**, 113 (1970).
[101]H. Haas and E. Kordes, Z. Kristallogr. Kristallgeom. Kristallphys. Kristallchem. **129**, 259 (1969).
[102]G. Demazeau, *et al.*, Mater. Res. Bull. **7**, 913 (1972).
[103]A. R. Schulze and H. M. Müller-Buschbaum, Z. Anorg. Allg. Chem. **471**, 59 (1980).
[104]J. M. Longo and M. Racah, J. Solid State Chem. **6**, 526 (1973).
[105]B. Grande, *et al.*, Z. Anorg. Allg. Chem. **428**, 120 (1977).
[106]Y. Hidaka, *et al*, Jpn. J. Appl. Phys. Part 2 **26**, L377 (1987).
[107]D. E. Cox, *et al.*, J. Mater. Res. **3**, 1327 (1988).
[108]S. W. Cheong, *et al.*, Phys. Rev. B **37**, 5916 (1988).
[109]A. I. Maksimov, *et al.*, Solid State Commun. **66**, 1077 (1988).
[110]P. J. Picone, *et al.*, J. Cryst. Growth **85**, 576 (1987).
[111]Y. Hidaka and T. Murakami, Kotai Butsuri **23**, 743 (1988).
[112]T. Inoue, *et al.*, Jpn. J. Appl. Phys. Part 2 **26**, L732 (1987).
[113]V. V. Voronkov, *et al.*, *Abstracts of Papers presented at First All-Union Conf. on High-Temperature Superconductivity*, Kharkov, 1988 [in Russian], Vol. 3, p. 193.
[114]I. Tanaka and M. Kojima, Nature (London) **337**, 21 (1989).
[115]C. Chen, *et al.*, Solid State Commun. **66**, 611 (1988).
[116]R. Yoshizaki, *et al.*, Jpn. J. Appl. Phys. Part 2 **26**, L311 (1987).
[117]T. Iwazumi, *et al.*, Jpn. J. Appl. Phys. Part 2 **26**, L386 (1987).
[118]A. S. Ivanov, *et al.*, Sverkhprovodimost' (KIAE) **2**(2), 21 (1988).

[119]H. Hasegawa, *et al.*, Jpn. J. Appl. Phys. Part 2 **26**, L673 (1987).
[120]S. Shamoto, *et al.*, Solid State Commun. **66**, 1151 (1988).
[121]I. Tanaka, *et al.*, J. Cryst. Growth **96**, 711 (1989).
[122]V. I. Voronkova and V. K. Yanovskiĭ, Sverkhprovodimost' (KIAE) 2(4), 81 (1989) [Superconductivity **2**, 101 (1989)].
[123]K. V. Gamayunov, *et al.*, *Abstracts of Papers presented at Second All-Union Conf. on High-Temperature Superconductivity*, Kiev, 1989 [in Russian], Vol. 2, Kiev (1989), p. 333.
[124]V. G. Veselago, *et al.*, Preprint No. 68 [in Russian], Institute of General Physics, Academy of Sciences of the USSR, Moscow (1989), p. 18.
[125]T. Onoda, *et al.*, Jpn. J. Appl. Phys. Part 2 **26**, L771 (1987).
[126]H. Oka, *et al.*, Bull. Electrotech. Lab. **52**, 764 (1988).
[127]K. Suzuki, *et al.*, Jpn. J. Appl. Phys. Part 2 **27**, L814 (1988).
[128]S. N. Barilo, *et al.*, Sverkhprovodimost' (KIAE) 2(8), 138 (1989) [Superconductivity **2**, 158 (1989)].
[129]A. B. Bykov, *et al.*, Pis'ma Zh. Eksp. Teor. Fiz. **46**, Prilozh. 19 (1987) [JETP Lett. **46**, Suppl., S15 (1987)].
[130]L. A. Muradyan, *et al.*, Kristallografiya **35**, 861 (1990) [Sov. Phys. Crystallogr. **35**, 506 (1990)].
[131]S. Takekawa and N. Iyi, Jpn. J. Appl. Phys. Part 2 **26**, L851 (1987).
[132]J. Zhang, *et al*, Supercond. Sci. Technol. **1**, 107 (1988).
[133]R. K. Grebenshchikov, *et al.*, *Abstracts of Papers presented at First All-Union Conf. on High-Temperature Superconductivity*, Kharkov, 1988 [in Russian], Vol. 3, p. 74.
[134]K. Oka, *et al.*, Jpn. J. Appl. Phys. Part 2 **27**, L1065 (1988).
[135]M. Neviva, *et al.*, J. Cryst. Growth **91**, 434 (1988).
[136]M. Neviva, *et al.*, Thermodyn. Acta **127**, 395 (1988).
[137]V. I. Shitova, *et al.*, Sverkhprovodimost' (KIAE) 2(9), 59 (1989) [Superconductivity **2**, 69 (1989)].
[138]M. Maeda, *et al.*, Jpn. J. Appl. Phys. Part 1 **28**, 1417 (1989).
[139]I. K. Garkushin, *et al.*, *Physicochemical Basis of Preparation of High-Temperature Superconducting Materials (Reference Data)* [in Russian], Sverdlovsk (1989), p. 27.
[140]S. R. Roth, *et al.*, Adv. Ceram. Mater. **2**, 303 (1987).
[141]T. Aselage and K. Keefer, J. Mater. Res. **3**, 1279 (1988).
[142]A. Ono and T. Tanaka, Jpn. J. Appl. Phys. Part 2 **26**, L825 (1987).
[143]J. Takada, *et al.*, Jpn. J. Appl. Phys. Part 2 **26**, L1707 (1987).
[144]F. Holtzberg, *et al.*, in *Chemistry of High-Temperature Superconductors* (Proc. Conf., New Orleans, LA, 1987, ed. by D. L. Nelson, M. S. Whittingham, and T. F. George), publ. by American Chemical Society, Washington, DC (1987), p. 79 [ACS Symposium Series, Vol. 351).
[145]F. Holzberg, *et al.*, J. Magn. Mater. **76–77**, 626 (1988).
[146]G. Balestrino, *et al.*, J. Cryst. Growth **85**, 585 (1987).
[147]F. Licci, *et al.*, J. Less-Common Met. **150**, 201 (1989).
[148]J. Z. Liu, *et al.*, Phys. Lett. A **121**, 305 (1987).
[149]K. Fisher, *et al.*, Cryst. Res. Technol. **23**, 1171 (1988).
[150]K. Oka, *et al.*, Jpn. J. Appl. Phys. Part 2 **28**, L219 (1989).
[151]K. Oka and H. Unoki, J. Cryst. Growth **99**, 922 (1990).
[152]T. Konaka, *et al.*, J. Cryst. Growth **91**, 278 (1988).
[153]H. Takei, *et al.*, Jpn. J. Appl. Phys. Part 2 **26**, L1425 (1987).
[154]S. N. Barilo, *et al.*, *Abstracts of Papers presented at Second All-Union Conf. on High-Temperature Superconductivity*, Kiev, 1989 [in Russian], Vol. 2, Kiev (1989), p. 320.
[155]D. L. Kaiser, *et al.*, J. Cryst. Growth **85**, 593 (1987).
[156]K. Hayashi, *et al.*, Jpn. J. Appl. Phys. Part 2 **26**, L1240 (1987).
[157]I. B. Bobylev, *et al.*, Sverkhprovodimost' (KIAE) **3**, 504 (1990) [Superconductivity **3**, 479 (1990)].
[158]J. G. Huang, *et al.*, Supercond. Sci. Technol. **1**, 110 (1988).
[159]J. McKittrick, *et al.*, J. Appl. Phys. **65**, 3662 (1989).
[160]X. Z. Zhou, *et al.*, J. Phys. D **20**, 1542 (1987).
[161]A. Ono, *et al.*, Jpn. J. Appl. Phys. Part 2 **27**, L340 (1988).
[162]J. P. Rice, *et al.*, J. Low Temp. Phys. **72**, 245 (1988).
[163]K. L. Klester, *et al.*, J. Cryst. Growth **91**, 295 (1988).
[164]C. N. W. Darlington, *et al.*, J. Cryst. Growth **91**, 308 (1988).
[165]S. Hayashi, *et al.*, Jpn. J. Appl. Phys. Part 2 **26**, L1197 (1987).
[166]Y. Hidaka, *et al.*, Jpn. J. Appl. Phys. Part 2 **26**, L726 (1987).
[167]J. Wójcik, *et al.*, J. Cryst. Growth **91**, 255 (1988).
[168]Y. Iye, *et al.*, Jpn. J. Appl. Phys. Part 2 **26**, L1057 (1987).
[169]L. Z. Avdeev, *et al.*, Pis'ma Zh. Eksp. Teor. Fiz. **46**, Prilozh., 86 (1987) [JETP Lett. **46**, Suppl., S74 (1987)].
[170]G. A. Emel'chenko, *et al.*, Pis'ma Zh. Eksp. Teor. Fiz. **46**, 162 (1987) [JETP Lett. **46**, 204 (1987)].
[171]K. Mori, *et al.*, Bull. Jpn. Inst. Met. **27**, 734 (1988).
[172]G. Balestrino, *et al.*, Mater. Res. Bull. **23**, 1119 (1988).
[173]R. Boutellier, J. Cryst. Growth **96**, 465 (1989).
[174]W. Sadowski, *et al.*, J. Less-Common Met. **150**, 129 (1989).
[175]S. Posi, *et al.*, J. Mater. Sci. Lett. **3**, 497 (1989).
[176]Th. Wolf, *et al.*, J. Cryst. Growth **96**, 1010 (1989).
[177]S. V. Moshkin, *et al*, *Abstracts of Papers presented at Second All-Union Conf. on High-Temperature Superconductivity*, Kiev, 1989 [in Russian], Vol. 2, Kiev (1989), p. 322.
[178]H. Wang, *et al.*, J. Cryst. Growth **99**, 929 (1990).
[179]B. N. Sun, *et al.*, J. Cryst. Growth **100**, 297 (1990).
[180]N. E. Alekseevskiĭ, *et al.*, Sverkhprovodimost' (KIAE) **3**, 78 (1990) [Superconductivity **3**, 75 (1990)].
[181]T. M. Dmitruk, *et al.*, *Abstracts of Papers presented at All-Union Conf. on Physics and Chemistry of High-Temperature Superconducitivity: Theoretical Problems*, Kharkov, 1989 [in Russian], p. 145.
[182]F. Holtzberg and C. Feild, J. Cryst. Growth **99**, 915 (1990).
[183]A. B. Bykov, *et al.*, Kristallografiya **34**, 1267 (1989) [Sov. Phys. Crystallogr. **34**, 763 (1989)].
[184]Q. Wu, *et al.*, Mater. Res. Bull. **24**, 1325 (1989).
[185]I. V. Vodolazskaya, *et al.*, Physica C (Utecht) **162–164**, 1213 (1989).
[186]V. I. Voronkova, *et al.*, Sverkhprovodimost' (KIAE) 2(2), 41 (1989) [Superconductivity **2**, 50 (1989)].
[187]Y. Hidaka, *et al.*, J. Cryst. Growth **85**, 581 (1987).
[188]F. Garzon and I. Raistrick, J. Electrochem. Soc. **136**, 2753 (1989).
[189]R. Moret and G. Collin, *High-Temperature Superconductors* (Proc. Symposium, Boston, MA, 1987, ed. by D. S. Capone, *et al.*), Materials Research Society, Pittsburgh (1988), p. 497.
[190]I. N. Makarenko, *et al.*, Pis'ma Zh. Eksp. Teor. Fiz. **47**, 52 (1988) [JETP Lett. **47**, 63 (1988)].
[191]E. Moran, *et al.*, Solid State Commun. **67**, 369 (1988).
[192]J. A. Campa, *et al.*, J. Cryst. Growth **91**, 334 (1988).
[193]A. Katsui, *et al.*, Jpn. J. Appl. Phys. Part 2 **26**, L1521 (1987).
[194]T. Iwata, *et al.*, J. Cryst. Growth **91**, 274 (1988).
[195]J. H. Weaver, *et al.*, Phys. Rev. B **38**, 4668 (1988).
[196]R. C. J. Droper, J. Mater. Sci. Lett. **7**, 1281 (1988).
[197]R. Wan, *et al.*, J. Appl. Phys. **64**, 3754 (1988).
[198]M. Hikita, *et al.*, Phys. Rev. B **36**, 7199 (1987).
[199]Y. Tajima, *et al.*, J. Cryst. Growth **85**, 662 (1987).
[200]T. Inoue, *et al.*, J. Cryst. Growth **91**, 287 (1988).
[201]T. Inoue, *et al.*, J. Cryst. Growth **99**, 925 (1990).
[202]M. J. Menken, *et al.*, J. Cryst. Growth **91**, 264 (1988).
[203]S. Hayashi, *et al.*, J. Cryst. Growth **91**, 331 (1988).
[204]D. Sun, *et al.*, Acta Phys. Sin. **3**, 2023 (1988).
[205]M. J. V. Menken, *et al.*, J. Cryst. Growth **96**, 1002 (1989).
[206]V. I. Aleksandrov, *et al.*, *Abstracts of Papers presented at Second All-Union Conf. on High-Temperature Superconductivity*, Kiev, 1989 [in Russian], Vol. 2, Kiev (1989), p. 325.
[207]Fang Minghu, Chin. J. Low Temp. Phys. **10**, 306 (1988).
[208]V. V. Moshchalkov, *et al.*, Physica C (Utrecht) **166**, 185 (1990).
[209]S. Takekawa, *et al.*, Jpn. J. Appl. Phys. Part 2 **26**, L2079 (1987).
[210]E. Hodorowicz, *et al.*, Physica C (Utrecht) **158**, 127 (1989).
[211]V. I. Voronkova, *et al.*, Physica C (Utrecht) **162–164**, 1211 (1989).
[212]H. J. Scheel, *et al.*, J. Cryst. Growth **94**, 281 (1989).
[213]P. Niedermann, *et al.*, J. Appl. Phys. **65**, 3274 (1989).
[214]M. Zange, *et al.*, Bull. Soc. Chim. Fr. 4470 (1972).
[215]T. L. Barry and R. Roy, J. Inorg. Nucl. Chem. **29**, 1243 (1976).
[216]T. Shishido, *et al.*, J. Cryst. Growth **85**, 599 (1987).
[217]J. Akimitsu, *et al.*, Jpn. J. Appl. Phys. Part 2 **27**, L2080 (1987).
[218]A. A. Bush, *et al.*, Sverkhprovodimost' (KIAE) 2(9), 38 (1989) [Superconductivity **2**, 45 (1989)].
[219]D. M. De Leeuw, *et al.*, Physica C (Utrecht) **152**, 39 (1988).
[220]K. G. Frase and D. K. Clark, Adv. Ceram. Mater. **2**, Spec. issue, 295 (1987).
[221]G. Wang, *et al.*, Adv. Ceram. Mater. **2**, Spec. issue, 313 (1987).
[222]B. Domenges, *et al.*, Europhys. Lett. **4**, 211 (1987).
[223]H. W. Zandbergen, *et al.* Phys. Status Solidi A **105**, 207 (1988).
[224]Y. Matsui, *et al.*, Jpn. J. Appl. Phys. Part 2 **26**, L777 (1987).
[225]E. Kaldis, *et al.*, *Abstracts of Papers presented at Symposium on High-Temperature Superconductors: Preparation and Applications* (Fall Meeting of European Materials Research Society), Strasbourg, 1988, Part AIII, p. 5.
[226]A. M. Balbashov, Sverkhprovodimost' (KIAE) 2(9), 138 (1989) [Superconductivity **2**, 156 (1989)].
[227]T. Inoue, *et al.*, Jpn. J. Appl. Phys. Part 2 **27**, L347 (1988).
[228]Y. Matsui and M. Maeda, Jpn. J. Appl. Phys. Part 2 **27**, L361 (1988).
[229]M. Fukunara, *et al.*, Mater. Lett. **6**, 398 (1988).
[230]Z. Ren, *et al.*, J. Cryst. Growth **92**, 677 (1988).
[231]S. Ikegawa, *et al.*, Annu. Rep. Eng. Res. Inst. Fac. Eng. Univ. Tokyo **47**, 79 (1988).
[232]A. Ono, *et al.*, Jpn. J. Appl. Phys. Part 2 **27**, L1213 (1988).
[233]Y. Ikeda, *et al.*, J. Jpn. Soc. Powder Met. **35**, 405 (1988).
[234]Yu. Ya. Skolis, *et al.*, Vestn. Mosk. Univ. Khim. **31**, 142 (1990).
[235]K. Tomomatsu, *et al.*, Appl. Phys. Lett. **55**, 298 (1989).

[236]K. Shigematsu, *et al.*, J. Cryst. Growth **100**, 661 (1990).
[237]P. A. Morris, *et al.*, Appl. Phys. Lett. **53**, 249 (1988).
[238]A. A. Bush, *et al.*, Sverkhprovodimost' (KIAE) **2**(3), 78 (1989) [Superconductivity **2**, 102 (1989)].
[239]L. N. Dem'yanets, *et al.*, Sverkhuprovodimost' (KIAE) **2** (12), 147 (1989) [Superconductivity **2**, 169 (1989)].
[240]Yu. D. Tret'yakov, *et al.*, Zh. Neorg. Khim. **35**, 1635 (1990).
[241]J. M. Tarascon, *et al.*, Phys. Rev. B **38**, 8885 (1988).
[242]A. Ono, Jpn. J. Appl. Phys. Part 2 **27**, L2276 (1988).
[243]B. Javaram, *et al.*, J. Phys. Condens. Matter. **1**, 477 (1989).
[244]S. A. Sunshine, *et al.*, Phys. Rev. B **38**, 893 (1988).
[245]U. Endo, *et al.*, Jpn. J. Appl. Phys. Part 2 **28**, L190 (1988).
[246]V. A. Murashov, *et al.*, *Abstracts of Papers presented at First All-Union Conf. on High-Temperature Superconductivity*, Kharkov, 1988 [in Russian], Vol. 3, p. 116.
[247]R. G. Buckley, *et al.*, Physica C (Utrecht) **156**, 629 (1988).
[248]R. M. Hazen, *et al.*, Phys. Rev. Lett. **60**, 1657 (1988).
[249]S. Iijama, *et al.*, Jpn. J. Appl. Phys. Part 2 **27**, L1168 (1988).
[250]J. I. Randell, Acta Crystallogr. **12**, 519 (1959).
[251]S. Nomura, *et al.*, Jpn. J. Appl. Phys. Part 2 **27**, L1251 (1988).
[252]J. Koike, *et al.*, Jpn. J. Appl. Phys. Part 2 **27**, L841 (1988).
[253]T. K. Cišzek, *et al.*, J. Cryst. Growth **91**, 312 (1988).
[254]Y. F. Yan, *et al.*, Mod. Phys. Lett. B **2**, 571 (1988).
[255]C. Cui, *et al.*, Solid State Commun. **68**, 331 (1988).
[256]Z. Zhao, *et al.*, Solid State Commun. **67**, 101 (1988).
[257]S. Takekawa, *et al.*, J. Cryst. Growth **92**, 687 (1988).
[258]S. Durčok, *et al.*, Czech. J. Phys. B **39**, 113 (1989).
[259]X. Z. Wang, *et al.*, Solid State Commun. **69**, 829 (1989).
[260]C. Chen, *et al.*, J. Cryst. Growth **96**, 547 (1989).
[261]T. Shishido, *et al.*, Jpn. J. Appl. Phys. Part 2 **28**, L791 (1989).
[262]P. A. J. Le Groot, *et al.*, J. Phys. Condens. Matter **1**, 5817 (1989).
[263]H. Wang, *et al.*, J. Cryst. Growth **96**, 221 (1989).
[264]B. Keszei, *et al.*, J. Less-Common Met. **155**, 229 (1989).
[265]S. Piñol, *et al.*, J. Cryst. Growth **100**, 286 (1990).
[266]S. J. Guo, *et al.*, J. Cryst. Growth **100**, 303 (1990).
[267]S. V. Moshkin, *et al.*, *Ural Crystallographic Meeting on Mineralogical Crystallography, Crystal Origin, and Crystal Synthesis*, Syktyvkar, 1990 [in Russian], p. 115.
[268]N. J. H. Gallo, *et al.*, Mater. Sci. Lett. **8**, 1262 (1989).
[269]Ren Zhifeng, *et al.*, J. Cryst. Growth **92**, 677 (1988).
[270]D. B. Mitzi, *et al.*, Phys. Rev. B **41**, 6564 (1990).
[271]B. Morosin, *et al.*, Physica C (Utrecht) **152**, 413 (1988).
[272]T. Kanai, *et al.*, Jpn. J. Appl. Phys. Part 2 **27**, L1435 (1988).
[273]H. Takei, *et al.*, Jpn. J. Appl. Phys. Part 2 **28**, L1193 (1989).
[274]M. A. Subramanian, *et al.*, Science **239**, 1015 (1988).
[275]W. Kritscha, *et al.*, Europhys. Lett. **12**, 179 (1990).
[276]A. A. Bush, *et al.*, *Abstracts of Papers presented at Fifth All-Union Conf. on Crystal Chemistry of Intermetallic Compounds*, L'vov, 1989 [in Russian], p. 267.
[277]A. M. Balbashov, *et al.*, Sverkhprovodimost' (KIAE) **2**(1), 57 (1990) [Superconductivity **2**, 51 (1990)].
[278]D. N. Zheng, *et al.*, Mod. Phys. Lett. B **4**, 145 (1990).
[279]S. Kishuda, *et al.*, J. Cryst. Growth **99**, 937 (1990).
[280]Ren Zhifeng *et al.*, J. Cryst. Growth **102**, 349 (1990).
[281]S. C. Gadkari, J. Cryst. Growth **102**, 685 (1990).
[282]Y. Matsui and H. Maeda, Jpn. J. Appl. Phys. Part 2 **27**, L827 (1988).
[283]T. Hatano, *et al.*, Jpn. J. Appl. Phys. Part 2 **27**, L2055 (1988).
[284]L. M. Leonyuk, *et al.*, *Abstracts of Papers presented at Second All-Union Conf. on High-Temperature Superconductivity*, Kiev, 1989 [in Russian], Vol. 2, p. 52.
[285]A. A. Bush, *et al.*, Sverkhprovodimost' (KIAE) **3**, 432 (1990) [Superconductivity **3**, 409 (1990)].
[286]Y. Wang, *et al.*, J. Cryst. Growth **99**, 933 (1990).
[287]K. Oka and H. Unoki, Jpn. J. Appl. Phys. Part 2 **28**, L937 (1989).
[288]S. Piñol, *et al.*, Physica C (Utrecht) **165**, 265 (1990).
[289]A. Cassanho, *et al.*, J. Cryst. Growth **96**, 999 (1989).
[290]J. M. Tarascon, *et al.*, Physica C (Utrecht) **162–164**, 285 (1989).
[291]J. M. Tarascon, *et al.*, Phys. Rev. B **40**, 4494 (1989).
[292]F. C. Matacotta, *et al.*, Preprint No. 332, International Centre for Theoretical Physics, Trieste (1989), p. 1.
[293]K. F. McCarty, *et al.*, Physica C (Utrecht) **157**, 135 (1989).
[294]M. C. Krantz, *et al.*, Phys. Rev. B **40**, 2635 (1989).
[295]N. N. Kolesnikov, *et al.*, Pis'ma Zh. Eksp. Teor. Fiz. **50**, 40 (1989) [JETP Lett. **50**, 47 (1989)].
[296]M. P. Kulakov, *et al.*, *Abstracts of Papers presented at Second All-Union Conf. on High-Temperature Superconductivity*, Kiev, 1989 [in Russian], Vol. 2, p. 336.
[297]T. Kotani, *et al.*, Jpn. J. Appl. Phys. Part 2 **28**, L1378 (1989).
[298]A. A. Maksimov, *et al.*, Zh. Eksp. Teor. Fiz. **97**, 1047 (1990) [Sov. Phys. JETP **70**, 588 (1990)].
[299]K. F. McCarty, *et al.*, Physica C (Utrecht) **156**, 119 (1988).
[300]R. Liu, *et al.*, Phys. Rev. B **40**, 2654 (1989).
[301]M. A. Subramanian, *et al.*, Physica C (Utrecht) **157**, 124 (1989).
[302]J. Y. Lee, *et al.*, J. Mater. Res. **4**, 763 (1989).
[303]A. A. Bush, *et al.*, Sverkhprovodimost' (KIAE) **3**, 599 (1990) [Superconductivity **3**, 566 (1990)].
[304]R. J. Cava, *et al.*, Nature (London) **332**, 814 (1988).
[305]J. P. Wignocourt, *et al.*, Solid State Commun. **65**, 1363 (1988).
[306]A. Katsui, Jpn. J. Appl. Phys. Part 2 **21**, L553 (1982).
[307]A. Katsui, *et al.*, J. Cryst. Growth **66**, 228 (1984).
[308]S. Hirano and S. Takahashi, J. Cryst. Growth **78**, 408 (1986).
[309]S. Hirano and S. Takahashi, J. Cryst. Growth **79**, 219 (1986).
[310]L. N. Dem'yanets, Dokl. Akad. Nauk SSSR **313**, 612 (1990) [Sov. Phys. Dokl. **35**, 601 (1990)].
[311]X. P. Jiang, *et al.*, Supercond. Sci. Technol. **1**, 102 (1988).

Translated by A. Tybulewicz